

**Autoantibodies to myelin oligodendrocyte glycoprotein
(MOG) in patients with demyelinating diseases of the
central nervous system (CNS): investigation of the clinical
spectrum and pathological potential**

Dissertation der Fakultät für Biologie
der Ludwig-Maximilians-Universität München

Melania Spadaro

München, 2017

Diese Dissertation wurde angefertigt
unter der Leitung von Prof. Dr. Edgar Meinl am Institut für Klinische
Neuroimmunologie (Biomedizinisches Centrum, Martinsried)
Ludwig-Maximilians-Universität München

Erstgutachter: Prof. Dr. Barbara Conradt
Zweitgutachter: Prof. Dr. Charles David

Tag der Abgabe: 30.03.2017

Tag der mündlichen Prüfung: 04.07.2017

ERKLÄRUNG

Ich versichere hiermit an Eides statt, dass meine Dissertation selbständig und ohne unerlaubte Hilfsmittel angefertigt worden ist.

Die vorliegende Dissertation wurde weder ganz, noch teilweise, bei einer anderen Prüfungskommission vorgelegt.

Ich habe noch zu keinem früheren Zeitpunkt versucht, eine Dissertation einzureichen oder an einer Doktorprüfung teilzunehmen.

München, den 30.03.2017

Melania Spadaro

Note on results obtained in collaboration:

Immunohistochemical stainings were performed and analyzed by Prof. Hans Lassmann, Brain Research Center in Vienna and Prof. Romana Höftberger, Allgemeines Krankenhaus (AKH) in Vienna.

In vivo experiments and perfusion of rats were performed by PD Dr. Naoto Kawakami of the Institute of Clinical Neuroimmunology (BioMedicine Center), Martinsried.

Summary

Antibodies (abs) to myelin oligodendrocyte glycoprotein (MOG) are known to induce demyelination in experimental animals and are found in a proportion of patients with different inflammatory diseases of the CNS.

In the first part of this thesis, the clinical spectrum of patients with MOG-specific abs was examined. To this end a cell-based assay (CBA) with transient transfection of full-length MOG was further optimized. A total of 260 adult patients from the outpatient clinic of the Institute of Clinical Neuroimmunology were analyzed for reactivity to human MOG by using this assay and 17 patients (6.5 %) tested positive. Recognized epitopes were determined with mutated variants of MOG. Some of these patients with abs to MOG were clinically classified as neuromyelitis optica spectrum disorders (NMOSD) and optic neuritis (ON), diseases in which it is already known that MOG-specific abs can occur. One of the 17 patients with MOG-specific abs had features overlapping with both multiple sclerosis (MS) and NMOSD and fulfilled only partially the criteria of these diseases. This patient had a severe disease course and underwent brain biopsy. The histopathological analysis revealed a MS type II pathology which is characterized by the deposition of the terminal complement complex C9neo. Moreover, this pattern of MS is expected to be antibody-mediated but the recognized antigen has not yet been identified. Here we describe for the first time the histopathology of MOG-antibody associated encephalitis and our findings suggest that the demyelination observed in our patient is mediated by abs to MOG. This could not directly be proven since MOG-specific abs of this patient did not cross-react with rodent MOG. The presence of MOG-specific abs in classical MS is a controversial issue since years. Inspired by our case report with MOG-antibody associated MS type II pathology, we specifically analyzed a cohort of MS patients selected for having severe ON and/or myelitis; we found that 5 % of these patients have abs to MOG.

The second part of this thesis aimed to analyze the pathogenic properties of human abs to MOG. To this end, patients with abs to MOG showing cross-reactivity to rodent MOG were identified. Abs to MOG from two patients were affinity purified. These abs bound human MOG by ELISA and in our CBA, stained myelin *in situ* and induced EAE exacerbation *in vivo*. As an additional experimental approach, recombinant abs to MOG were generated from one of these patients. To this end, MOG-specific B lymphocytes in the peripheral blood and *in vitro* differentiated B lymphocytes were identified by the employment of MOG tetramers and subsequently single-cell sorted, Ig chains were cloned and recombinant abs were produced. The recombinant abs obtained from these cells recognized MOG by ELISA with low affinity, but neither bound MOG in our CBA nor stained brain tissue. Moreover, the recombinant

antibody with the highest affinity for MOG was tested *in vivo* for its potential pathogenicity but no EAE exacerbation was observed.

Together, this thesis extends the knowledge about the clinical spectrum of adult patients with abs to MOG and describes the histopathology of anti-MOG associated encephalomyelitis. Further, it shows that abs to MOG, affinity purified from the peripheral blood of patients diagnosed with demyelinating disease, can enhance pathology in an animal model.

Zusammenfassung

Antikörper gegen das Myelin-Oligodendrozyten-Glykoprotein (MOG) wirken in Tiermodellen demyelinisierend und kommen in manchen Patienten mit unterschiedlichen entzündlichen Erkrankungen des ZNS vor.

Im ersten Teil dieser Arbeit wurde das klinische Spektrum von erwachsenen Patienten mit MOG-spezifischen Antikörpern untersucht. Zu diesem Zweck wurde ein zellbasierter Assay mit transienter Transfektion von voll-längen MOG weiter optimiert. Insgesamt wurden 260 erwachsene Patienten aus der ambulanten Klinik des Instituts für Klinische Neuroimmunologie auf die Reaktivität von hMOG getestet: 17 Patienten (6,5%) mit Antikörpern gegen MOG wurden identifiziert. Die Antigen Epitope wurden Anhand von unterschiedlichen MOG Varianten analysiert. Einige der Patienten mit Antikörper gegen MOG wurden mit Neuromyelitis optica Spektrum-Erkrankungen (NMOSD) und Neuritis nervi optici (ON) diagnostiziert. Bei Patienten mit diesen Krankheiten ist bereits bekannt, dass MOG-spezifische Antikörper auftreten können. Einer von 17 Anti-MOG-positiven Patienten zeigte eine Überlappung an Krankheitssymptomen von Multipler Sklerose (MS), als auch NMOSD-spezifischen Eigenschaften und erfüllte daher nur teilweise die klassifizierenden Kriterien dieser Erkrankungen. Da dieser Patient einen schweren Krankheitsverlauf hat, wurde ihm eine Hirnbiopsie entnommen. Die histopathologische Analyse ergab ein MS-Typ-II-Pattern, das durch Ablagerung des terminalen Komplementkomplexes C9neo gekennzeichnet ist. Weiterhin ist bekannt, dass die Erkrankung vom Typ-II Antikörper assoziiert ist, wobei deren Antigene überwiegend noch nicht identifiziert wurden. Diese Arbeit beschreibt zum ersten Mal die Histopathologie eines Patienten mit MOG-Antikörpern assoziierter Enzephalitis. Die Ergebnisse weisen darauf hin dass die Demyelinisierung in diesem Patienten von MOG-Antikörpern vermittelt wird. Dies konnte nicht direkt in Tiermodellen nachgewiesen werden, da die MOG-spezifische Antikörper dieses Patienten keine Kreuzreaktivität gegen Maus und Ratten MOG aufwiesen. Die Detektion von Antikörpern gegen MOG bei klassischer MS ist seit Jahren ein umstrittenes Thema. Daher wurde eine weitere Kohorte von MS-Patienten, die mit schwerer optischer Neuritis und / oder Myelitis diagnostiziert wurden, ausgewählt und in dieser Arbeit auf MOG-Antikörpern untersucht. In 5% dieser Patienten wurden die entsprechenden Antikörper nachgewiesen.

Der zweite Teil dieser Arbeit zielte darauf ab, die pathogenen Eigenschaften der menschlichen Antikörper gegen MOG zu analysieren. Zu diesem Zweck wurden Patienten mit Antikörpern gegen MOG, die eine Kreuzreaktivität gegen Maus und Ratten MOG zeigten, identifiziert. Es konnten MOG-spezifische Antikörper von zwei Patienten aufgereinigt werden. Diese Antikörper zeigten sowohl im ELISA, als auch in einem Zell-basierten Assay eine Reaktivität gegen hMOG. Zusätzlich färbten diese Antikörper Hirngewebe und induzierten eine Verschlechterung der EAE (Experimentelle autoimmune Enzephalomyelitis) *in vivo*. Als

zusätzlicher experimenteller Ansatz wurden rekombinante Antikörper gegen MOG von einem dieser Patienten hergestellt. Hierfür wurden MOG-spezifische B Zellen in PBMCs (Peripheral blood mononuclear cells) und *in vitro* differenzierten B-Lymphozyten des Patienten durch den Einsatz von MOG-Tetrameren identifiziert, auf Einzelzell-Ebene sortiert, die IgG Ketten kloniert und rekombinante Antikörper wurden produziert. Die aus diesen Zellen erhaltenen rekombinanten Antikörper erkannten MOG mit geringer Affinität im ELISA aber zeigten weder im Zell-basierten Assay, noch im Hirngewebe Reaktivität gegen MOG. Darüber hinaus wurde der rekombinante Antikörper mit der höchsten Affinität für MOG *in vivo* auf seine potentielle Pathogenität getestet. Im Gegensatz zu den aufgereinigten Antikörpern, induzierte dieser Antikörper keine Verschlechterung der EAE.

Diese Arbeit erweitert das aktuelle Wissen über das klinische Spektrum von erwachsenen Patienten mit Antikörpern gegen MOG und beschreibt die Histopathologie der mit diesen Antikörpern assoziierten Enzephalitis. Darüber hinaus konnte gezeigt werden, dass Antikörper gegen MOG, die aus dem Blut von Patienten mit einer demyelinisierenden Erkrankung aufgereinigt wurden, die Pathologie im Tiermodell verschlechtern können.

Acknowledgments

First of all, I want to thank my supervisor **Prof. Dr. Edgar Meinl** for all his support and advice, for always being available for my questions and for his faith in this project. He gave me the opportunity to develop my own ideas and helped me to become an independent scientist.

I want to express my appreciation also to **Prof. Dr. Reinhard Hohlfeld** who gave me the opportunity to perform my PhD in his department at the Institute of Clinical Neuroimmunology of the LMU.

I am grateful to **Prof. Dr. Barbara Conradt**, my doctoral thesis supervisor at the Faculty of Biology, for her time and helpful suggestions during the last years.

I want to thank all the members of my thesis advisory committee, **PD Dr. Naoto Kawakami**, **PD Dr. Dieter Jenne** and **Prof. Dr. Barbara Conradt** for their support, guidance, constructive criticism and discussions. Especially thanks to Naoto for his contribution to this work, for his endless patience and his precious suggestions.

Thank you also to all the members of my thesis examination committee, namely **Prof. Dr. Charles David**, **Prof. Dr. Nicolas Gompel** and **PD Dr. Serena Schwenkert**, for their time.

I want to acknowledge all our collaboration partners. I am grateful to **Dr. Eduardo Beltran** and **Dr. Simone Brändle** for their time and for sharing with me their knowledge about recombinant antibodies. Thanks also to **Prof. Hans Lassmann**, **Prof. Romana Höftberger** and to all our collaborators of the outpatient clinic of the Institute of Clinical Neuroimmunology.

I want to thank all the members of the Meinl lab and of the whole department for providing a wonderful atmosphere during the last years. I am endless grateful to **Ramona, Sissi, Mara, Julia, Bella, Franziska, Kerstin, Simone, Cathrin, Stephan, Caterina, Nikos, Michalis, Sarah** and **Anita**. Thanks for all the unforgettable moments in the lab and outside which made my time as a PhD student a memorable experience.

Thank you **Lucy** for being always there. Thank you for being a great friend, a sister, and for all your support.

I am grateful to my lovely **family** and to my **HEART** for their endless love. Grazie ai miei genitori e a mio fratello per aver sempre creduto in me e grazie a te, Vita Mia, per essere sempre al mio fianco. Questa tesi la dedico a voi.

Table of contents

1	Introduction	1
1.1	Inflammatory demyelinating diseases of the central nervous system (CNS).....	1
1.1.1	Role of B cells and autoantibodies	3
1.1.2	Therapeutic interventions targeting B cells and autoantibodies	4
1.2	Myelin Oligodendrocyte Glycoprotein (MOG)	5
1.3	MOG-specific abs in Experimental Autoimmune Encephalomyelitis (EAE).....	6
1.3.1	Pathogenic potential of abs to MOG: evidences from animal studies	7
1.4	Different detection methods of MOG-specific abs	7
1.4.1	Investigation of MOG-specific abs by using ELISA or Western blot.....	7
1.4.2	Abs to conformational-intact MOG	8
1.5	Possible pathogenic mechanisms of MOG-specific abs in humans	9
1.6	Aims of this project.....	11
2	Materials and Methods.....	12
2.1	Materials	12
2.1.1	Oligonucleotides	12
2.1.2	Restriction enzymes.....	13
2.1.3	Plasmids	14
2.1.4	Antibodies	15
2.2	Methods	16
2.2.1	Molecular biological methods.....	16
2.2.2	Microbiological methods.....	19
2.2.3	Cell biological methods	19
2.2.4	Isolation of human B cells	21
2.2.5	Recombinant protein expression.....	22
2.2.6	Protein analysis	22
2.2.7	Patient material.....	25
2.2.8	Immunological methods	25
2.2.9	Single cell sorting of MOG-binding B cells	28

2.2.10	Immunohistochemistry.....	28
2.2.11	Animal experiments.....	29
3	Results.....	30
3.1	Optimization of the CBA for the detection of MOG-specific abs.....	30
3.2	Occurrence of abs against conformation-intact hMOG in adult patients.....	33
3.2.1	Isotyping of MOG-specific abs.....	34
3.2.2	Epitope mapping on conformation-intact MOG.....	35
3.2.3	Recombinant expression of rat MOG and binding of human sera.....	37
3.3	Histopathology and clinical course of MOG-associated encephalomyelitis.....	39
3.3.1	Abs to MOG in index patient 1819.....	39
3.3.2	Neuropathological examination.....	41
3.4	Abs to MOG in a distinct subgroup of adult multiple sclerosis.....	43
3.4.1	Clinical phenotype of anti-MOG IgG positive patients with MS.....	44
3.5	Detection of MOG-specific abs by ELISA.....	47
3.6	Affinity purified anti-MOG abs from patients 1771 and 2246.....	49
3.6.1	Detailed analysis of patient sera 1771 and 2246.....	49
3.6.2	Establishment and validation of affinity purification of MOG-specific abs.....	50
3.6.3	Validation of affinity purification by FACS and ELISA.....	53
3.6.4	Pathogenicity of affinity purified abs against MOG.....	55
3.6.5	Histopathological analysis.....	56
3.7	Recombinant abs from patient 2246.....	57
3.7.1	MOG-specific B cells identified after <i>in vitro</i> stimulation.....	57
3.7.2	Validation of human MOG tetramers and staining of PBMC <i>ex vivo</i>	60
3.7.3	Recombinant expression of IgG from patient 2246.....	62
3.7.4	Functional analysis of recombinant abs from patient 2246.....	63
3.7.5	Transfer of human recombinant abs in Lewis rats.....	64
4	Discussion.....	66
4.1	Clinical spectrum of patients with abs to MOG.....	66
4.2	Histopathology of anti-MOG encephalomyelitis.....	68
4.3	Features of abs to MOG.....	69

4.4	Repertoire of abs to MOG	71
4.5	Pathogenicity of abs to MOG	73
4.6	Conclusions	73
5	References	75
6	List of Abbreviations.....	86
7	Publications and Conferences.....	88
7.1	Publications	88
7.2	Conferences	88
8	Curriculum Vitae	90

1 Introduction

1.1 Inflammatory demyelinating diseases of the central nervous system (CNS)

Inflammatory demyelinating diseases of the CNS comprise a spectrum of diseases including multiple sclerosis (MS), neuromyelitis optica spectrum disorders (NMOSD), optic neuritis (ON) and acute disseminated encephalomyelitis (ADEM). They consist in a clinically heterogeneous group of diseases regarding age of onset, clinical course, treatment, magnetic resonance imaging (MRI) and cerebrospinal fluid (CSF) features. It is sometimes difficult to make an accurate diagnosis, especially at disease onset, since these diseases sometimes show overlapping features in clinical, MRI or serum/CSF findings (Figure 1).

MS is the most common chronic inflammatory disease of the CNS. In the majority of MS patients, the disease is characterized at the beginning by a relapsing-remitting course (RRMS), which is followed after several years by a secondary progressive phase (SPMS). In some patients the disease is progressive from the onset (PPMS) (Confavreux, Vukusic et al. 2000). During the early stages of MS, inflammatory demyelination leads to the formation of focal plaques localized in the white matter, while later stages are characterized by a diffusion of demyelination in the cerebral and cerebellar cortex, as well as by degenerative processes in the white and grey matter (Kutzelnigg, Lucchinetti et al. 2005). Since T cells are able to induce a blood-brain barrier disruption and to induce CNS inflammation (Kebir, Kreymborg et al. 2007), MS has been for long time considered a T-cell driven disease, however, there are many evidences that B cells and autoantibodies play a key role in MS pathogenesis (Krumbholz, Derfuss et al. 2012, Hohlfeld, Dornmair et al. 2016).

The term NMOSD was introduced in 2007 after the revision of the diagnostic criteria for neuromyelitis optica (NMO) due to the discovery of NMO-immunoglobulin G (IgG) or Aquaporin-4 (AQP4)-specific antibodies (abs) (see below) (Wingerchuk, Lennon VA et al. 2006). Patients diagnosed with NMOSD have recurrent, isolated longitudinal extensive transverse myelitis (LETM, spinal cord lesion that extends over three or more vertebrae) or ON. These conditions can be associated or not with autoimmune disorders or brain lesions (hypothalamic, corpus callosal, periventricular, or brainstem) typical for NMO (Wingerchuk, Lennon VA et al. 2007).

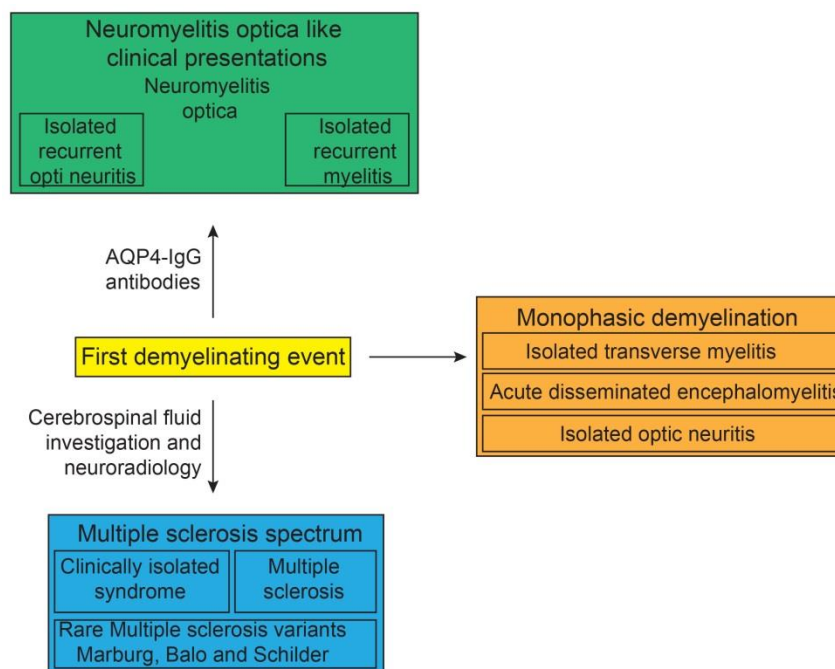


Figure 1: CNS inflammatory demyelinating diseases. Most patients present with clinically isolated syndrome (CIS) and subsequently develop MS or rare MS variants, such as Marburg, Balo or Schilder disease (MS spectrum). A first demyelinating event could also herald NMO or NMO-like disease, such as isolated (recurrent) ON or transverse myelitis. A third group of patients develop monophasic demyelinating diseases such as ADEM, isolated ON or transverse myelitis. Modified from (Reindl, Di Pauli et al. 2013).

ON is a demyelinating inflammation of the optic nerve that can appear as an isolated condition or in association with MS or NMOSD. Clinical features of this disease include a sudden unilateral vision loss, visual field loss, abnormal color vision, reduced contrast sensitivity function as well as the Uhthoff phenomenon that consists in a decrease of visual acuity due to high body temperature (Hickman, Dalton et al. 2002). Patients who experienced an episode of unilateral ON have a possibility of the 38% to develop MS in the next ten years. This percentage increases in the case of brain lesions in MRI (Beck, Trobe et al. 2003).

The original definitions for ADEM have been updated in 2013 (Krupp, Tardieu et al. 2013). This disease occurs predominantly during early childhood and has often a monophasic course. Monophasic ADEM is characterized by single polyphasic CNS event with encephalopathy (alteration in behavior or consciousness) and inflammatory demyelination during the first three months after disease onset. A small proportion of patients is diagnosed with multiphasic ADEM (Neuteboom, Boon et al. 2008) in which two ADEM episodes are separated by at least three months.

The patients who participated in this study are adults diagnosed with MS, ON, NMOSD or encephalomyelitis.

1.1.1 Role of B cells and autoantibodies

Several evidences suggest that B cells and autoantibodies are key players in inflammatory demyelinating diseases of the CNS:

- the CSF of MS patients is characterized by the presence of locally produced oligoclonal bands (OCB) (Obermeier, Mentele et al. 2008) and clonally expanded B cells (Von Büdingen, Gulati et al. 2010);
- demyelinating areas of MS lesions in a subset of patients show IgG and activated complement deposition (Lucchinetti, Brück et al. 2000);
- plasma exchange is beneficial in a subset of patients with MS type II pathology (Keegan, König et al. 2005);
- B-cell follicles have been reported in the meninges of some patients with progressive MS (Serafini, Rosicarelli et al. 2004);
- active NMO lesions showed IgM deposition and complement activation (Lucchinetti, Mandler et al. 2002, Misu, Höftberger et al. 2013);
- B-cell depleting therapies with anti-CD20 show a reduction of relapses in a subset of patients with MS and NMO (Hauser, Waubant et al. 2008, Krumbholz, Derfuss et al. 2012, Trebst, Jarius et al. 2014)

Apart from their role to generate antibody-producing cells, B cells perform a spectrum of additional functions which are crucial for the pathogenesis of MS and related disorders (Figure 2) (Krumbholz, Derfuss et al. 2012, Hoffmann and Meinl 2014, Krumbholz and Meinl 2014).

The important role of autoantibodies in demyelinating diseases of the CNS is highlighted by the discovery of pathogenic IgG in NMO patients. These abs bind selectively to the water channel AQP4, localized on astrocytes (Lennon, Wingerchuk et al. 2004) and are considered a valuable biomarker in distinguishing NMO from MS. Their pathogenicity has been demonstrated by transfer studies in which human NMO IgG or human sera containing AQP4-specific abs were injected in mice with experimental autoimmune encephalomyelitis (EAE), (Bradl, Misu et al. 2009, Saadoun, Waters et al. 2010, Saini, Rifkin et al. 2013, Wu, Zhou et al. 2013), the animal model that most closely resembles clinical and neuropathological features of human MS. Moreover, several *in vivo* experiments showed that autoantibodies can induce disease exacerbation only after a breaching of the blood-brain barrier (Genain, Nguyen et al. 1995, Derfuss, Parikh et al. 2009, Mayer and Meinl 2012).

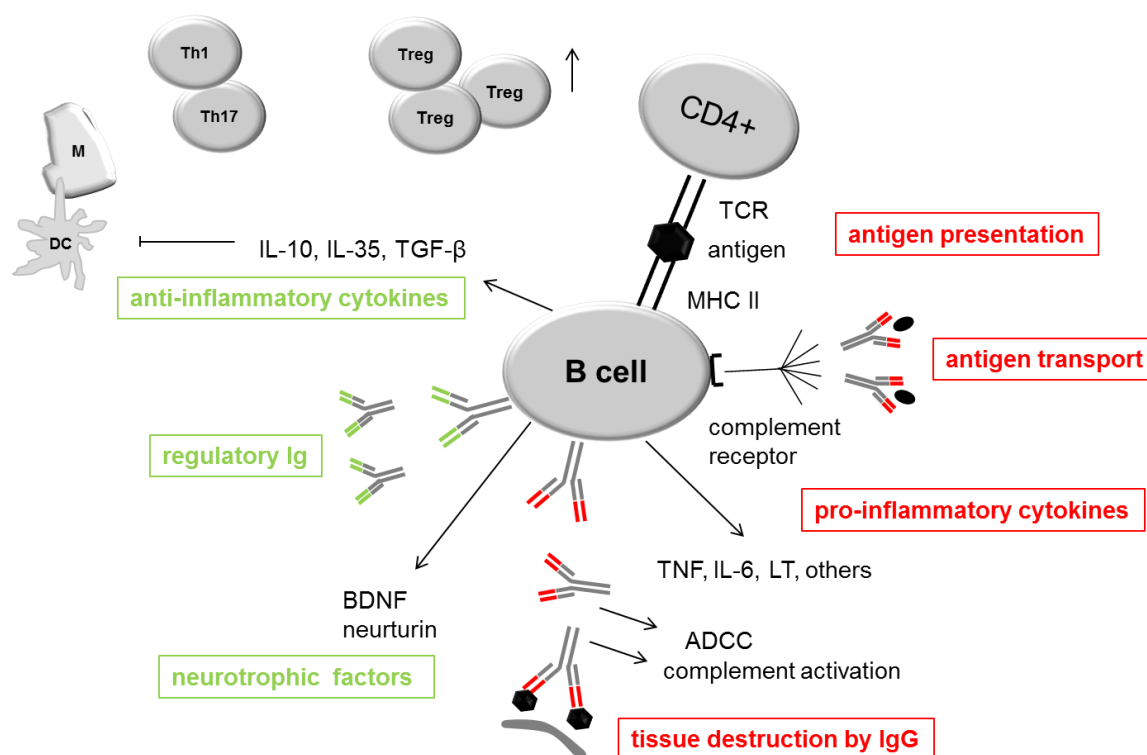


Figure 2: Inflammatory and regulatory functions of B cells. B cells exert various pro-inflammatory and immunoregulatory functions: they produce autoantibodies that can induce complement activation and ADCC. They are involved in inflammatory cytokine production (i.e. TNF, IL-6, LT), antigen-presentation and follicular antigen-transport. On the other hand, they produce anti-inflammatory cytokines (IL-10, IL-35 and TGF- β), which induce expansion of Treg cells, reduce Th1 and Th17 differentiation, and inhibit macrophage (M) and dendritic cell (DC) activity. Furthermore, B cells produce abs with potential immunoregulatory function and neurotrophic factors. Modified from (Hoffmann and Mehl 2014).

1.1.2 Therapeutic interventions targeting B cells and autoantibodies

The discovery of the pathogenic role of B cells and autoantibodies in CNS inflammation provided a strong rationale for the development and use of new therapeutic approaches over the last decades:

B cell-depleting monoclonal antibodies

Different monoclonal abs (mAb) target the CD20 molecule which is expressed throughout different maturation stages of the human B-cell lineage, from pre-B cells to early plasmablasts, and is lost during plasmacell differentiation (Krumbholz, Derfuss et al. 2012). Rituximab, a chimeric mAb, depletes CD20⁺ B cells efficiently from the circulation and reduces inflammatory brain lesions and clinical relapse in RRMS patients (Hauser, Waubant et al. 2008). It can reduce the levels of AQP4-specific abs in some but not all patients with NMO (Jarius and Wildemann 2010) and is also effective as a second line therapy in NMO

patients in which it does not affect AQP4-specific abs levels (Pellkofer, Krumbholz et al. 2011).

Other drugs targeting the CD20 molecule include humanized mAbs: ocrelizumab reduces the relapse rate and disease progression in RRMS (Hauser, Comi et al. 2015), while ofamatumumab reduces MRI lesions in RRMS patients (Sorensen, Lisby et al. 2014). These mAbs appear to have similar therapeutic efficiency in MS as rituximab. B cells are also targeted, simultaneously with T cells by the anti-CD52 mAb alemtuzumab, recently approved for the treatment of RRMS (Cohen, Coles et al. 2012).

Targeting antibodies

Abs can be removed from the circulation by plasma exchange or immunoadsorption (IA). The main difference between these two approaches is that the latter one allows the specific removal of abs and immune complexes by implying columns containing hydrophobic amino acids (Yoshida, Tamura et al. 2000). Plasma exchange and IA are used for steroid-resistant relapse in MS and NMO (Heigl, Hettich et al. 2013, Krumbholz and Meinl 2014).

1.2 Myelin Oligodendrocyte Glycoprotein (MOG)

Myelin Oligodendrocyte Glycoprotein (MOG) was identified for the first time as the target of *in-vitro* demyelinating abs obtained from guinea pigs immunized with homologues CNS tissue (Lebar, Lubetzki et al. 1986). Full length human MOG (hMOG) consists of 218 amino acids and belongs to the immunoglobulin superfamily (Pham-Dinh, Mattei et al. 1993). It is expressed exclusively in the CNS where it is localized on the outer surface of myelin (Figure 3) and represents less than 0.05% of total myelin proteins (Brunner, Lassmann et al. 1989).

The exact function of MOG is not known, however, it has been shown recently that MOG might be involved in the modulation of axon growth and survival since it directly interacts with the nerve growth factor (NGF) (von Büdingen, Mei et al. 2015). MOG might also be able to regulate the classical complement pathway through its interaction with the complement component C1q (Johns and Bernard 1997). The structure and localization of this protein suggests also a role as adhesion molecule (Clements, Reid et al. 2003), however, a MOG knockout mice did not show any obvious phenotype (Delarasse, Daubas et al. 2003).

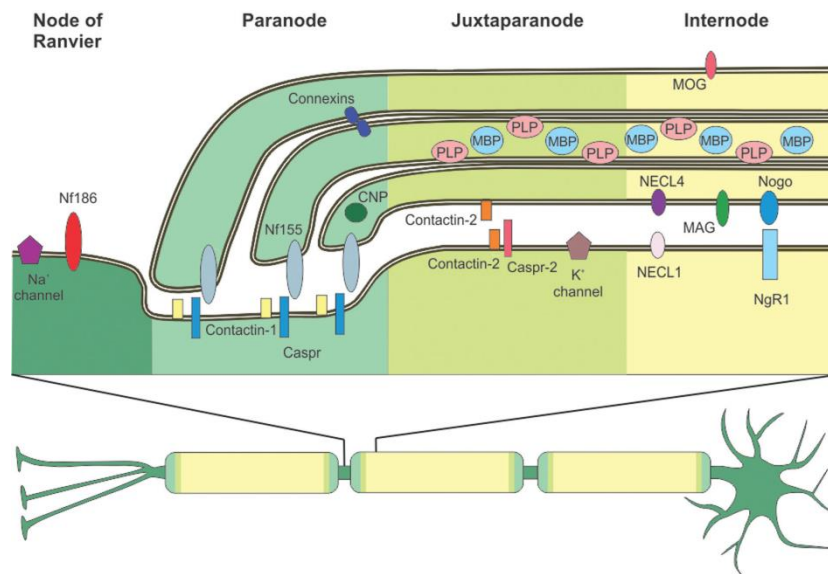


Figure 3: Distribution of CNS myelin proteins. Typical myelin proteins are found at the internode: Proteolipid protein (PLP) and Myelin basic protein (MBP) are the major myelin proteins, the quantitatively minor MOG is found at the outermost surface of the myelin sheath. Figure taken from (Mayer and Mehl 2012).

Among numerous antigens that have been proposed as antibody targets in MS and related disorders, MOG has received the greatest attention for the following reasons: it is localized on the outermost myelin sheath (Brunner, Lassmann et al. 1989) and is therefore easily accessible for pathogenic abs present in the extracellular milieu (Mayer and Mehl 2012); studies in animal models showed that MOG is the target of demyelinating abs (see below).

1.3 MOG-specific abs in Experimental Autoimmune Encephalomyelitis (EAE)

A first evidence of the potential involvement of MOG in the pathogenesis of demyelination derived from a study performed in guinea pigs with chronic relapsing EAE: the sera of these animals were able to induce, after injection in the subarachnoid space, *in vivo* demyelination in normal rats and this demyelinating activity directly correlated with their anti-MOG antibody titers (Linington and Lassmann 1987). Subsequently, evidences from different animal models showed that, upon active immunization, MOG is able to trigger both an antibody-mediated demyelinating as well as an encephalitogenic T-cell response in Lewis rats (Adelmann, Wood et al. 1995), SJL/J mice and primates (Bourquin, Schubart et al. 2003, 't Hart, Laman et al. 2004). Studies performed in C57Bl/6 mice, on the other hand, led to interesting results since in this animal model only the immunization with human MOG, and not rat MOG, induced B-cell-dependent EAE (Marta, Oliver et al. 2005).

1.3.1 Pathogenic potential of abs to MOG: evidences from animal studies

Anti-MOG mAbs are pathogenic both in rats (Schluesener, Sobel et al. 1987, Lassmann, Brunner et al. 1988, Linington, Bradl et al. 1988) and in primates (Genain, Nguyen et al. 1995) in which EAE was obtained either after active immunization with MBP or upon adoptive transfer of MBP-specific T cells. On the other hand, MBP-specific EAE in the absence of anti-MOG abs is characterized only by an inflammatory response without demyelination. MOG-specific abs exert their demyelinating activity in a complement dependent manner (Piddlesden, Lassmann et al. 1993) and require breakdown of the blood-brain barrier to enhance pathology (Litzenburger, Fässler et al. 1998) However, recent publications proposed a possible effector mechanism which brought new insights in the sophisticated interplay that occurs between T cells, B cells and abs during disease. These studies showed that MOG-specific abs can trigger inflammation by increasing the antigen presentation to myelin-reactive T cells in the CNS and therefore promote their expansion and encephalitogenic differentiation (Flach, Litke et al. 2016, Kinzel, Lehmann-Horn et al. 2016).

1.4 Different detection methods of MOG-specific abs

Studies performed over the last decades to identify the occurrence of abs to MOG in humans, gave controversial results. This can partially be explained by methodical variations regarding antigen preparation and antibody detection.

1.4.1 Investigation of MOG-specific abs by using ELISA or Western blot

Initial investigations were performed to detect the presence of abs to MOG in MS patients: a first study aimed to determine by ELISA the presence of MOG-specific abs in the serum and the CSF of 30 MS patients and showed that these abs not only occurred in the CSF of a subset of MS patients but they were also present in control groups (Xiao, Linington et al. 1991). In a more recent report abs to MOG were analyzed by using refolded rat MOG expressed in *Escherichia coli*. IgG and IgM to MOG could not be detected neither in MS patients nor in controls (Gori, Mulinacci et al. 2011). Abs to MOG were also detected by using MOG peptides: autoantibodies from MS patients and normal healthy controls (HC) were affinity purified and tested for reactivity against a panel of MOG peptides (Haase, Guggenmos et al. 2001). The authors found that epitope specificity was quite heterogeneous in both groups and that only one of the 17 tested MS patients and none of the nine HC abs were able to bind full length MOG expressed in its native state on the surface of fibroblasts. Therefore, even though abs recognizing MOG peptides can be detected both in MS patients and in HC, only a subset of patients has also abs that bind the full length protein and these are absent in healthy individuals. This is an important observation since it is known from

animal experiments that only abs that recognize cell-bound MOG, in its native and glycosylated state, are able to induce demyelination in EAE models (Brehm, Piddlesden et al. 1999, Ohtani, Kohyama et al. 2011).

Several studies analyzed abs to MOG by Western Blot, in which MOG is in its denatured state: MOG-specific abs were detected in MS patients, HC (Lindert, Haase et al. 1999, Reindl, Linington et al. 1999) and patients with clinically isolated syndrome (CIS). These authors found that CIS patients with MBP- or MOG-specific abs, had a higher relapse risk and a higher probability to develop MS (Berger, Rubner et al. 2003). However, these results could not be confirmed by other studies which used the same methods (Kuhle, Pohl et al. 2007, Pelayo, Tintoré et al. 2007).

1.4.2 Abs to conformational-intact MOG

The observation that only MOG-specific abs that are able to bind to conformational-intact MOG can determine demyelination *in vivo* highlights the importance of the use of cell-based assays (CBA) when detecting these abs in serum and CSF.

Abs to MOG in children. An important milestone in this context is represented by the studies performed by O'Connor and colleagues (O'Connor, McLaughlin et al. 2007): the authors used a sensitive assay based on self-assembling radiolabeled tetramers in which the native folding of the protein was guaranteed by *in vitro* translation system with endoplasmic reticulum microsomes. They could detect abs to MOG in a subset of ADEM patients but not in adult MS. These results were subsequently confirmed in other reports in which antibody detection was performed by using flow cytometry and immunocytochemistry (McLaughlin, Chitnis et al. 2009, Lalive, Hausler et al. 2011). The prevalence of MOG-specific abs was higher in a subset of patients with a younger age at disease onset and during a first episode of CNS demyelination (Brilot, Dale et al. 2009, McLaughlin, Chitnis et al. 2009, Fernandez-Carbonell, Vargas-Lowy et al. 2015). Moreover, longitudinal analysis of anti-MOG reactivity revealed that, while in pediatric MS abs to MOG tend to remain stable over time (Probstel, Dornmair et al. 2011), in ADEM patients they disappear and this was associated with a more favorable clinical outcome (Di Pauli, Mader et al. 2011, Probstel, Dornmair et al. 2011). Further studies revealed that abs to conformational-intact MOG are also present in children with recurrent ON (Rostasy, Mader et al. 2012).

Abs to MOG in adults. A subset of AQP4-IgG negative NMO/NMOSD patients harbor a MOG-directed immune response and seem to have a more favorable clinical outcome when compared to patients with a typical AQP4-antibody mediated disease (Mader, Gredler et al. 2011, Kitley, Woodhall et al. 2012, Kitley, Leite et al. 2013). However, this finding could not be confirmed by more recent studies (Kim, Woodhall et al. 2015, Jarius, Ruprecht et al.

2016). Abs to MOG have also been observed in adults with bilateral and recurrent ON (Ramanathan, Reddel et al. 2014) and rarely in patients with anti-N-methyl-D-aspartate (NMDA)-receptor encephalitis (Titulaer, Hoftberger et al. 2014).

Epitope mapping on conformational-intact MOG. The mapping of epitopes is important to understand autoantibody function and pathogenicity. Moreover, knowing the autoantibody epitope target and its conservation among species, can contribute to develop epitope-specific therapies and pathogenic studies in animal models. The use of a panel of MOG mutants allowed in a previous study to get an insight into the epitope determination on native human MOG in different pediatric patient groups (Mayer, Breithaupt et al. 2013): human abs to MOG recognize epitopes that connect the β strands of the extracellular IgV-like domain of MOG. The most frequently recognized epitope was P42, which is not present in rodent MOG. In addition, only 20% of patients had abs that recognize the epitope His103; Ser104 which is the main target of the 8-18C5 antibody used in animal studies. In some cases, the recognition of specific amino acids can induce epitope-specific effects: behavioral studies in rats showed that the injection of two different mAbs recognizing different epitopes on the smaller form of the glutamate decarboxylase (GAD65) can induce distinct neurological effects (Hampe, Petrosini et al. 2013). On the other hand, the analysis of antibody binding to MOG did not reveal any relevant difference between the analyzed patient groups (Mayer, Breithaupt et al. 2013).

1.5 Possible pathogenic mechanisms of MOG-specific abs in humans

Evidences for a pathogenic role of human abs to MOG have emerged from several studies. MOG-specific abs from children with CIS or ADEM have a natural killer mediated cytotoxic effect on MOG-expressing cells *in vitro*, moreover, antibody-dependent cell-mediated cytotoxicity (ADCC) correlated with antibody titer (Brilot, Dale et al. 2009). The majority of abs to MOG has the complement-activating IgG1 isotype which can activate complement and bind to the Fc receptors (McLaughlin, Chitnis et al. 2009). Another study showed that abs to MOG are able to induce at high titers the activation of the complement cascade, leading to the formation of the terminal complement complex (TCC) and to the internalization of these abs. This resulted in a complement dependent lysis of MOG-transfected cells (Mader, Gredler et al. 2011). In addition, a recent report revealed that purified IgG from MOG antibody-positive patients are able to induce cytoskeletal changes in cultured oligodendrocytes, however, no cell death was observed (Dale, Tantsis et al. 2014).

A possible pathogenic role of MOG-specific abs arises also from *in vivo* experiments. Transfer of sera from MS patients with MOG-specific abs to EAE rats showed an

enhancement of demyelination (Zhou, Srivastava et al. 2006). On the other hand, the injection of total IgG obtained from MOG-antibody positive NMO patients into mouse brains induced myelin changes and altered expression of axonal proteins that were reversible (Saadoun, Waters et al. 2014). Furthermore, this study did not reveal any complement involvement, suggesting therefore a different pathogenic mechanism.

1.6 Aims of this project

The main aims of this study were:

- Definition of the clinical spectrum of adult patients with abs to conformational-intact MOG, with a particular focus on the anti-MOG reactivity in adult MS and the histopathological features of MOG-associated encephalomyelitis.
- Investigation of the pathogenic potential of patient derived MOG-specific abs and of the antibody repertoire. MOG-specific abs were obtained by combining different experimental approaches:
 - Affinity purification
 - Isolation of MOG-specific B cells from peripheral blood with MOG-tetramers and generation of recombinant abs.

Affinity purified and recombinant abs were subsequently analyzed for binding to MOG in a CBA, by ELISA and for binding to myelin *in situ* by immunohistochemistry. The pathogenic potential of these abs was investigated by *in vivo* transfer experiments in Lewis rats upon determination of antibody cross-reactivity to rodent MOG.

2 Materials and Methods

2.1 Materials

2.1.1 Oligonucleotides

All oligonucleotides used in this study were synthesized by Metabion (Martinsried, Germany).

Table 1: Primer for MOG and vector backbones

Description	Name	Sequence
ratMOG full lenght	ratMOG-for	5'GGTGTGTGGAGCCTTTCTCTGC
ratMOG full lenght	ratMOG-rev	5'CTTAGCTCTTCAAGAACTGTCC
wt hMOG soluble_Cterm AviTag	wtMOGtetr-for-in	5'GCATATCTCCTGGGAAGAACGCTACAGGCATGG
wt hMOG soluble_Cterm AviTag	wtMOGtetr-rev-in	5'CCATGCCTGTAGCGTTCTTCCCAGGAGATATGC
wt hMOG soluble_Cterm AviTag	wtMOGtetr-for-out	5'AAGCTTGGGCAGTTCAGAGTGATAGG
wt hMOG soluble_Cterm AviTag	wtMOGtetr-rev-out	5'GC GGC CGC TCA GTG GTG GTG GTG GTG GTG GCCGCTGCCCGCGCTAGGGCTCACC CAGTATAG
CMV promoter	CMV-for	5'CGCAAATGGGCGGTAGGCGTG
pTT5 backbone	pTT5-for	5'GGGGTGAGTACTCCCTCTCAAAGC

Primer for single-cell analysis

Description	Name	Sequence
RT Primer	scRT-HG	5'GGGCTCAACTTTCTTGTCCA
RT Primer	scRT-Cmu	5'GGGACGAAGACGCTCACTT
RT Primer	scRT-AID	5'GCCAGACCTGTGTTCTTCT
RT Primer	scRT-Kappa	5'CTGTAGGTGCTGTCCTTGCT
RT Primer	scRT-Lambda	5'CATTCTGTAGGGGCCACTGT
Outer primer	V-Heavy1-for-out	5'ACAGGTGCCCCACTCCCAGGTGCAG
Outer primer	V-Heavy3-for-out	5'AAGGTGTCCAGTGTGARGTGCAG
Outer primer	V-Heavy4/6-for-out	5'CCCAGATGGGTCTGTCCCAGGTGCAG
Outer primer	V-Heavy5-for-out	5'CAAGGAGTCTGTTCCGAGGTGCAG
Outer primer	V-Kappa1/2-for-out	5'ATGAGGSTCCCYGCTCAGCTGCTGG
Outer primer	V-Kappa3-for-out	5'CTCTTCCTCCTGCTACTCTGGCTCCCAG
Outer primer	V-Kappa4-for-out	5'ATTTCTCTGTTGCTCTGGATCTCTG
Outer primer	scHG-rev-out	5'AGGTGTGCACGCCGCTG
Outer primer	scKappa-rev-out	5'CACACAACAGAGGCAGTTCC
Inner primer	V-Heavy1/5/7-for-in	5'CTGCAACCGGTGTACATTCCGAGGTGCAGCTGGTGCAG
Inner primer	V-Heavy1-for-in	5'CTGCAACCGGTGTACATTCCCAGGTGCAGCTGGTGGAG
Inner primer	V-Heavy3-for-in	5'CTGCAACCGGTGTACATTCTGAGGTGCAGCTGGTGGAG
Inner primer	V-Heavy4-for-in	5'CTGCAACCGGTGTACATTCCCAGGTGCAGCTGCAGGAG
Inner primer	V-Kappa-pan-for-in	5'ATGACCCAGWCTCCABYCWCCCTG
Inner primer	scHG-rev-in	5'AGTTCACGACACCGTCAC

Description	Name	Sequence
2246_D7 IG VH cloning	2246_IGVH_D7-for	5'GGCGGCTCCGCGGTGGGTCTGTCCCAGGTGCAGCTGCAGGAGTCGG
2246_D7 IG VH cloning	2246_IGVH_D7-rev	5'CCAGAGGTTCGACCTGGAGCAGGGCGCCAGGGGGAA GACCGATGGGCCCTTGGTGGAAGCTGAGGAGACGG
2246_D7 IG VK cloning	2246_IGVK_D7-for	5'GGCTCCGAGGCGCGCGATGTGACCTCCAGATGACCC AGTCTCCATCCTCCCTGTCTGCATCTGTAGG
2246_D7 IG VK cloning	2246_IGVK_D7-rev	5'GGAAGATGAAGACAGATGGCGCCGCCACAGTTCGTT TGATTTCACCTTGGTCCCTCC
2246_E6 IG VH cloning	2246_IGVH_E6-for	5'GGCGGCTCCGCGGTGGGTCTGTCCGAGGTGCAGTT GGTGAGAGGGGGGGGGGGTGGTTACAGCTGGAGG
2246_E6 IG VH cloning	2246_IGVH_E6-rev	5'CCAGAGGTTCGACCTGGAGCAGGGCGCCAGGGGGAA GACCGATGGGCCCTTGGTGGAAGCTGAGGAGACGG
2246_E6 IG VK cloning	2246_IGVK_E6-for	5'GGCTCCGAGGCGCGCGATGTGACATCCAGATGACCC AGTCACCAAGCAGCCTGAGCGCCAGCGTGGGCGACA
2246_E6 IG VK cloning	2246_IGVK_E6-rev	5'GCTCATCAGATGGCGGGAAGATGAAGACAGATGGC GCCGCCACAGTTGTCTGATCTCC
2246_E3 IG VH cloning	2246_IGVH_E3-for	5'GGCGGCTCCGCGGTGGGTCTGTCCCAGGTGCAGCT GGTGACAGCGGCGCGGAAGTGAAACGCCCGGGG
2246_E3 IG VH cloning	2246_IGVH_E3-rev	5'CCAGAGGTTCGACCTGGAGCAGGGCGCCAGGGGGAA GACCGATGGGCCCTTGGTGAGGCTGAGGAGACGGTT
2246_E3 IG VK cloning	2246_IGVK_E3-for	5'GGCTCCGAGGCGCGCGATGTGAAATTGTGTTGACGC AGTCTCC AGGCACCCTGTCTTTGTCTCCAGG
2246_E3 IG VK cloning	2246_IGVK_E3-rev	5'GGAAGATGAAGACAGATGGCGCCGCCACAGTTCGTT TGATATCCACTTTGGTCC
2246_A2 IG VH cloning	2246_IGVH_A2-for	5'GGTAGCTGCTCCGCGGTGGGTCTGTCCCAGGTGCA GCTGCAGGAGTCGGGCCAGGACTGGTGAGGGCTTC
2246_A2 IG VH cloning	2246_IGVH_A2-rev	5'CCAGGGGTCTGAACCAGAGAGACCACTGTTCTCTGAC CAGGTGTATCCCCGACACTCTCGCACAGTAATACATGG CCGTGTCCGCTGCGGTAC
2246_A2 IG VK cloning	2246_IGVK_A2-for	5'GCTCCGAGGCGCGCGATGTGAAATTGTGTTGACGCA GTCTCCAGGCACCCTGTCTTTGTCTCCAGGGGAAAGAG
2246_A2 IG VK cloning	2246_IGVK_A2-rev	5'GGAAGATGAAGACAGATGGCGCCGCCACAGTTCGTT TGACATCAACTGTGGTCCCAGGGCCGAAAGTGAATGA
2246_F6 IG VH cloning	2246_IGVH_F6-for	5'GGCGGCTCCGCGGTGGGTCTGTCCGAGGTGCAGTT GGTGAGAGGGGGGGGGGGTGGTTACGCTGGAGG
2246_F6 IG VH cloning	2246_IGVH_F6-rev	5'CCAGAGGTTCGACCTGGAGCAGGGCGCCAGGGGGA AGACCGATGGGCCCTTGGTGGAAGCTGAGGAGACGG
2246_F6 IG VK cloning	2246_IGVK_F6-for	5'GGCTCCGAGGCGCGCGATGTGACATCCAGATGACCC AGTCACCAAGCAGCCTGAGCGCCAGCGTGGGCGACA

2.1.2 Restriction enzymes

All restriction enzymes used in this study were purchased from NEB (New England Biolabs, Germany)

Table 2: Restriction enzymes

Enzyme	Restriction site
BssHII	G'CGCGCGC
EcoRI	G'AATTC
HindIII	A'AGCTT
KasI	G'GCGCC
NotI	GC'GGCCGC
SacII	CCGC'GG
SalI	G'TCGAC

2.1.3 Plasmids

Table 3: Plasmids used for this study

Vector	Insert	Expression	Origin
pEGFP-N1	/	cell surface	CLONTECH Laboratories
pEGFP-N1	hMOG wt	cell surface	AG Meinl
pEGFP-N1	hMOG-N31D	cell surface	AG Meinl
pEGFP-N1	mMOG	cell surface	AG Meinl
pEGFP-N1	hMOG-R9G/H10Y	cell surface	AG Meinl
pEGFP-N1	hMOG-P42S	cell surface	AG Meinl
pEGFP-N1	hMOG-R86Q	cell surface	AG Meinl
pEGFP-N1	hMOG-S104E	cell surface	AG Meinl
pEGFP-N1	H103A-S104E	cell surface	AG Meinl
pEGFP-N1	ratMOG	cell surface	AG Meinl
pTT5	/	soluble	AG Jenne
pTT5	hMOG_Cterm AviTag	soluble	AG Meinl
pTT5	hMOG-gly	soluble	AG Meinl
pTT5	mMOG	soluble	AG Krishnamoorthy
pTT5	ratMOG	soluble	AG Krishnamoorthy
pTT5	NF155	soluble	AG Meinl
pTT5	NF186	soluble	AG Meinl
pTT5	omgP	soluble	AG Meinl
pTT5	8-18C5_IGVH	soluble	AG Dornmair
pTT5	8-18C5_IGVK	soluble	AG Dornmair
pTT5	AB3_IGVH	soluble	AG Dornmair
pTT5	AB3_IGVK	soluble	AG Dornmair
pTT5	2246_D7_IGVH	soluble	AG Meinl
pTT5	2246_D7_IGVK	soluble	AG Meinl
pTT5	2246_E6_IGVH	soluble	AG Meinl
pTT5	2246_E6_IGVK	soluble	AG Meinl
pTT5	2246_E3_IGVH	soluble	AG Meinl
pTT5	2246_E3_IGVK	soluble	AG Meinl
pTT5	2246_A2_IGVH	soluble	AG Meinl
pTT5	2246_A2_IGVK	soluble	AG Meinl
pTT5	2246_F6_IGVH	soluble	AG Meinl
pTT5	2246_F6_IGVK	soluble	AG Meinl

2.1.4 Antibodies

Table 4: Antibodies used in this study

Target Specificity	Catalogue Nr.	Source	Provider	Conjugate
MOG	/	mouse	C.Linington, Glasgow	/
MOG	/	mouse	AG Meinel	/
MOG	/	human	AG Dornmair	/
human CD3	RM 1907S	rabbit	Neomarkers	/
human CD8	M7103	mouse	DAKO	/
human CD20	MS 340S	mouse	Neomarkers	/
human CD68	MO814	mouse	DAKO	/
human CD19	555413	mouse	BD Pharmingen	PE
human CD27	25027942	mouse	eBioscience	PE-Cy7
human CD38	48-0388-41	mouse	eBioscience	V450
mouse B220	45045280	rat	eBioscience	PerCP
human Ig	RPM 1003	sheep	Amersham	/
human IgG (H +L)	109066098	goat	Jackson Immuno Research	Biotin
mouse IgG (H+L)	115066003	goat	Jackson Immuno Research	Biotin
human IgG	BA3000	goat	Vector Laboratories	biotin
human IgM	17999842	mouse	eBioscience	APC
human IgM	48999841	mouse	eBioscience	V450
human IgG1	905428	mouse	Southern Biotech	Biotin
human IgG2	906008	mouse	Southern Biotech	Biotin
human IgG3	921008	mouse	Southern Biotech	Biotin
human IgG4	920008	mouse	Southern Biotech	Biotin
human IgG (H+L)	109036003	goat	Jackson Immuno Research	HRP
mouse IgG (H+L)	715036150	donkey	Jackson Immuno Research	HRP
Histidine	A70581VL	mouse	Sigma-Aldrich	HRP
human C9 neo	/	rabbit	P.Morgan, Glasgow	/
B7	/	mouse	P.Morgan, Glasgow	/
p22phox	sc-20781	rabbit	Santa Cruz	/
PLP	MCA 839G	mouse	Serotec	/
CNPase	SMI91	mouse	Sternberger Monoclonals	/
Neurofilament	AB 1981	mouse	Chemicon	/
GFAP	Z334	rabbit	DAKO	/
Aquaporin 1 and 4	sc20810	rabbit	Santa Cruz	/

Table 5: Other reagents used for flow cytometry

Name	Conjugate	Catalogue Nr.	Provider
Propidium Iodide	/	P4170	Sigma-Aldrich
Streptavidin	FITC	11431787	eBioscience
Streptavidin	Dye Light 649	16190084	Jackson Immuno Research
TO-PRO-3 Iodide	/	T3605	Invitrogen Life Technologies

2.2 Methods

2.2.1 Molecular biological methods

2.2.1.1 Reverse-transcriptase polymerase chain reaction (RT-PCR)

cDNA from single cell sorted B cells was obtained by using the Qiagen One Step RT-PCR Kit (Qiagen, Germany). The use of this kit allows both the reverse transcription and the PCR amplification to take place in the same reaction mix in a “one step” reaction. The reaction was performed according to the protocol provided by the manufacturer and by using gene specific primers (RT primers) as described in (Beltran, Obermeier et al. 2014).

2.2.1.2 Polymerase chain reaction (PCR)

IgG gene amplification. IgH and Igk V gene transcripts were amplified by two independent rounds of nested PCR. All PCR reactions were performed in 96 well plates containing a final volume of 20 µl per well. The first PCRs were performed with forward primer mixes specific for the leader region and reverse primers specific for the IgH and Igk gene constant regions (for-out and rev-out primers). 10 µl of cDNA were used as template. After the reverse transcription, reactions were heated to 95 °C for 15 minutes, this allowed the activation of the HotStarTaq DNA polymerase of the RT-PCR enzyme mix and the simultaneous inactivation of the reverse transcriptase. 2 µl of the first PCR product were used as template for the second PCRs which were performed by using forward primer mixes specific for FWR1 and respective nested reverse primers specific for the IgH and Igk J genes or constant regions. These PCRs were carried out by using the Taq DNA polymerase (Roche, Penzberg, Germany). PCRs for IgG gene amplification were performed in cooperation with Dr. Eduardo Beltran from the Dornmair group of our institute.

FIRST PCR using Qiagen OneStep RT-PCR kit (20µl)

2 µl	10X Reaction Buffer
0.4 mM	dNTPs
0.2 µM	forward OUT primer
0.2 µM	reverse OUT primer
20 U	enzyme mix
10 µl	cDNA template

PCR Program

Denaturation	95°C 15 min	
Denaturation	94 °C 30 sec	} 30 cycles
Annealing	57 °C 30 sec	
Elongation	72 °C 55 sec	
Elongation	72 °C 10 min	

SECOND nested PCR using Roche Taq reagents (20µl)

2 µl 10X reaction buffer
 0.4 mM dNTPs
 0.5 µM forward IN primer
 0.5 µM reverse IN primer
 1 U TaqDNA polymerase
 2 µl template

PCR Program

Denaturation 95°C 15 min

Denaturation	94 °C 30 sec	} 30 cycles
Annealing	55 °C 30 sec	
Elongation	72 °C 45 sec	
Elongation	72 °C 10 min	

Introduction of restriction sites by gradient PCR. A third PCR was performed to introduce restriction sites for restriction endonucleases SacII, Sal I, Kas I and BssHII (New England Biolabs, Germany) for the heavy and the light chain, respectively. All reagents used for these PCRs were provided from NEB. The annealing temperatures for the gradient were primer-specific.

Phusion PCR reaction (20 µl)

4 µl 5X GC reaction buffer
 0.2 mM dNTPs
 0.5 µM forward primer
 0.5 µM reverse primer
 0.2 µl Phusion DNA polymerase (1.0 unit/50 µl PCR)
 20 ng template
 0.6 µl DMSO

PCR program

Denaturation 98°C 30 sec

Denaturation	98 °C 15 sec	} 35 cycles
Annealing	primer specific	
Elongation	72 °C 45 sec	
Elongation	72 °C 10 min	

Rat MOG. The construct for the full length rat MOG was ordered at Eurofins MWG GmbH (Germany) (NCBI reference sequence: NM_022668.2). The construct was designed with restriction sites for the endonucleases XhoI and EcoRI and subcloned into the pEGFP-N1 vector (CLONTECH Laboratories, Mountain View, CA).

Recombinant hMOG. The construct for recombinant hMOG was ordered at Eurofins MWG GmbH (Germany). It contained the extracellular domain of wild type (wt) hMOG which was

connected via a flexible 11-amino acid linker GSGMGMGMGMM, from (O'Connor, McLaughlin et al. 2007) to a C-terminal Avi-tag sequence (GLNDIFEAQKIEWH), used for site-specific biotinylation, and a poly-His-tag sequence. It was digested with the restriction endonucleases NheI and NotI and subcloned into the pTT5 expression vector.

2.2.1.3 Agarose gel electrophoresis

Agarose gels were prepared by dissolving agarose powder (Biozyme, Germany) in TAE buffer. For visualization of DNA under UV ($\lambda = 254\text{-}366\text{ nm}$) SYBR Safe (Life Technologies, Germany) 1:10000 or ethidium bromide ($1\mu\text{g/ml}$) were added. The percentage of the gel depended on the size of the analyzed DNA product and ranged from 1-2 %. DNA samples were mixed with gel loading dye (6x) (Serva, Germany), and loaded on the gel. The size of the samples was determined by comparison with a molecular weight standard (peqGOLD 50bp, Peqlab, Germany; Gene Ruler 100bp and 2-LoG-ladder, NEB, Germany).

2.2.1.4 DNA extraction from agarose gel

DNA fragments of interest were cut out from the gel with a scalpel and extracted by using the QIAquick GelExtraction Kit or the QIAquick PCR Purification Kit (Qiagen) in accordance to the protocol provided by the manufacturer.

2.2.1.5 Determination of DNA quantification

DNA was quantified by using a Nanodrop spectrophotometer (Peqlab). A blank measurement was done with the DNA TE buffer (Qiagen) or with water, afterwards, $1\mu\text{l}$ of the DNA sample was loaded for photometric measurement at 260 nm to determine DNA concentration and purity.

2.2.1.6 Restriction digest

Restriction endonucleases cleave DNA at a specific recognition site. All restriction enzymes were used according to the protocol provided from the manufacturer. 1 U of enzyme corresponds to the amount required to cleave $1\mu\text{g}$ of DNA in 1 hour in a total volume of $20\mu\text{l}$.

2.2.1.7 Ligation of DNA

Ligation was performed by using the T4 DNA Ligase (NEB) and following the instructions of the manufacturer. 50 ng of vector and a molar ratio of 1 (vector) to 3 (insert) were used. Reactions were carried out for 1-3 hours at RT or overnight at 16°C .

2.2.1.8 Sequence analysis of DNA

All DNA samples were sent for sequencing to the sequencing facility of the LMU Biocenter (Martinsried, Germany).

2.2.2 Microbiological methods

2.2.2.1 Transformation of competent bacterial cells by heat shock

Competent *E. coli* DH5 α or purchased NEB 5-alpha Competent *E. coli* (High efficiency) (NEB) were used for plasmid amplification. For the transformation of competent *E. coli* DH5 α , 300 ng of plasmid were used to transform 50 μ l of thawed bacterial cells. Cells were incubated for 20 minutes on ice and then heat-shocked for 90 seconds at 42 °C. This was followed by a incubation for 5 minutes on ice. 400 μ l of LB medium was added and cells were put on a shaker at 150 rpm for 30 minutes at 37 °C. Afterwards, 200 μ l of cells were plated on a LB-Amp or LB-Kan agar plate and incubated overnight at 37 °C. The rest of the bacterial culture was stored at 4 °C. LB medium (for 1 L in water) consisted of: 10 g Bacto-tryptone (BD Biosciences, Germany), 5 g yeast extract (BD Biosciences), and 10 g NaCl (Sigma-Aldrich, Germany); it was brought to pH 7.5 using NaOH and sterilized by autoclaving. For LB-agar, 15 g of agar were dissolved in 1L of LB and sterilized by autoclaving. For LB-Amp agar, ampicillin (Sigma-Aldrich) was added to a final concentration of 100 μ g/mL, while for LB-Kan agar, kanamycin (Sigma- Aldrich) was added to a final concentration of 50 μ g/ml. 20 mL of LB agar was poured onto 10 cm culture plate (Greiner, Germany) for casting and the plates were stored at 4 °C until use. The transformation of NEB 5-alpha Competent *E. coli* (High efficiency) (NEB) was performed according to the manufacturer's protocol with the following modifications: 10 ng of plasmid or 3 μ l of ligation product were added to 30 μ l of thawed bacterial cells. Next steps were performed as indicated and cells were recovered by adding 200 μ l of room temperature SOC medium (Invitrogen). Cells were placed on a shaker at 250 rpm for 30 minutes at 37 °C and then plated on LB agar plates.

2.2.2.2 Plasmid DNA purification from bacterial cells

Plasmid DNA was purified from *E. coli* by using Miniprep, Midiprep and Maxiprep kits (Qiagen) and by following the protocol provided from the manufacturer. The resulting plasmid DNA was sent for sequence verification, used for further cloning procedures or cell transfection.

2.2.3 Cell biological methods

2.2.3.1 Cell culture of HeLa cells

HeLa cells were cultivated in T75 cell culture flasks (BD Biosciences) at 37 °C and 10% CO₂. Cells were passaged every 48 hours at a 1:10 ratio. In detail, cell culture medium was removed, cells were washed with 10 ml PBS (Invitrogen) and 2 ml Trypsin-EDTA (Invitrogen) were added. Cells were incubated for 5-10 minutes at 37 °C and trypsinization was neutralized by adding 8 ml of culture medium.

HeLa culture medium**Dulbecco's modified Eagle Medium (DMEM) (Invitrogen)**

10 % fetal calf serum (FCS) (Gibco)
1 % Penicillin/Streptomycin (Gibco)

2.2.3.2 Cell culture of HEK 293 EBNA 1 cells

HEK 293 EBNA 1 cells were cultured in suspension in an incubator (Multitron Pro) with humidified atmosphere at 37 °C, 8 % CO₂ and 110 rpm. Cells were passaged every 48-60 hours to a density of 200.000 cells/ml.

HEK 293 EBNA 1 culture medium**Freestyle 293 Expression medium (Gibco)**

1 % Pluronic F-68 10 % (Gibco)
25 µg/ml Geneticin G418 (Gibco)

2.2.3.3 Cell count and viability

Cell count was determined by using a Neubauer improved hemocytometer (Marienfeld-Superior). The cell suspension was diluted with 0.05 % Trypan blue solution and then the number of cells in four big quadrants was counted. Trypan blue is able to pass through the membrane of dead cells and allows therefore the determination of the number of living cells. The average of counted cells was multiplied by the dilution factor and by 10⁴ in order to determine the number of cells/ml.

Trypan blue solution

0.4 % Trypan blue (Sigma-Aldrich)
1X PBS (Invitrogen)

2.2.3.4 Isolation of human peripheral blood mononuclear cells (PBMC) by density gradient centrifugation

Fresh blood was obtained from adult healthy volunteers and from adult patients of the outpatient clinic of the Institute of clinical Neuroimmunology of the Klinikum Großhadern (Munich, Germany). The blood was collected in 9 ml EDTA tubes (Sarstedt) in order to prevent clotting. PBS and blood were mixed in a 1:1 ratio in a 50 ml Falcon tube (BD) and then transferred to a second Falcon tube containing 15 ml Pancoll (human Pancoll density 1.077 g/l PanBiotech). Samples were centrifuged at 4 °C for 35 minutes at 400 g without break. After centrifugation, erythrocyte sediment on the bottom layer while plasma and PBMC are on the top of the Pancoll layer. Plasma was carefully removed and stored at – 20 °C. PBMCs were transferred to a new 50 ml Falcon tube, washed by adding 20 ml of PBS and centrifuged at 4 °C for 10 minutes at 300 g. This process was repeated three times. Afterwards, cells were counted and frozen in 5x10⁶ cell aliquots at -80 °C in freezing medium (FCS, 10 % DMSO). Cells were transferred to liquid nitrogen for long term storage.

2.2.3.5 Isolation of murine splenocytes

Spleens from wt and transgene Th (IgH^{MOG}) C57BL/6 mice were kindly provided by Dr. Kerstin Berer. Th mice were used because the BCR of their B cells carries a rearranged heavy chain of a MOG-specific antibody (Litzenburger, Fässler et al. 1998). To prepare a single cell suspension of spleen cells, the spleen was put into a cell strainer (BD) which was localized on the top of an empty 50 ml Falcon tube. Spleens were mashed through the strainer into the tube by using the plunger of a 20 ml syringe (BD). Plunger and cell strainer were rinsed by adding 5 ml of RPMI complete medium. This procedure was repeated three times. Cells were centrifuged at 400 g for 7 minutes. Supernatant was discarded and erythrocytes were lysed by incubating the cell pellet in 2.5 ml ACK lysing buffer for 2 minutes. As a next step, 45 ml of RPMI complete medium were added and the cells were centrifuged at 400 g for 7 minutes. The cell pellet was suspended again in RPMI complete medium. This procedure was repeated three times. Cells were counted, suspended in freezing medium (FCS, 10 %DMSO) and stored in 5x10⁶ aliquots at -80 °C.

RPMI complete medium

RPMI-1640 Medium (Invitrogen)

10 % FCS (Gibco)
1 % Penicillin/Streptomycin (Gibco)
1 % Sodium Pyruvate (Gibco)
1 % Non-essential Amino Acids (Gibco)
10 mM L-glutamine (100mM, Gibco)

10x ACK lysing buffer

1.5 M NH₄Cl
100 mM KHCO₃
10 mM Na₂EDTA

2.2.3.6 Human B cell stimulation with Resiquimod and IL-2

Naive human B cells were stimulated in order to obtain Ig-secreting cells. PBMCs from healthy donors or from patients were suspended in RPMI complete medium at a concentration of 300.000 cells/ml. Resiquimod (R848, Sigma-Aldrich) and recombinant human IL-2 (R&D) were added at a concentration of 2.5 µg/ml and 1000 UI/ml, respectively (Pinna et al, 2006). Cells were cultivated for 7 and 10 days at 37 °C, 5 % CO₂.

2.2.4 Isolation of human B cells

Human B cells were isolated from fresh PBMC by using the B-cell isolation kit (Miltenyi Biotec). Isolation was performed according to the instructions provided by the manufacturer.

2.2.5 Recombinant protein expression

2.2.5.1 *Optimization of the expression of hMOG on HEK and HeLa cell*

The expression of MOG on HEK and HeLa cells was tested by using two different transfection reagents: Lipofectamine 2000 (Invitrogen) and FuGene (Promega). HeLa and HEK cells were seeded in a 96 well culture dish (BD) at a density of 0.25×10^6 cells/ml and 0.35×10^6 cells/ml respectively. After 24 h cells were transiently transfected according to the instruction of the manufacturer. In detail, for the transfection with Lipofectamine 2000, 25 μ l of Optimem transfection medium (Invitrogen) were mixed with either 100 or 200 ng DNA. In a second tube, the same amount of Optimem was mixed with 0.5 μ l Lipofectamine 2000 (1:50 ratio). The mixtures were incubated separately for 5 minutes, after that the Lipofectamine mixture was added to the DNA mixture followed by an incubation time of 20 minutes at room temperature (RT). The cell medium was completely removed and the transfection mixture was added to the cells for 2 h at 37 °C. As a next step, the transfection mixture was completely replaced by fresh DMEM. The transfection was also performed in the presence of FCS by adding the transfection mixture directly to the cell culture medium. For the transfection with FuGene, DMEM and FuGene were mixed in a 1:15 ratio while in a second tube the same amount of DMEM was mixed for 5 minutes with 100 or 200 ng of DNA. As a next step, the content of the two tubes were mixed, incubated for 15 min at RT and added to the cells. For both transfection reagents, cells were also transfected with the pEGFP N1 vector (CLONTECH Laboratories) as a control.

2.2.5.2 *Generation of recombinant hMOG and IgG in the HEK 293 EBNA 1 cell line*

The extracellular domain of hMOG and the heavy and light chains of human IgG were expressed in serum free condition in suspension HEK 293 EBNA 1 cells (Durocher, Perret et al. 2002). Cells were adjusted for transfection to a density of 1×10^6 cells/ml. Polyethylenimine (PEI) transfection reagent (Polypro Transfection) and DNA were added separately to Optipro serum free transfection reagent (Invitrogen), mixed and incubated for 30 minutes at RT. 1 μ g DNA and 2 μ g PEI were used for 1 ml of cell suspension. Optipro was used in a volume corresponding to 1/10 of the cell suspension volume. The transfection mixture was added dropwise to the cell suspension. After 24 h incubation, Bacto TC Lactalbumin Hydrolysate (BD Biosciences) was added to a final concentration of 0.5 %.

2.2.6 Protein analysis

2.2.6.1 *Purification of recombinant protein by immobilized affinity chromatography (IMAC)*

His Trap HP columns (GE Healthcare) were used to purify recombinant hMOG and recombinant abs from the supernatant of HEK 293 EBNA 1 cells. The proteins carry a C-

terminal 6x His Tag which allows the binding to the nickel on the column. The culture supernatants were centrifuged at 400 g for 5 minutes at 4 °C, transferred to a new centrifuge tube and centrifuged again at 550 g for 20 minutes at 4 °C. As a next step, culture supernatants were filtered through a 0.22 µm filter (Merck Millipore) and concentrated at least threefold by using a Minimate TFF System (Pall Corporation) at a pressure of 200 kPa. Supernatants were dialyzed overnight at 4 °C against binding buffer (100 mM Na₂HPO₄, 500 mM NaCl, 10 mM imidazole, pH 7.4). For purification, the column was equilibrated with 10 column volumes binding buffer, then the sample was applied. Column was washed with 10 column volumes binding buffer and then bounded protein was eluted by performing a linear imidazole gradient from 10 mM to 1 M imidazole. Wash and elution fraction were analyzed by SDS-Page, the fractions containing the purified protein were pooled and dialyzed against PBS overnight at 4 °C. Human MOG carrying the C-terminal Avi Tag has a size of 21.3 kDa while the purified IgG has a size of 150 kDa.

2.2.6.2 *Enzymatic biotinylation of hMOG*

MOG was biotinylated by using the BirA biotin ligase Kit (Avidity) according to the instruction of the manufacturer. The final reaction mixture was incubated overnight at 30 °C. Free biotin was removed by using 3 K centrifugal filters (Merck Millipore) and the sample was suspended in PBS (Invitrogen Life Technologies). Biotinylated hMOG was used to perform the affinity purification of MOG abs, to screen patient sera by ELISA and to generate hMOG tetramers.

2.2.6.3 *Generation of human MOG tetramers*

Biotinylated MOG and fluorescently labeled streptavidin (Jackson Immuno Research) were incubated in a molar ratio of 4:1. The required volume of streptavidin was divided into six aliquots which were added one by one to the biotinylated MOG. Each aliquot was incubated in the dark at RT for 15 minutes. The efficiency of the tetramer generation was tested by staining splenocytes from Th (IgH^{MOG}) C57BL/6 mice (Litzenburger, Fässler et al. 1998).

2.2.6.4 *Sodium dodecyl sulfate polyacrylamide gel electrophoresis (SDS PAGE)*

Gel electrophoresis was performed by using 4-12 % Bis Tris gels (Invitrogen) and a Xcell Mini Cell electrophoresis chamber (Invitrogen) filled with NuPAGE MOPS SDS Running buffer (Invitrogen Life Science Technologies). Samples were prepared by adding to 1-2 µg of protein NuPAGE LDS sample buffer (Invitrogen Life Science Technologies) and, if electrophoresis was performed under reducing conditions, NuPAGE sample reducing agent (Invitrogen). The samples were then incubated at 95 °C for 5 minutes and then loaded on the gel. Electrophoresis was carried out at 130 V for 90 minutes.

10x NuPAGE MOPS SDS Running buffer	250 mM Tris 1.92 M Glycine 1 %(g/V) SDS
-------------------------------------------	-----------------------------------------------

2.2.6.5 *Determination of protein concentration*

Protein concentration was measured by using the Bicinchoninic acid (BCA) protein assay kit (Pierce, Rockford, USA) according to the instructions of the manufacturer.

2.2.6.6 *Protein detection by Coomassie blue staining*

After gel electrophoresis, gels were incubated on a shaker for 15 minutes with Coomassie blue staining solution (0.1 % Coomassie brilliant-blue R-250, 40 % methanol, 10 % acetic acid) followed by incubation for 1 hour with destain solution (50 %methanol, 7 % acetic acid). Destain solution was changed from time to time. Gel was stored overnight in a 7 % acetic acid solution at RT.

2.2.6.7 *Mass spectrometry*

Bands of interest were analyzed by mass spectrometry. Bands were cut out from the gel with a scalpel and stored in 100 µl of water at -4 °C. Mass spectrometry analysis was performed at the core facility of the LMU.

2.2.6.8 *Antibody purification by protein G*

IgG from HC were purified by using a HiTrap Protein G column (GE Healthcare). Human plasma was centrifuged at 4000 g for 20 minutes at 4 °C and then filtered through a 45 µm filter (Merck Millipore). Dialysis against binding buffer (20 mM Sodium Phosphate, pH 7.4) was carried out at overnight at 4 °C by using a 50 k cutoff dialysis tube (SpectrumLabs, Germany). The column was equilibrated with 10 column volumes binding buffer, sample was loaded and unbound protein was removed by washing the column again with 10 column volumes binding buffer. Bound IgG was eluted with elution buffer and immediately neutralized with 1 M Tris-HCl pH 8.8. The eluted fractions were concentrated with Amicon Ultra centrifugation filters (Merck Millipore) and dialyzed against PBS overnight at 4 °C. After testing their binding to MOG, purified abs were frozen in small aliquots at 4 °C.

IgG elution buffer, pH 2.5, 1x	100 mM Glycine 150 mM NaCl
---------------------------------------	-------------------------------

2.2.6.9 *Affinity purification of MOG-specific antibodies*

Biotinylated hMOG was diluted at a concentration of 1 mg/ml in solubilization buffer. A prepacked HiTrap Streptavidin HP column (GE Healthcare, Munich, Germany) was washed with 10 column volumes solubilization buffer, afterwards the protein was loaded on the column at a flow rate of 0.5 ml/min. Plasma samples were prepared as follows: plasma was

thawed and placed on a magnet stirrer. Slowly an equal amount of a saturated ammonium sulfate solution (4.1 M, pH 7.4) was added until the solution became cloudy. After 1 hour incubation at RT the antibody/ammonium sulfate solution was centrifuged at 8000 g for 30 minutes at 4 °C. Pellets were dissolved in 30-50 ml PBS and transferred to 50 k cutoff dialysis tubes (SpectrumLabs). Tube was placed into PBS and dialysis was carried out at 4 °C without stirring for the first 24 hours. Afterwards PBS was changed and dialysis was continued for another 48 hours at 4 °C with stirring. The dialyzed material was centrifuged at 8000 g at 4 °C for 1 hour, filtered with a 0.45 µm filter (Merck Millipore) and diluted 1:10 in 10x solubilization buffer. The sample was loaded on the column in rotation overnight at 4 °C at a flow rate of 0.5 ml/min. The column was washed again with 10 column volumes solubilization buffer. The next steps were carried out as described in section 2.2.6.8

Solubilization buffer, pH 7.4, 1x

150 mM NaCl
6 mM Tris base
3 mM Tris-HCl
1 % Octyl- β-D-glucopyranoside

2.2.7 Patient material

The detection of MOG-specific abs and the recognized epitopes on MOG were performed by using sera from patients and healthy donors. Sera were provided by the medical staff of the Institute of clinical Neuroimmunology of the Klinikum Großhadern (Munich, Germany).

Original samples were stored at -80 °C while working aliquots of 50 µl were stored at -20°C. PBMC and plasma were obtained from 20-500 ml volume blood after performing a density gradient centrifugation (described in section 2.2.3.4).

2.2.8 Immunological methods

2.2.8.1 Serum screening by FACS

Autoantibodies against conformational-intact MOG were detected by performing a cell-based flow cytometry assay (Spadaro and Meinel 2016). HeLa cells were transiently transfected with full length hMOG fused C-terminally to the EGFP N1 (CLONTECH Laboratories, Mountain View, CA) vector or with EGFP alone (control cells). 24 hours after transfection, cells were plated in a 96 well FACS plate at a density of 50.000 cells/ well. Cells were pelleted by centrifugating them at a speed of 400 g for 5 minutes. Control and MOG-transfected cells were incubated with 100 µl of a 1:50 dilution of each serum and incubated for 45 minutes at 4 °C. As a next step, cells were washed three times with 150 µl PBS/ 1 % FCS. MOG-specific IgG was detected with 100 µl of a 1:500 dilution of a biotin-SP-conjugated goat anti-human IgG (Jackson ImmunoResearch, West Grove, PA, USA). Cells were incubated for 30 minutes at 4 °C. After three washing steps, cells were incubated with 100 µl of a 1:2000 dilution of

Alexa Fluor® 647-conjugated Streptavidin (Jackson ImmunoResearch, West Grove, PA, USA) and incubated in the dark for 30 minutes at 4 °C. After three washes, dead cells were stained with 100 µl of propidium iodide (Sigma-Aldrich) diluted 1:2000 in PBS. FACS analysis was performed on a BD FACSVerse flow cytometer and data was analyzed with FlowJo (Tree Star Inc., Ashland, USA). The mAb 8-18C5 was used as a positive control at a concentration of 0.5 µg/ml. The same protocol was used for the determination of the recognized epitopes on MOG. In this case sera were incubated with different MOG mutants already available in our laboratory. Binding percentage was calculated as $\text{mean fluorescence intensity (MFI) (mutant)} - \text{MFI (EGFP only)} / \text{MFI (wt hMOG)} - \text{MFI (EGFP only)} \times 100\%$ as described in (Mayer, Breithaupt et al. 2013).

2.2.8.1.1 Isotyping by FACS

The isotype of the MOG-specific autoantibodies was determined by performing the assay as described in section 2.2.8.1. Instead of the biotin-conjugated anti-human IgG antibody, the following abs were used: mouse anti-human IgG1 (Fc)-BIMA (1:500, Clone HP 6001), mouse anti-human IgG2 (Fc)-EIOT (1:500, Clone 31-7-4, Southern Biotech), mouse anti-human IgG3-BIOT (1:500, Clone HP 3050, Southern Biotech), mouse anti-human IgG4-BIOT (1:500, Clone HP 6025, Southern Biotech), biotin-SP-conjugated anti-human IgA (1:500, Jackson ImmunoResearch) and allophycocyanin-labeled anti-human IgM (1:10, Clone: SA-DA4, eBioscience San Diego, CA).

2.2.8.2 Serum screening by streptavidin ELISA

Sera were also screened for reactivity against recombinant MOG by ELISA. After enzymatic biotinylation, hMOG was diluted in PBS at a concentration of 3 µg/ml and immobilized on a streptavidin coated 96 well plate (Nunc, Thermo Scientific) for 2 hours at room temperature on a shaker. Each well was then washed three times with 200 µl PBS/ 0.05 % Tween (PBST) and incubated at 4 °C overnight with 100 µl of a 1:100 dilution of each sera. After three washes, each well was incubated with 100 µl of a 1:5000 dilution of a horseradish peroxidase labeled goat anti-human IgG (Jackson Immuno Research) in the dark for 1 hour at RT on a shaker. After washing, 100 µl of TMB (Sigma-Aldrich) were added and the reaction was stopped after 7-8 minutes by using 50 µl of 1 M sulfuric acid. Optical density was measured with a Victor2 plate reader (Perkin Elmer Life Sciences) at 450 nm and 540 nm for plate background. Data was analyzed by using PrismGraphPad (La Jolla, USA). For comparison between streptavidin coated plates and maxisorp plates, serum was diluted 1:200 and wells containing BSA were used as negative control. The anti-MOG reactivity was calculated as follows: $\Delta\text{OD (450 nm-540 nm)}$. For sera screening sera from patients and HC were diluted 1:100 and wells containing streptavidin without hMOG were used as negative controls. The anti-MOG reactivity was calculated as $\Delta\text{OD (streptavidin + hMOG)} - (\text{streptavidin only})$.

2.2.8.3 Quantification of antibodies by ELISA

The purified abs and the supernatants of stimulate B cells were quantified by human IgG and IgM ELISA development kit (Mabtech) according to the protocol of the manufacturer. Maxisorp plates (Nunc, Thermo Scientific) were coated with a MT145 antibody or a monoclonal anti-IgM antibody diluted to 2 µg/ml in PBS and incubated overnight at 4 °C. Wells were washed twice with 200 µl PBS and blocked by adding 200 µl/well of incubation buffer (PBS with 0.05% Tween, 0.1% BSA) for 1 hour at RT. Wells were washed five times with PBST and incubated for 2 hours at RT with 100 µl of serial dilutions of human IgG or IgM standard solutions (7.8 ng/ml to 500 ng/ml in PBS) and antibody samples. Elution and wash fractions were diluted 1:100 and 1:200, plasma and flow through were diluted 1:1000 and then 1:50 and 1:100. The supernatants of not stimulated and stimulated B cells were diluted respectively 1:2 and 1:80. After washing, wells were incubated for 1 hour at RT with 100 µl of MT78-ALP or anti-IgM-ALP detection antibody diluted 1:1000 in incubation buffer. Wells were again washed and 100 µl/well of pNPP substrate (Sigma-Aldrich) was added. Optical density was measured at 405 nm after suitable developing time.

2.2.8.4 Binding activity of purified abs by FACS

Binding of affinity purified abs to MOG was tested by performing the CBA described in section 2.2.8.1 with the following modifications: 50.000 HeLa cells transfected with human, mouse and rat MOG were incubated with 50 µl of eluted sample diluted in PBS/1 % BSA to a final concentration of 12 µg/ml. Plasma, wash fraction and flow through were tested at the same concentration.

2.2.8.5 Binding activity of affinity purified and recombinant antibodies by ELISA

Affinity purified and recombinant abs were also tested by ELISA. In detail, maxisorp plates (Nunc, Thermo Scientific) were coated overnight at 4 °C with 100 µl/well of recombinant human, mouse and rat MOG diluted in coating buffer (100 mM sodium carbonate, pH 9.5) to a final concentration of 10 µg/ml. Each well was washed three times with 200 µl PBST (PBS with 0.05 % BSA) and then incubated with 100 µl blocking buffer (3 % BSA in PBS) for 2 hours at RT. After washing three times, each well was incubated for 2 hours at RT with the samples diluted in incubation buffer (0.5 % BSA in PBS). Affinity purified abs were tested at a concentration of 6 µg/ml and 12 µg/ml while recombinant abs were serial diluted from a concentration of 50 µg/ml to 1 µg/ml. The next steps were carried out as described in section 2.2.8.2. The same protocol was used to perform saturation binding experiments to determine antibody K_D values. Affinity purified and recombinant abs were used at a concentration ranging from 10 to 160 nM and 6.6 nM to 8000 nM, respectively. Negative controls were used at the same concentrations. To determine the K_D values, saturation binding data were analyzed with GraphPad Prism 7 using nonlinear regression analysis.

2.2.8.6 Western Blot

Proteins were separated by SDS-Page and then transferred by semidry electroblotting (60 mA, 90 minutes, Bio-Rad) onto a PVDF membrane, which was first activated in 100 % methanol. The membrane was blocked in 5 % skim milk in 0.05 % PBST at RT for 1 hour and then incubated with the abs HRP-anti-His (Sigma- Aldrich), at a dilution of 1:1000 and HRP-anti-human IgG (Jackson ImmunoResearch), at a dilution of 1:2500, at RT for 1 hour. The membrane was washed three times in 0.05 % PBST and bound HRP-conjugates were visualized by adding enzymatic chemiluminescence (ECL, GE Healthcare) for 1 minute. Visual analysis was performed with Odyssey ® CLx Imaging System (LI-COR Biosciences).

2.2.9 Single cell sorting of MOG-binding B cells

First, human B cells isolated from fresh PBMC were stained with PE-CD19 (BD Pharmingen), PE-Cy7-CD27 (eBioscience), V450-IgM (eBioscience) and APC-hMOG tetramer. Subsequently CD19+CD27+IgM-MOG-binding B cells were sorted as single cells by using a BD FACSAria™ 2 flow cytometer. In vitro differentiated MOG-specific B cells were stained with PE-CD19 (BD Pharmingen), PE-Cy7-CD27 (eBioscience), V450-CD38 (eBioscience) and a FITC-mMOG tetramer. MOG tetramers were used at a concentration range of 0.150 ng-1 µg/ml. Single cell sorting was performed in collaboration with Dr. Markus Moser at the Max Planck Institute for Biochemistry.

2.2.10 Immunohistochemistry

For neuropathological analysis tissues were fixed in 4 % phosphate buffered paraformaldehyde and routinely embedded in paraffin. Paraffin sections were stained with hematoxylin & eosin, Luxol fast blue myelin stain and Bielschowsky silver impregnation for basic neuropathological classification. Serials section were then stained by immunocytochemistry with antibodies against the following targets: CD3 (RM 1907S, Neomarkers), CD8 (M7103, DAKO), CD20 (MS 340S, Neomarkers), CD68 (MO814, DAKO), p22phox (sc-20781, Santa Cruz), MOG (8-18C5, gift from C. Linington, Glasgow), PLP (MCA 839G, Serotec), CNPase (SMI91, Sternberger Monoclonals), Neurofilament (AB 1981, Chemikon), GFAP (Z=334, DAKO), Aquaporin 4, Aquaporin 1 (sc 20810, Santa Cruz), human immunoglobulin (RPM 1003, Amersham) and activated terminal complement (C9, C9neo, rabbit polyclonal and mouse monoclonal B7; gift from P. Morgan, Glasgow). Immunocytochemistry was performed with a biotin avidin peroxidase technique as described in (Fischer, Wimmer et al. 2013). Prof. Hans Lassmann performed the histopathological analysis of human biopsy tissue sections, rat brain and spinal cord and provided the information for this text. For binding of human affinity purified or recombinant IgG to rat MOG, rat brains were fixed in 4 % paraformaldehyde (PFA) for 1 hour, cryoprotected with 40 % sucrose for 48 hour, and snap frozen in chilled isopentane. Seven micron thick sagittal

sections were incubated with 0.3 % hydrogen peroxide for 20 minutes, with 10 % donkey serum in PBS for 1 hour, and then labeled with patient or control sample (1:200) at 4 °C overnight. The next day, sections were labeled with a donkey-anti-human secondary antibody (1:2000) for 2 hours at RT and visualized with an avidin-biotin-diaminobenzidine (DAB) reaction. Analysis was performed by Prof. Romana Höftberger who provided the information for this text.

2.2.11 Animal experiments

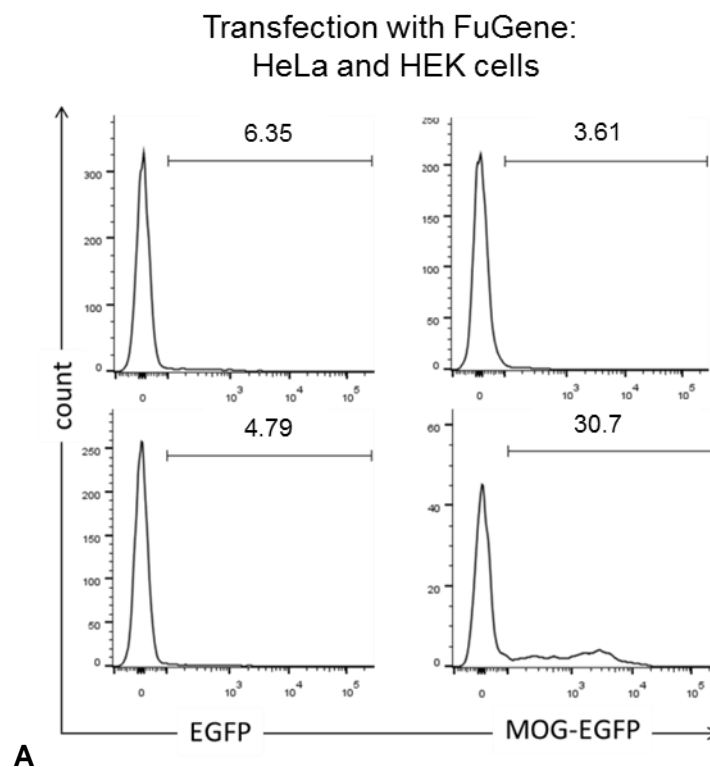
MOG-specific T cell lines were generated using antigen-primed donors. To induce mild EAE, freshly restimulated MOG-specific T cells were injected intravenously (i.v) in Lewis rats. Clinical scores were evaluated as follows: 0 = normal; 0.5 = loss of tail tonus; 1 = tail paralysis; 2 = gait disturbance; 3 = hind-limb paralysis; 4 = fore-limb paralysis; 5 = moribund. Two days after EAE induction, the following abs were injected intrathecally (i.t) : 90 µg of affinity purified patient abs and IgG from a healthy donor used as negative control, 500 µg of the recombinant ab r2246_D7 and the negative control AB3. The mAb 8-18C5 and the humanized r8-18C5 (Brändle, Obermeier et al. 2016) abs were used as positive controls, respectively. A mouse IgG1 antibody (eBioscience) was used as isotype control. For the monitoring of clinical score, animals were followed until full recovery and were then sacrificed. For subsequent immunohistochemical analysis, 72 hours after antibody injection, animals were perfused with PBS and 4 % PFA in PBS under terminal anesthesia; the spinal cord and brain were then postfixed with 4 % PFA in PBS at 4 °C. Animal experiments were performed by PD Dr. Naoto Kawakami who provided the information for this text.

3 Results

Parts of the following results were published in (Spadaro, Gerdes et al. 2015, Spadaro, Gerdes et al. 2016).

3.1 Optimization of the CBA for the detection of MOG-specific abs

The first aim of this study was to optimize the CBA for the detection of MOG-specific abs already established in our laboratory. To this end, the transfection reagents Lipofectamine and FuGene and the HeLa and HEK cell lines were compared. HeLa and HEK cells were transiently transfected with EGFP (control cells) or MOG-EGFP by using FuGene (Figure 4A) and Lipofectamine 2000 (Figure 4B and C) as transfection reagents. Since transfection is usually performed by using serum reduced medium, for the transfection with Lipofectamine 2000 we also tested the influence of FCS present in the cell culture medium on the transfection efficiency (Figure 4B and C).



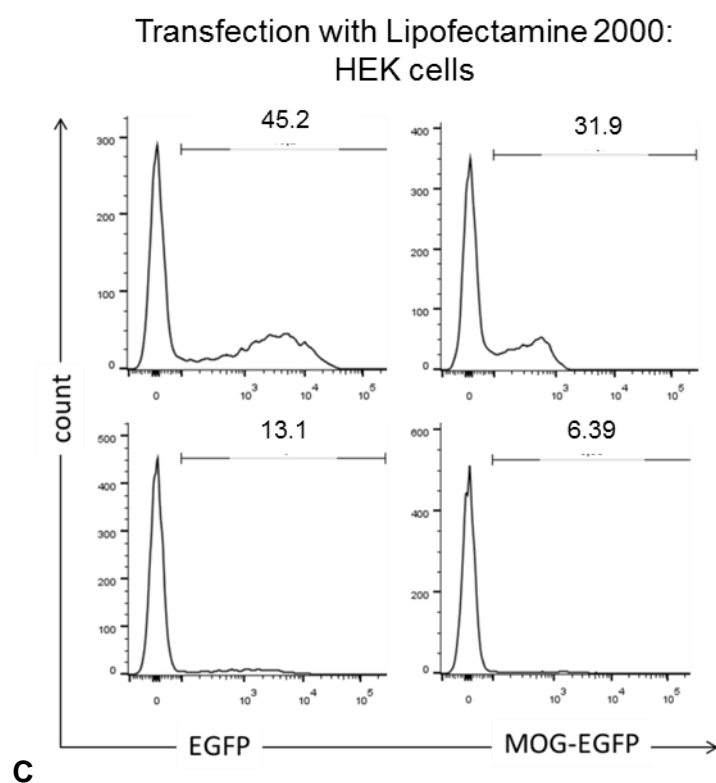
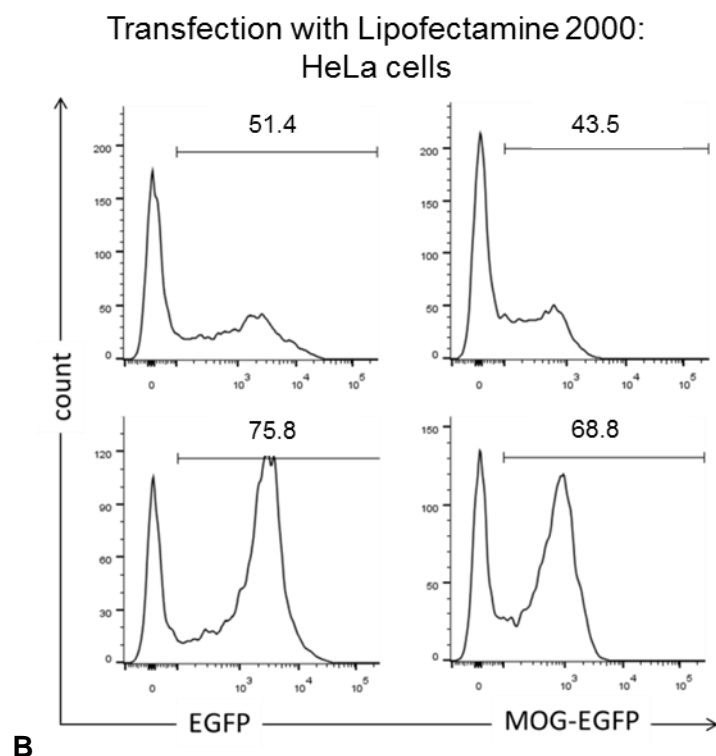


Figure 4: Optimization of transfection efficiency. Transfection efficiency of HeLa cells by using FuGene (A, upper histograms) or Lipofectamine 2000 (B) as transfection reagents and comparison with HEK cells (A, lower histograms and C, respectively). Transfection with Lipofectamine 2000 was also tested in the presence and absence of FCS in the culture medium (B for HeLa cells, upper and lower histograms, respectively and C for HEK cells). Numbers indicate the percentage of cells with a transfection efficiency >100 in the FITC channel.

The transfection efficiency was determined by gating on the cells showing a signal > 100 in the FITC channel. Cells transfected with FuGene showed an efficiency between 4.8 % and 30 %, and 6.3 % and 3.6 % for HEK and HeLa cells, respectively (Figure 4A). As expected, the use of Lipofectamine 2000 in the presence of FCS induced a reduction of the transfection efficiency (Figure 4B for HeLa cells and 4C for HEK cells). The highest transfection efficiency was obtained with HeLa cells transfected with Lipofectamine 2000 in the absence of FCS (Figure 4B, higher histograms). Therefore, we decided to use this protocol, which is described in detail in section 2.2.5.1. In order to determine the presence of anti-MOG abs, we increased the sensitivity of the assay: we used for our analysis only cells with a transfection intensity >500 in the FITC channel and acquired at least 30.000 events at the flow cytometer. The murine anti-MOG mAb 8-18C5 was used as a positive control (Figure 5).

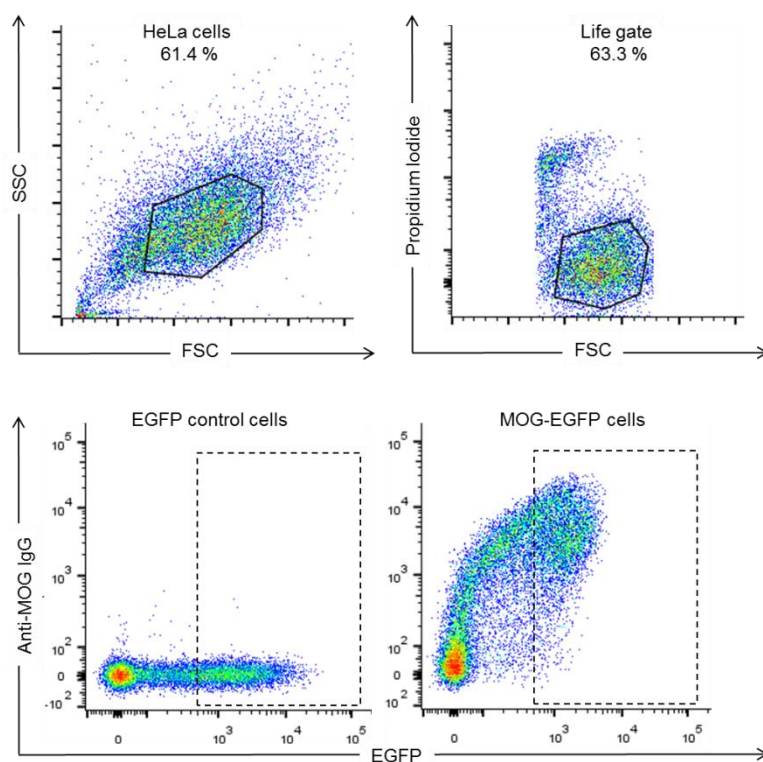


Figure 5: Gating strategies and validation with the 8-18C5 mAb. HeLa cells transfected with EGFP or hMOG-EGFP were incubated with the anti-MOG mAb 8-18C5. We gated on HeLa cells (upper plot, left) and excluded from our analysis the dead cells (upper dot, right). To quantify the anti-MOG reactivity, we set the gates on the cells expressing high levels of EGFP or hMOG-EGFP (dashed rectangle) and calculated the FACS ratio as MFI (MOG-EGFP)/ MFI (EGFP only).

3.2 Occurrence of abs against conformation-intact hMOG in adult patients

We used our CBA to screen sera from a total of 260 patients: NMOSD (n=18), ON (n=14), MS (n=104 including: RRMS n=94, SPMS n=4 and CIS n=6), encephalomyelitis (n=8), autoimmune syndromes (n=61) and with other forms of encephalomyelitis (n=55). Patients with non-inflammatory neurological diseases (NIND, n=45) and HC (n=39) were used as controls (Figure 6). The threshold for anti-MOG reactivity was set to the mean plus 3 SD of n=39 adult HC (Figure 6), which resulted in a FACS ratio of 2.27. The experiments were performed according to the protocol described in section 2.2.8.1. We found anti-MOG reactivity in a total of 17/260 (6.5%) patients, these included: 4/18 NMOSD patients, 4/14 ON patients, 5/94 RRMS patients and 4/8 patients with encephalomyelitis. None of the patients diagnosed with SPMS or CIS tested positive for anti-MOG abs. 53 % of the anti-MOG abs positive patients were female and 47 % male. The age at the time point of first sample collection was between 23 and 66 years. One patient with NMOSD (serum ID 2347), one with relapsing encephalomyelitis (serum ID 2144) and two HC showed a reactivity which was at the detection limit (FACS ratio 2.4 and 3.0, respectively). Also one patient of the NIND control group tested positive (FACS ratio 3.98). As shown in Table 6, patients with the highest anti-MOG reactivity were diagnosed with unilateral or bilateral ON, these patients showed in our CBA a FACS ratio ≥ 15 (Mean FACS ratio 67.08). 3 of the 17 patients who tested positive for anti-MOG abs, were also diagnosed with an autoimmune syndrome: two with familial mediterranean fever (FMF) and one patient with cryopyrin-associated autoinflammatory syndrome (CAPS).

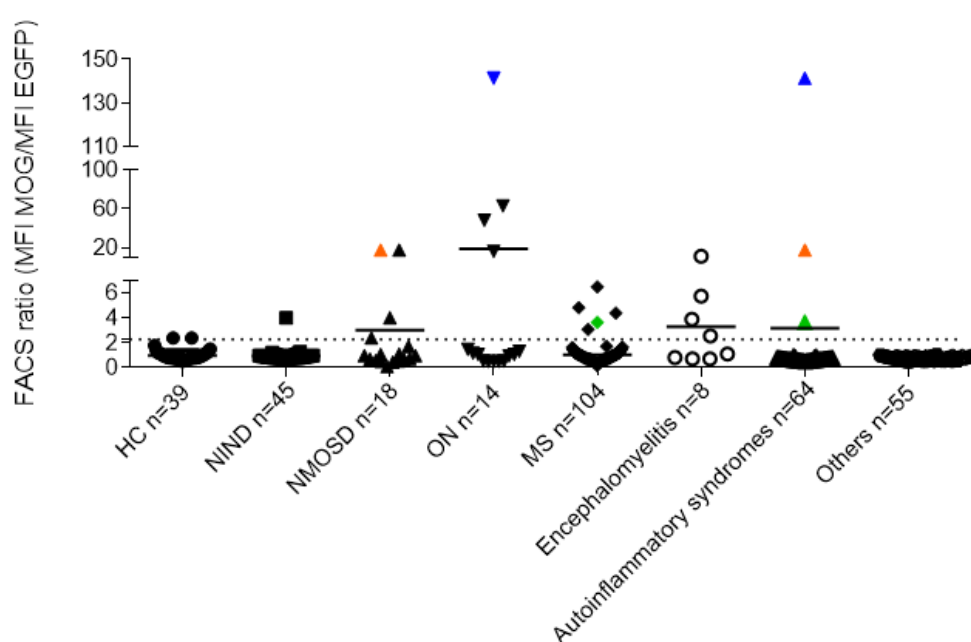


Figure 6: Anti-MOG reactivity by flow cytometry. Serum screening by FACS using hMOG included samples from patients with NMOSD (n=18), ON (n=14), MS (n=104), encephalomyelitis (n=8) and autoinflammatory syndromes (n=64). The dotted line indicates the cutoff for anti-MOG reactivity (2.27). Values for each anti-MOG IgG-positive patient represent the mean of ≥ 2 independent measurements. The three patients with anti-MOG abs and an autoinflammatory syndrome are indicated with the orange (serum ID 2215), blue (serum ID 1771) and green (serum ID 0211) symbols twice.

Therefore, in order to determine whether MOG-specific abs also occur in patients with these diseases, we screened additional 61 sera from patients with autoinflammatory diseases, none of them tested positive.

Table 6: Characteristics of patients with abs to MOG

ID	Disease	Gender	Therapy	Ratio*
2174	NMOSD	m	AZA	4,0
2347	NMOSD	f	RX	2,4
3278	NMOSD	m	AZA	17,15
2215	NMOSD/FMF	m	no	17,3
2246	Relapsing unilateral ON	m	AZA	62,9
3202	Relapsing bilateral ON	m	AZA	48,04
2816	Relapsing bilateral ON	f	AZA	15,90
1771	Relapsing bilateral ON/ CAPS	f	no	141,3
1819	Relapsing encephalomyelitis	f	RX	3,5
2144	Relapsing encephalomyelitis	m	Tocilizumab	3,0
724	Relapsing Encephalomyelitis	m	no	4,7
2471	Monophasic encephalitis	f	no	11,4
2169	RRMS	f	IFN	4,8
467	RRMS	m	NAT	4,4
558	RRMS	f	RX	6,5
2703	RRMS	f	NAT	3,1
0211	RRMS/FMF	f	RX	3,6

* $n \geq 2$ independent measurements. AZA: Azathioprine, RX: Rituximab, NAT: Natalizumab, IFN: interferon, FMF: familial Mediterranean fever, CAPS: cryopyrin-associated inflammatory syndrome.

3.2.1 Isotyping of MOG-specific abs

Sera containing anti-MOG abs, were further analyzed to determine the Ig subclasses IgG1-IgG4 and the IgM and IgA classes by using the procedures described in section 2.2.8.1. We identified the presence of the complement-activating IgG1 subclass in 8/17 patients (Figure 7). The full-length humanized r8-18C5 mAb (Brändle, Obermeier et al. 2016) was used as a positive control. This antibody contains the human IgG1- and κ - constant regions. The observation that we could not determine the IgG isotype in all 17 anti-MOG antibody positive

patients is in line with the fact that the polyclonal goat anti-human IgG secondary antibody that we used for serum screening is much more sensitive than the IgG subclass secondary abs. One NMOSD patient (serum ID 1771) tested also positive for anti-MOG IgM (see section 3.6.1 for additional details). None of the patients had anti-MOG abs belonging to the IgG2-4 subclasses or the IgA class.

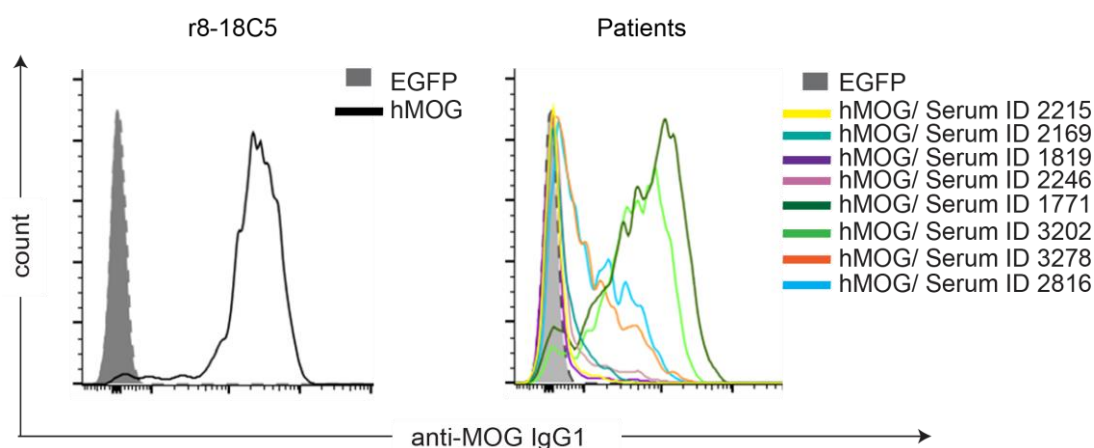


Figure 7: Isotype of MOG-specific abs. The abs responsible for anti-MOG reactivity were isotyped by flow cytometry (right). The humanized r8-18C5 mAb was used as a positive control (left). Anti-MOG reactivity was determined by the incubation of a 1:50 dilution of the sera with EGFP transfected control cells (closed gray graphs, shown here for one patient as an example) and hMOG-EGFP transfected cells (coloured lines). Sera were diluted 1:50, the r8-18C5 antibody was used at a 0.5 $\mu\text{g/ml}$ concentration.

3.2.2 Epitope mapping on conformation-intact MOG

The 17 sera with anti-MOG abs were also analyzed for epitope specificity. Six variants of human MOG were previously generated in our laboratory and used to investigate the antibody binding in a cohort of 111 pediatric patient sera (Mayer, Breithaupt et al. 2013). These constructs carry a C-terminal intracellular EGFP tag and include the not glycosylated variant of hMOG (N31D) and the mutants R9G/H10Y, P42S, R86Q, S104E and H103A/S104E. The amino acids that were exchanged in these constructs are localized at different loops of the protein (Figure 8A): P42 is localized on the CC' loop, H103 and S104 on the FG' loop, R9 and H10 at the AA' loop and R86 at the EF' loop. The transfection of HeLa cells with the different mutants showed a comparable efficiency (Mayer, Breithaupt et al. 2013), this allowed us to use them for the analysis and comparison of antibody binding. We used as positive controls the mouse mAb Z2 and the humanized r8-18C5. The humanized r8-18C5 antibody offered the advantage to use the same detection system as for human samples. Previous studies showed that different murine MOG-specific mAbs recognize different epitopes (Breithaupt, Schäfer et al. 2008, Mayer, Breithaupt et al. 2013): while the 8-18C5 antibody does not bind to the MOG variants containing the S104E

mutation, the Y11 antibody recognizes all MOG variants. We observed that the Z2 antibody has the same epitope pattern as the 8-18C5 antibody (Figure 8B).

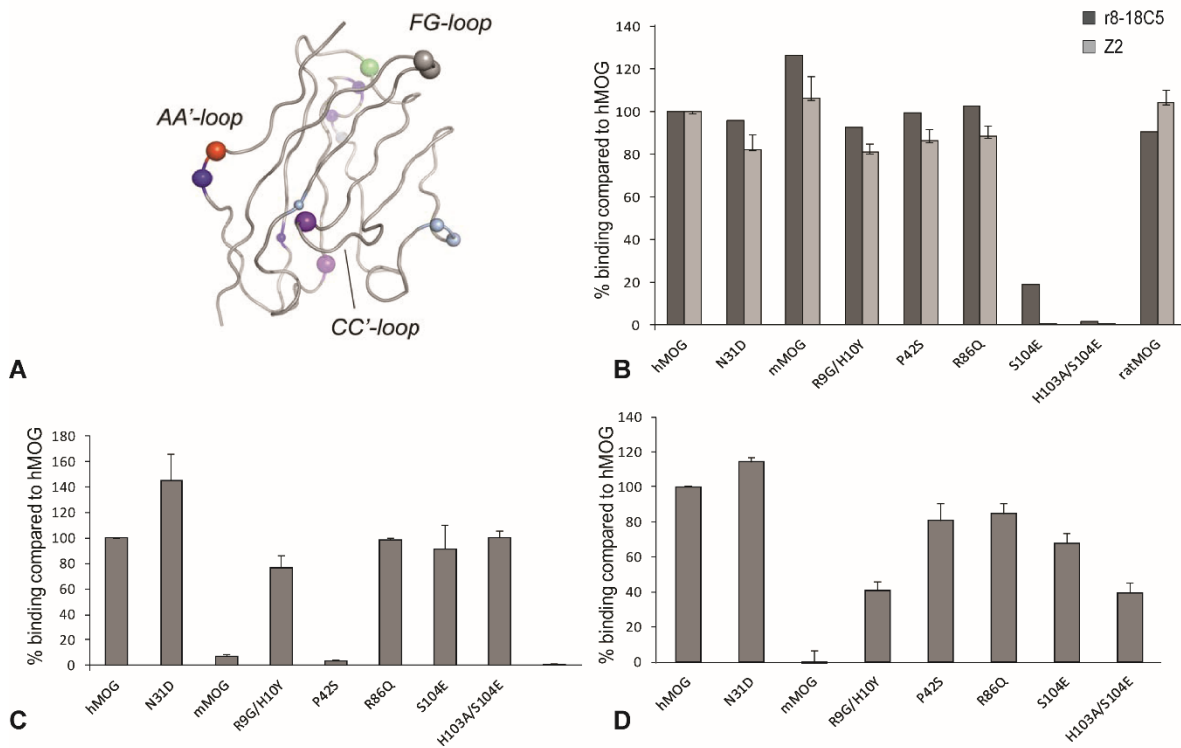


Figure 8: Epitope mapping on conformational-intact hMOG. Sequence conservation of mMOG and hMOG mapped onto the three-dimensional structure of mMOG: C α -atoms of residues that were mutated are shown as largest spheres: R9G/H10Y in red and blue, N31D greenish, H103A/S104E in gray, and P42S and R86Q in purple. C α -atoms of nonconserved residues, which were not mutated are shown as midsized spheres: G59A/D60E, D74E/A75T and G77S. These C α -atoms are highlighted in blue, indicating conservative amino acid differences between mMOG and hMOG. C α -atoms of non conserved residues with side chains located inside the protein are shown as small spheres: V20A and F98Y. Figure taken from (Mayer, Breithaupt et al. 2013), Copyright 2013, The American Association of Immunologists, Inc.(A); HeLa cells transfected with hMOG variants, mouse and ratMOG were incubated with a 0.5 μ g/ml concentration of the r8-18C5 or Z2 abs. Values obtained with wt hMOG were set at 100% and the other reactivities were calculated as described in section 4.2.2 (B); example of anti-MOG response directed against one epitope in one ON patient (serum ID 2816): binding to mutant P42S and to mMOG is >90% reduced (C); example of anti-MOG response directed against multiple epitopes in one encephalomyelitis patient (serum ID 2144): binding to mutants R9G/H10Y and H103A/S104E is reduced of a 50% while binding to mMOG is absent (D). Depicted are the mean values of ≥ 2 independent experiments \pm SEM.

In 40 % of our anti-MOG-IgG positive patients, the antibody binding was directed against only one single epitope. These patients included three of four ON patients, three of four NMOSD patients and two of five RRMS patients. The autoantibodies in the remaining 60 % showed a reactivity directed against multiple epitopes: one ON patient, one NMOSD patient, three RRMS patients and three encephalomyelitis patients had a reactivity which was directed against two different epitopes (either against loops FG' and CC', loops AA' and FG' or loops CC' and EF') (Figure 9A). The fourth patient with encephalomyelitis was the only one who showed an anti-MOG reactivity against three different epitopes (CC', AA' and FG'

loops) and will be described in detail in section 3.3. 13 of 17 patients showed a higher reactivity to the not glycosylated variant of MOG (N31D), one patient recognized this mutant at least as good as wt hMOG while the remaining three patients showed a lower binding (Figure 9B). In two of these three patients binding to the not glycosylated MOG was reduced to 50 % compared to wt hMOG while in the third patient the decreased binding was not significant. We observed a more than 2-fold higher reactivity also against other mutated variants of MOG: one encephalomyelitis patient showed an increased binding to the single mutant S104E and the double mutant H103A/S104E; one ON patient had a 6.4-fold higher reactivity against the P42S variant and a 5-fold higher reactivity against mouse MOG (mMOG). This patient will be described in more detail in section 3.6.1.

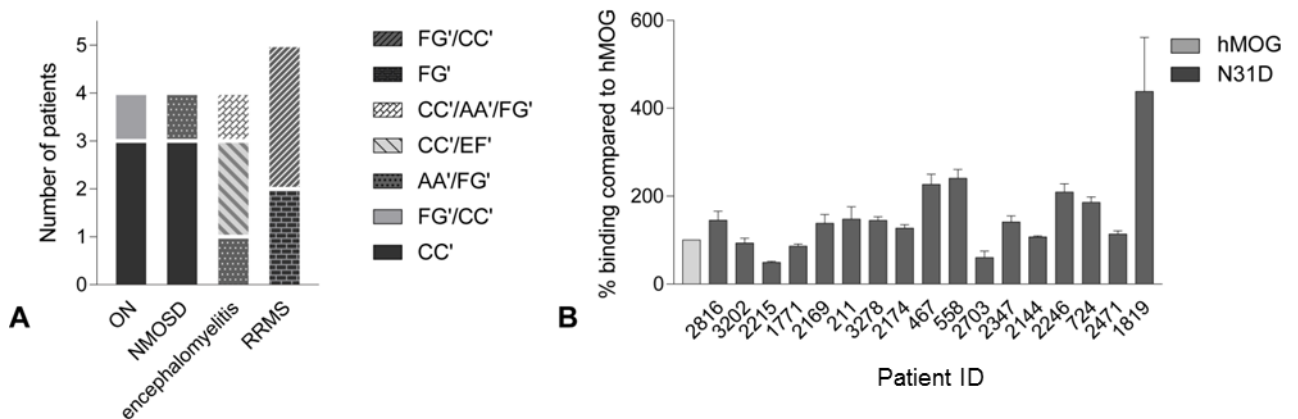


Figure 9: Recognized epitopes by anti-MOG abs positive patients. Anti-MOG response directed against the different loops on MOG (A); Binding percentage against the mutant N31D compared to the binding percentage against wild type hMOG (set to 100 %). Binding percentage was calculated as described in section 2.2.8.1. Depicted are the mean values of $n=3$ independent experiments \pm SEM.

3.2.3 Recombinant expression of rat MOG and binding of human sera

One aim of this study was to investigate the pathogenicity of human MOG-specific abs in animal models. Since these animal experiments were planned to be performed in an EAE model in the Lewis rat, we analyzed specifically also the cross-reactivity to rat MOG. A previous study in our laboratory with pediatric samples showed that only a minority of patients has MOG-specific abs that recognize rodent MOG (Mayer, Breithaupt et al. 2013). In order to determine in this study if sera from adult patients are reactive against mouse and rat MOG, HeLa cells were transiently transfected, according to the protocol described in section 2.2.8.1, with full length rat or mouse MOG-EGFP and the transfection efficiency was compared to that of hMOG-EGFP (Figure 10A). Surface expression and correct folding of rat MOG was evaluated with the mAbs 8-18C5 and Z2 (Figure 10B). Of the 17 sera that tested

positive for anti-hMOG reactivity, three (serum ID 1771, 2246 and 3202) showed also strong binding to rat MOG (Figure 10C). In these three sera we observed to rat MOG a mean FACS ratio of 53.8 ± 8.8 SEM compared to the mean FACS ratio of 1.6 ± 0.3 SEM observed in sera without anti-rat MOG abs. FACS ratio was calculated as described in section 2.2.8.1.

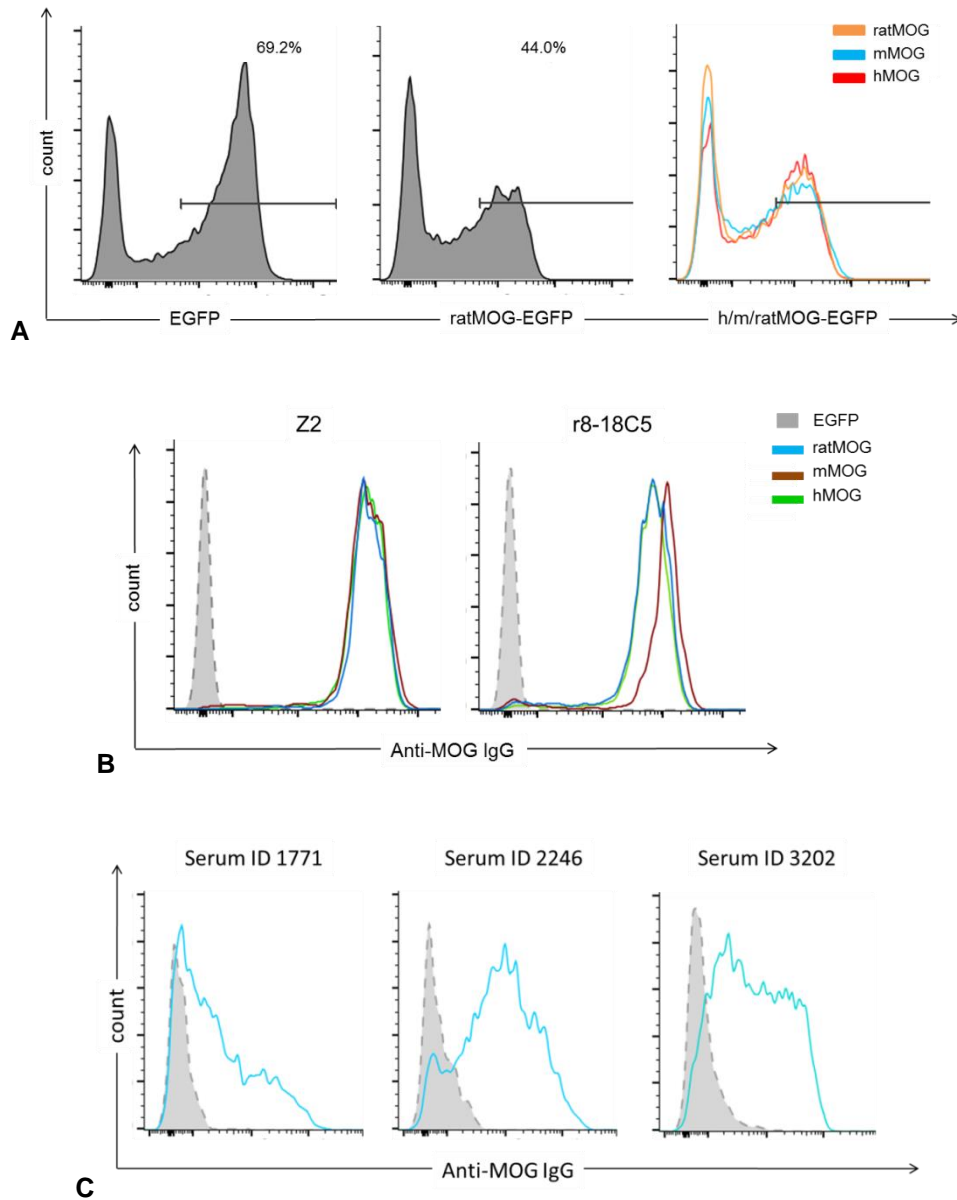


Figure 10: Reactivity to conformational-intact rat MOG. HeLa cells were transiently transfected with EGFP (control) and rat MOG-EGFP. Transfection efficiency was calculated by gating on cells with an EGFP signal >500 (A, left and middle); comparison of the transfection efficiency with hMOG and mMOG (A, right). Transfected HeLa cells were incubated with a concentration of $0.5\mu\text{g/ml}$ of the mAbs Z2 and r8-18C5 (B). Transfected HeLa cells were incubated with a 1:50 dilution of each serum. The MFI in the APC-channel was used to determine antibody binding and FACS ratio was calculated as previously described. Shown is one representative histogram of $n \geq 2$ independent measurements.

3.3 Histopathology and clinical course of MOG-associated encephalomyelitis

Among the four encephalomyelitis patients who showed anti-MOG reactivity in our CBA, we focused our attention on a 66-years old Caucasian woman (serum ID 1819). The clinical phenotype of this patient is summarized in Table 7. The performance of a brain biopsy, carried out to exclude a progressive multifocal leukoencephalopathy, allowed us to describe the histopathology.

Table 7: Clinical features in a patient with MOG-associated encephalomyelitis (index patient 1819).

	Similarities	Differences
MS	MS type II histopathology relapsing-remitting disease course	no oligoclonal bands no typical periventricular lesions
NMOSD	brainstem and spinal cord large lesion in the splenium	no LETM no optic nerve involvement

LETM: long extensive transverse myelitis.

3.3.1 Abs to MOG in index patient 1819

The anti-MOG abs of index patient 1819 had the complement-activating IgG1 isotype at months 19 (data not shown) and 32 (Figure 11A) after disease onset. There was no evidence for intrathecal production of MOG-specific abs (Figure 11B). We identified amino acids on MOG (R9/H10, P42, S104) as critical for antibody binding and noted that the not glycosylated MOG was recognized better than wt hMOG (Figure 11C-D). No cross-reactivity to murine MOG was observed (Figure 11C). This is consistent with the fact that mouse and rat MOG contain the mutant amino acids G9/Y10 and S42. The pattern of epitope recognition stayed constant over time (Figure 11D). We performed longitudinal analysis of anti-MOG response for an observation time of 24 months (Figure 11E): the anti-MOG reactivity increased until month 32 after disease onset, when the biopsy was performed, and subsequently dropped as a consequence of immunoadsorbance (IA).

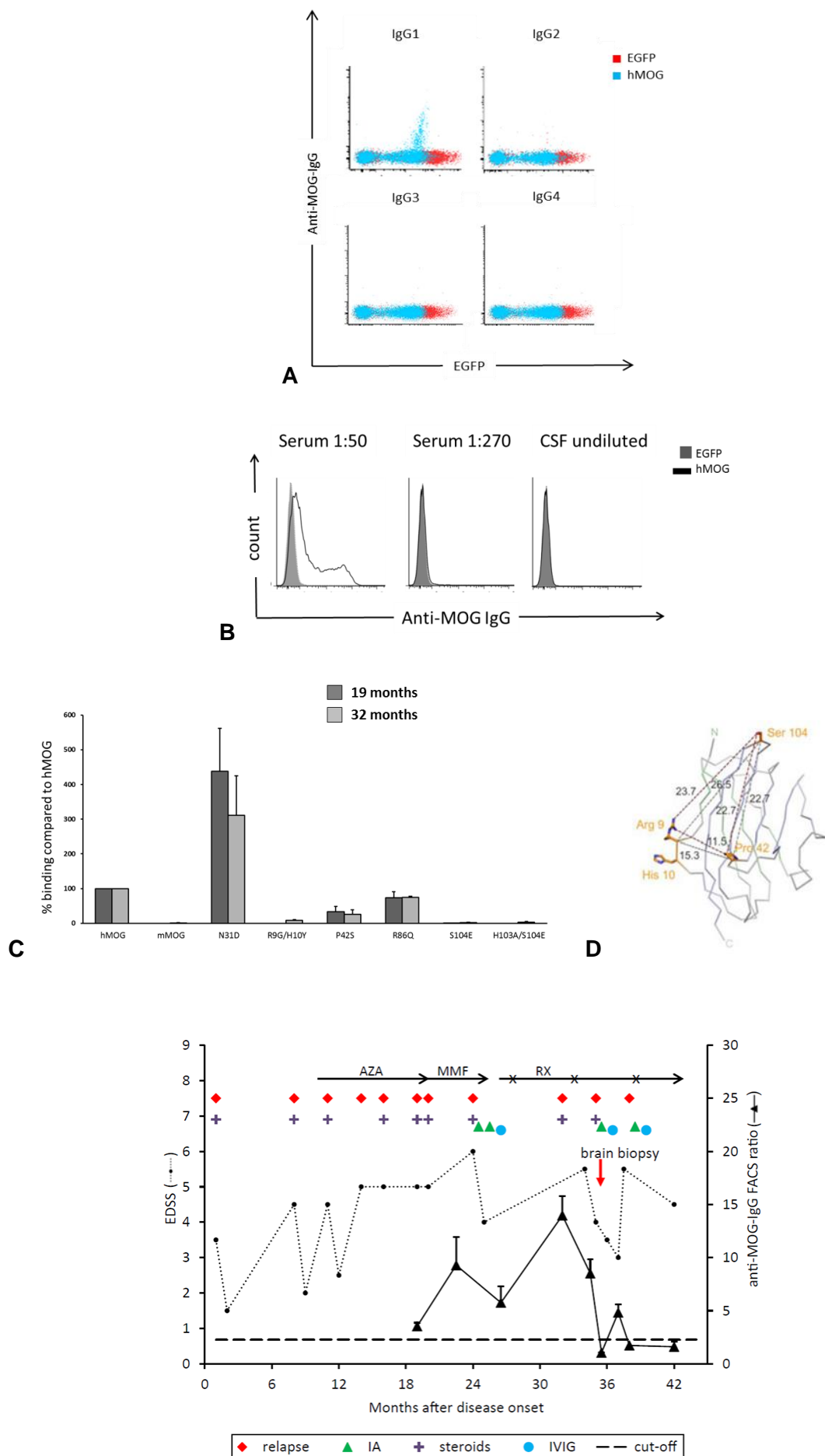


Figure 11: Clinical course and antibodies to MOG in index patient 1819. The isotype of the MOG-specific abs was analyzed by using the serum sample obtained 32 months after disease onset (A). For the analysis of intrathecal production of abs to MOG, serum and CSF were adjusted to the same IgG concentration and incubated with EGFP control cells (grey) and hMOG transfected cells (black line) (B); Reactivity to MOG variants after 19 (black) and 32 (gray) months after disease onset. Sera were diluted 1:50 and incubated with different MOG mutants. Binding percentage was calculated as described in section 2.2.8.1 (C). Visualization of amino acids recognized by the patient's autoantibodies (this figure was prepared by Prof. C. Breithaupt). The structure of the hMOG model is shown as C α -trace. C α -atoms of the front β -sheet are colored blue, those of the back β -sheet green. The amino acids involved in antibody binding are shown as stick models. C α -C α and minimum side chain distances are given in Å (D). Figures taken from (Spadaro, Gerdes et al. 2015). The dashed horizontal line indicates the threshold of anti-MOG positivity. This figure was prepared in collaboration with Dr. Lisa Ann Gerdes (E). Mean \pm SEM of three replicates. AZA: Azathioprine, MMF: mycophenolat mofetil; RX: Rituximab; IA: immune adsorption; EDSS: expanded disability status scale.

3.3.2 Neuropathological examination

During the observation period of three years, the patient's lesions spread in a caudo-cranial direction, starting with multifocal spinal cord lesions, followed by brainstem involvement and subsequently by a large bihemispheric white matter lesion which showed regression over time (Figure 12). The appearance of this large lesion corresponded to month 32 after disease onset. At this time point a brain biopsy was performed and histological analysis was carried out from our coworkers from the Center for Brain research in Vienna.

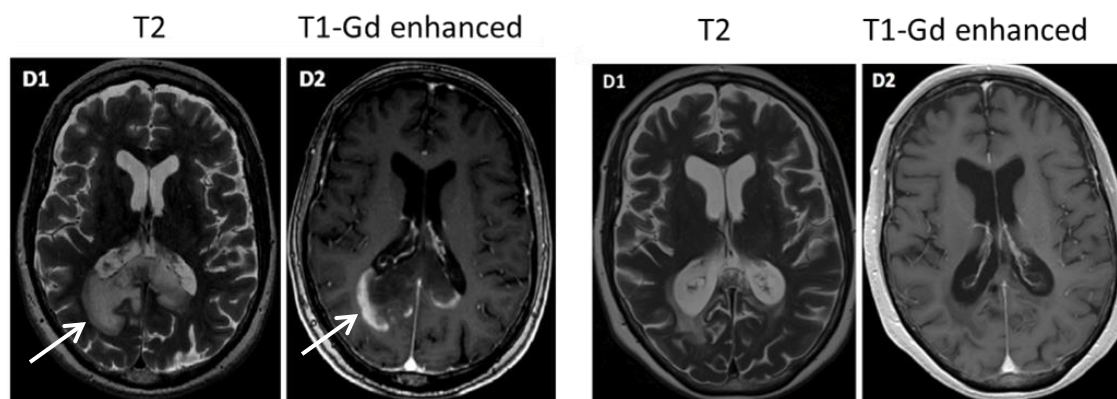


Figure 12: Cerebral MRI of index patient 1819. Cerebral MRI D1 and D2, 32 months after disease onset: the arrows indicate a bihemispheric, sharply demarcated confluent tumefactive parieto-occipital lesion across the splenium of the corpus callosum with rim-enhancing pattern; regression of large bihemispheric lesion in the splenium of the corpus callosum and lack of Gd-enhancement 47 months after disease onset. Scale bars, 50 μ m. Modified from (Spadaro, Gerdes et al. 2015).

Histopathological analysis revealed an inflammatory demyelinating lesion with partial axonal preservation and reactive astrocytic scarring (Figure 13). Inflammation was reflected by T-lymphocytes and activated macrophages or microglia. Areas of active demyelination were characterized by profound reactivity for C9neo indicating terminal complement activation, and accumulation of IgG. These were not observed in the normal appearing white matter or in the inactive lesion core (Figure 13) and were the main features of the histological defined MS pattern II (Lucchinetti, Brück et al. 2000). In the lesion center, numerous CNPase-positive premyelinating oligodendrocytes were present, but fully remyelinated lesion areas

were not contained within the biopsy specimen. Astrocytes showed changes of protoplasmatic and fibrillary gliosis without loss of AQP-4 or-1 reactivity. Neurofilament staining showed preservation of axons in the demyelinated lesion (Figure 13).

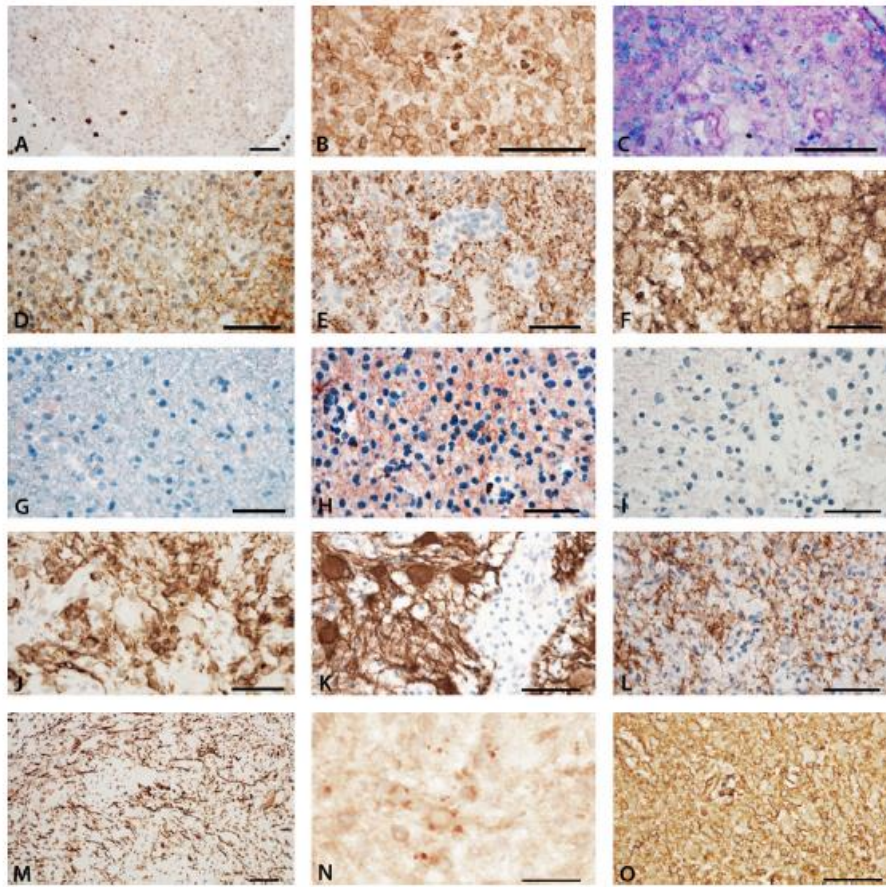


Figure 13: Histopathological analysis of index patient 1819. (A) Moderate tissue infiltration by CD8⁺ T lymphocytes. (B) activated macrophages, expressing the p22 component of the NADPH oxidase complex. (C) macrophages contain luxol fast blue-positive myelin degradation products. (D) loss of MOG immunoreactivity at the active site of the lesion; MOG-positive granules can be seen in the cytoplasm of macrophages (early active lesion). (E) more intense immunoreactivity for PLP; PLP is also seen in granular form in the cytoplasm of macrophages. (F) the most intense immunoreactivity for myelin-related proteins is seen for CNPase; (H) immunoreactivity for activated complement (C9neo antigen) is only present at the active lesion edge, but not in the normal appearing white matter (G), or the inactive lesion center (I). (H) At the active lesion edge C9neo reactivity is seen on myelinated fibers and in myelin degradation products within macrophages. In the lesion center complete demyelination is seen; (J) immunocytochemistry for CNPase shows numerous immunoreactive cells (premyelinating oligodendrocytes) and a fine meshwork of CNPase reactive fibers; (K) astrocytes within the lesion are preserved, show reactive gliosis as seen by GFAP staining and (L) express aquaporin 4; (M) immunocytochemistry for phosphorylated neurofilament shows preservation of axons in the demyelinated lesion; (N) sections stained for amyloid precursor protein reveal a moderate number of axons with disturbed fast axons transport. (O, serial section to H) Staining for human immunoglobulin G shows profound accumulation of IgG in early active lesions; IgG is diffusely deposited in the lesions, but shows accentuation on fibrillar structures in a similar pattern as depicted for complement C9neo staining. Magnification bars: 50 μ m. CNPase, cyclic nucleotide phosphodiesterase; PLP, proteolipid protein (B). This figure was taken from (Spadaro, Gerdes et al. 2015).

3.4 Abs to MOG in a distinct subgroup of adult multiple sclerosis

Abs to MOG were found in 5/104 patients (Figure 6) who fulfilled the diagnostic criteria for MS and were preselected for a specific clinical phenotype (severe spinal cord, optic nerve and brainstem involvement). Since we identified a patient with biopsy proven MS pattern II (described in section 3.3) we investigated two additional cohorts for the presence of anti-MOG IgG: n=22 biopsied patients with demyelinating diseases of the CNS (n=19 with RRMS and n=3 with ADEM), four of whom classified as MS type II, and n=55 sex and age-matched, otherwise unselected MS patients (see table 8 for clinical characteristics of the three groups). None of the patients of these two additional groups tested positive for anti-MOG reactivity (Figure 14A). The intensity of anti-MOG reactivity in these patients was similar to what we observed in the patient with MOG-associated encephalomyelitis. The availability of follow up samples allowed us to perform in these five MS patients the anti-MOG a longitudinal analysis of the anti-MOG response with a mean observation period of 7 years. In three of these patients, we noted intermittent disappearance and reappearance of the anti-MOG response (Figure 14B). This was particularly striking in patient 558 in whom a strong anti-MOG response transiently disappeared and then reappeared 7 years later at a similar intensity (Figure 14C).

Table 8: Clinical characteristics of patient groups 1-3

	Sex (f/m)	Age years, mean (range)	Diagnosis	Disease duration, years, mean (range)	EDSS, mean (range)	MSSS, mean (range)	Details
Group 1, n=104	65/39	37 (19-62)	RRMS=94 SPMS=4 CIS=6	8 (0-31)	3.7 (1-8.5)	5.97 (0.56- 9.74)	severe/recurrent ON n=50, 48% (n=14 bilateral ON); brainstem n=56, 54%; severe/recurrent myelitis n=61, 59%; severe spinal cord involvement n=18, 17% PLEX performed n=38 response to PLEX n=28
Group 2, n=55	30/25	39 (18- 70)	RRMS=53 SPMS=2	8 (0-31)	2.5 (0- 6.5)	3.92 (0.35- 9.63)	age/sex matched, otherwise unselected multiple sclerosis patients
Group 3, n=22	18/4	45 (25- 73)	RRMS=11, SPMS=2, CIS=6, ADEM=3	5.9 (0-28.7)	3.27 (1-9.5)	5.42 (0.74- 9.99)	brain biopsy classification: Type I=4, Type II=4, Type III=3, no classification possible=11

MSSS=multiple sclerosis severity scale. This table was taken from (Spadaro, Gerdes et al. 2016) and prepared by Dr. Lisa Ann Gerdes.

The anti-MOG response in this patient showed the same epitope specificity 9 and 16 years after disease onset (Figure 14D).

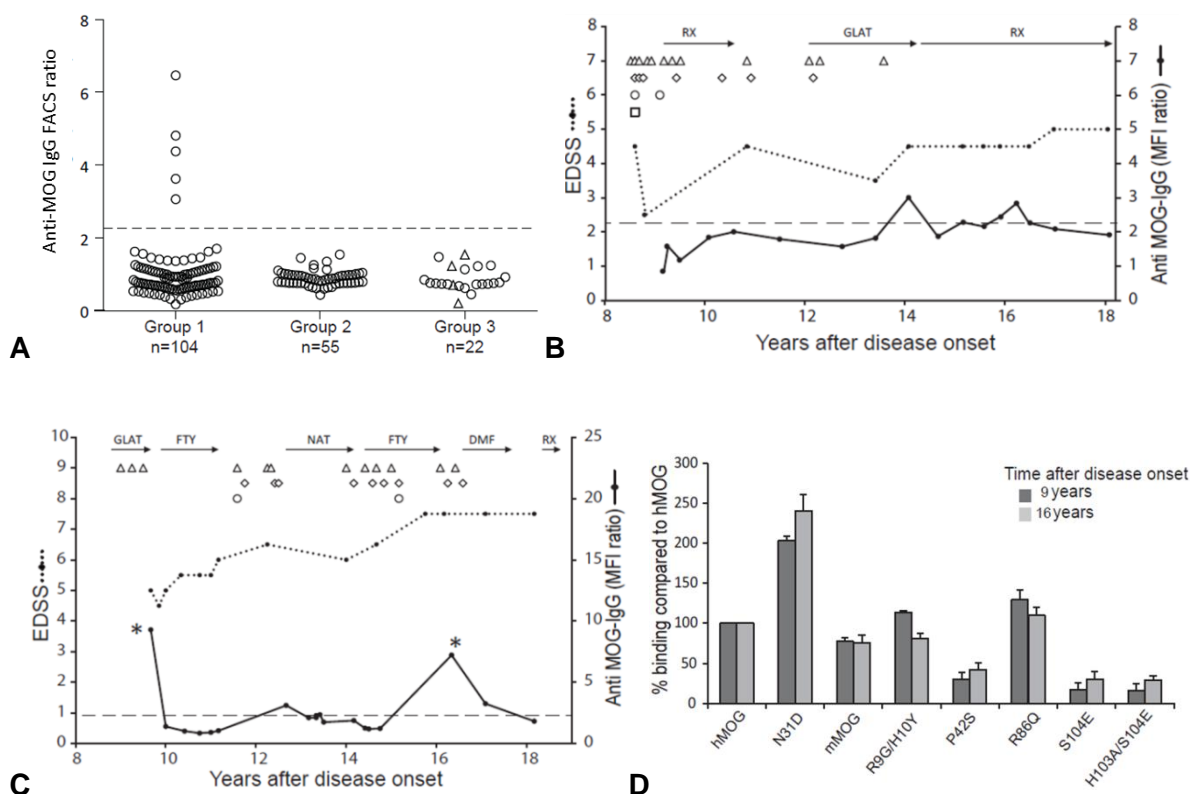


Figure 14: Anti-MOG reactivity in adult MS. Sera from three groups of patients with MS were analyzed for anti-MOG reactivity. Group 1: patients with MS with a specific clinical phenotype (severe or recurrent myelitis and/or severe or recurrent optic neuritis, and/or brainstem syndrome) (n=5/104). Group 2: unselected patients with MS matched for age and sex (n=55). Group 3: biopsied patients (n=22), 4 with MS type II pathology (empty triangles). The dashed line indicates the cutoff for anti-MOG positivity (2.27). Values shown for each anti-MOG IgG-positive patient represent the mean of 3 independent measurements using the first serum sample analyzed, which was 14, 16, 3, 18, and 9 years after disease onset for patients 1 through 5 (A). Clinical features, therapies, and longitudinal analysis of abs to MOG in two MS patients, corresponding to sera 0211 and 558 in table 7. (B,C). Analysis of the epitope specificity of the MOG reactivity of the samples indicated with asterisks in C. Mean \pm SEM of three independent replicates. DMF = dimethyl fumarate; DMT = disease-modifying therapy; EDSS = Expanded Disability Status Scale; FTY = fingolimod; GLAT = glatiramer acetate; IVIG = IV immunoglobulins; MFI = mean fluorescence intensity; NAT = natalizumab; PLEX = plasma exchange; RX = rituximab. Figures modified from (Spadaro, Gerdes et al. (2016)).

3.4.1 Clinical phenotype of anti-MOG IgG positive patients with MS

Clinical information of the analyzed patients was provided by PD Dr. Tania Kümpfel and Dr. Lisa Ann Gerdes. All five patients with MS had a typical RRMS with several relapses over time, typical CSF findings with presence of OCBs, and MS-typical cerebral MRI features from the beginning of the disease. When we compared the clinical features of the five anti-MOG-positive patients with MS to anti-MOG-negative patients of group 1, we noted that four

patients with abs to MOG had concomitant severe spinal cord and brainstem involvement, while this combination was seen in only 7 of 99 patients without abs to MOG. A combination of all three specific clinical characteristics (severe/recurrent ON, severe/recurrent myelitis, and brainstem syndrome) was observed in three of five patients with abs to MOG and in 3 of 99 patients without abs to MOG (Table 9). All five patients with MS who had MOG-specific abs showed an active disease course as indicated by high relapse rates and therapy failure to several disease modifying therapies (DMTs) (Table 9). Severe relapses at the beginning of MS led to Expanded Disability Status Scale (EDSS) scores 4.0 in four patients early on. Three of the five patients with abs to MOG responded favorably to plasma exchange (PLEX) therapy (Table 9). Serum samples from MOG antibody–positive patients were not available from disease onset; however, we could analyze the anti-MOG response longitudinally in all five patients with a mean observation period of seven years (Figure 15).

Table 9: Clinical characteristics of anti-MOG positive patients compared to anti-MOG negative patients in selected MS patients (group 1)

Clinical characteristics	Anti-MOG abs + (n=5)	Anti-MOG abs - (n= 99)
severe/recurrent ON	4 of 5	50 of 99
brainstem syndrome	4 of 5	53 of 99
severe/recurrent myelitis	5 of 5	56 of 99
severe myelitis and brainstem syndrome	4 of 5	7 of 99
severe ON and myelitis and brainstem syndrome	3 of 5	9 of 99
response to PLEX	3 of 3	25 of 35
DMT ≥3	4 of 5	21 of 99

Table modified from (Spadaro, Gerdes et al. 2016).

The anti-MOG reactivity fluctuated over time and only partially correlated with clinical disease activity. In patients 0211 and 558, anti-MOG reactivity reappeared during episodes of clinical and/or radiologic disease activity (Figure 15). Patient 2703 tested positive for MOG-specific abs during a severe brainstem and ON relapse, but tested negative seven and eight years later during a phase of clinical stabilization while under natalizumab therapy (Figure 15A). Patient 2169 could be tested only twice during a time interval of two years and showed ongoing disease activity accompanied by positive anti-MOG reactivity at both time points (Figure 15B). Patient 467 had a stable disease course. In this patient abs to MOG fluctuated during continuous natalizumab treatment (Figure 15C).

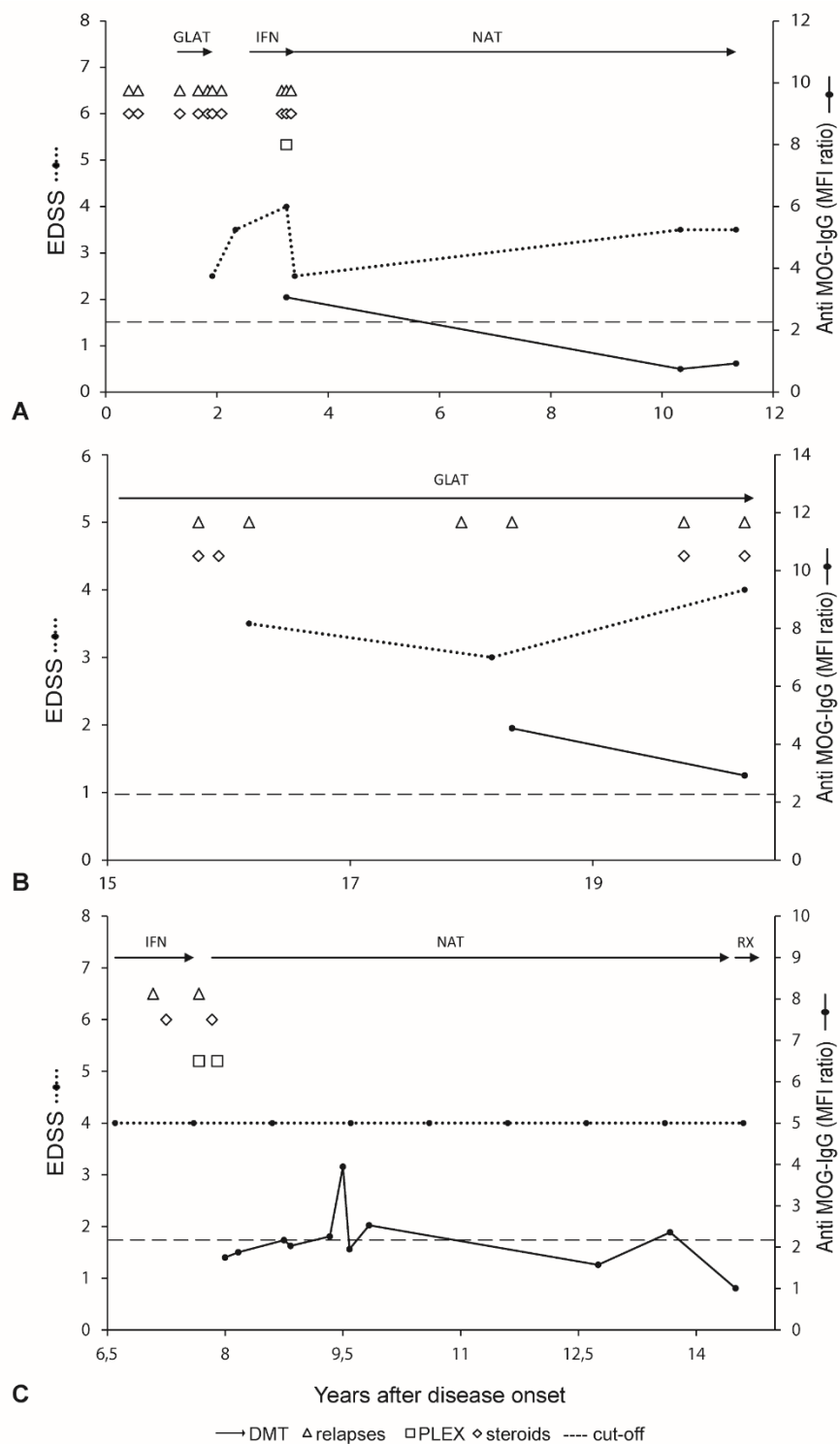


Figure 15: Longitudinal analysis of MOG-specific abs and clinical score. MS Patients 2703 (A), 2169 (B) and 467 (C). Figures modified from (Spadaro, Gerdes et al. 2016).

3.5 Detection of MOG-specific abs by ELISA

MOG-specific abs were also tested by ELISA. In this method, the antigen is adsorbed on a solid support. The use of streptavidin coated plates and of biotinylated hMOG as coating antigen, allowed us to increase the sensitivity compared to the ELISA performed with maxisorp plates (Figure 16A). Moreover, the presence of a flexible linker between the extracellular domain of MOG and the biotinylation site (see section 2.2.6.2) offers the advantage that epitopes on MOG are more accessible for antibody binding (Figure 16B). For comparison between streptavidin coated plates and maxisorp plates, sera 1771 was diluted 1:200, the mAb 8-18C5 was used at 0.5 µg/ml.

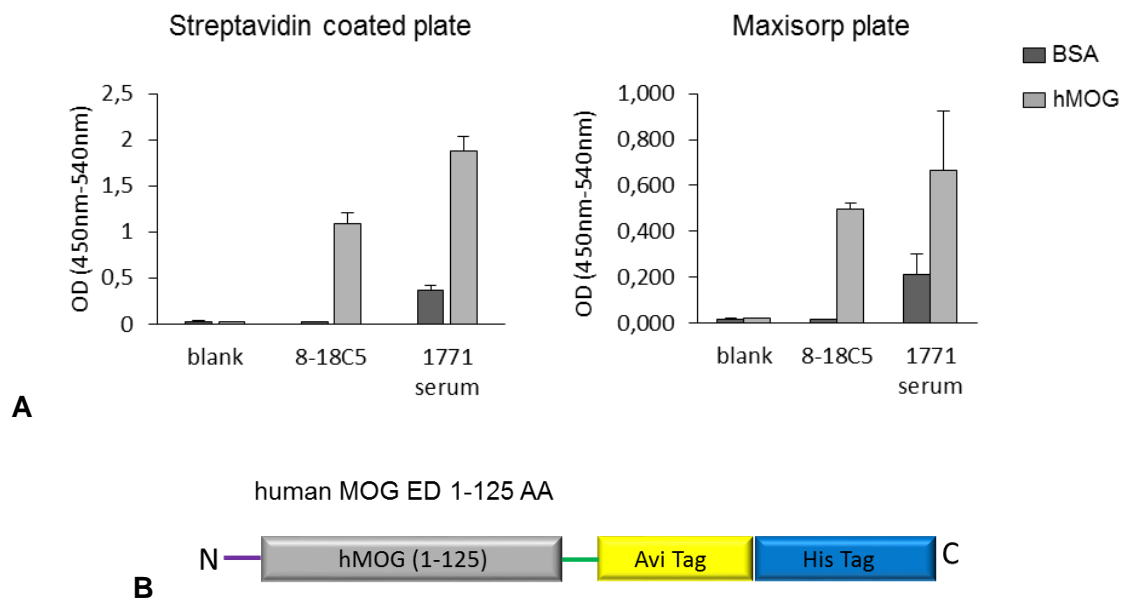


Figure 16: ELISA optimization by using biotinylated hMOG as coating antigen. Reactivity of the 8-18C5 mAb and human serum 1771 against hMOG or BSA (used as a negative control) is shown here. The streptavidin plate was coated with 3 µg/ml of biotinylated hMOG (left), while the maxisorp plate was coated with 10 µg/ml of hMOG (right). ELISA reactivity is shown here as OD (450 nm-540 nm). Serum was used at a 1:200 dilution, the 8-18C5 mAb was used at a 0.5 µg/ml concentration. Mean \pm SD, $n \geq 2$ (A); the construct used for the streptavidin ELISA contains the extracellular domain (ED) of hMOG (in grey). The flexible linker between this part of hMOG and the biotinylation site (Avi Tag) is depicted in green. The violet line represents the Igk leader sequence (B).

Wells were coated for serum screening with biotinylated hMOG at a 3 µg/ml concentration. Wells containing only streptavidin were used as a negative control. We tested by ELISA 116 patients and 87 HC (Figure 17A). The patient cohort included the 17 patients which showed anti-MOG reactivity by FACS and 89 RRMS, 6 CIS and 4 SPMS patients. All the patient samples were also tested in the CBA.

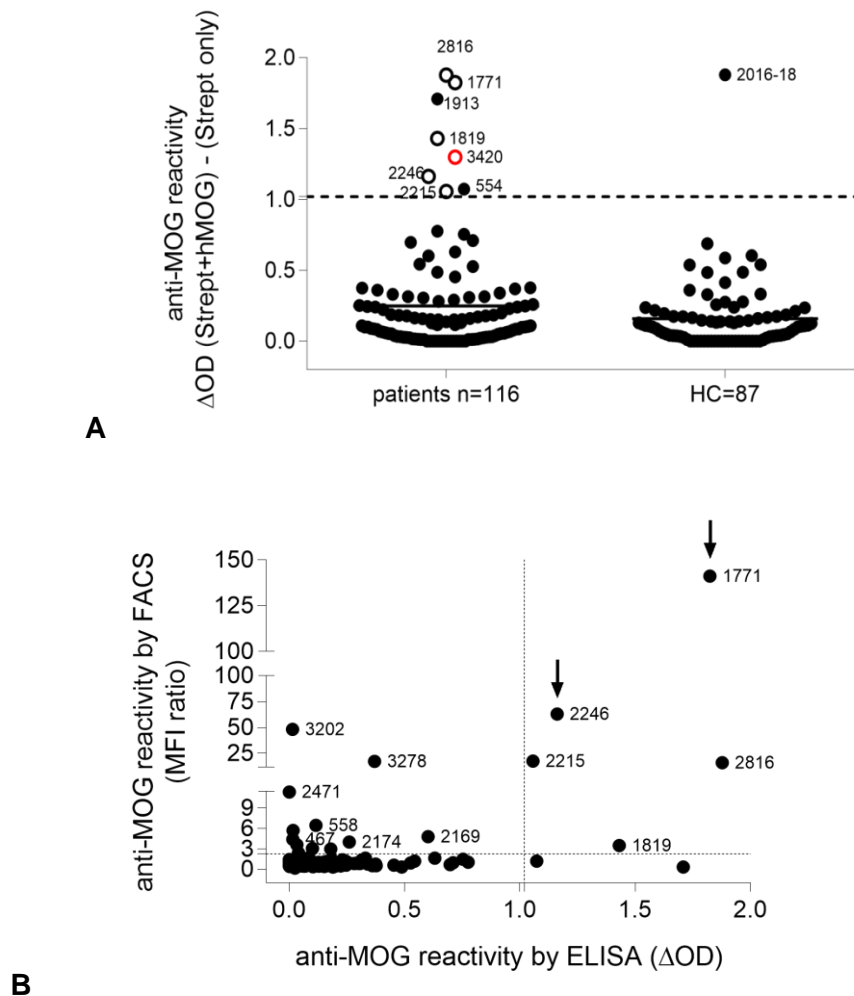


Figure 17: Reactivity to MOG by ELISA. Screening of 116 patients and 87 HC by ELISA. Biotinylated hMOG was added to streptavidin coated plates. The anti-MOG reactivity is expressed as ΔOD (streptavidin + hMOG) – (streptavidin only). See section 2.2.8.2 for more details. Open circles represent sera that scored positive by FACS, red circle corresponds to the human serum used daily control. The dashed line represents the cutoff value which was calculated as mean of the anti-MOG reactivity (ΔOD) of the HC+3SDs (A). Correlation between the anti-MOG reactivity (MFI ratio) measured by FACS and the anti-MOG reactivity (ΔOD) measured by ELISA. Sera indicated by the arrows were the only ones that showed high reactivity in both assays, these patient sera were affinity-purified. Numbers indicate patient sera that tested positive by FACS (B).

7/116 patients (6%) showed by ELISA anti-MOG reactivity above or close the cutoff value (1.02): 5 of these patients (open circles) tested also positive in our CBA (three ON patients, one NMOSD patient and one patient with relapsing encephalomyelitis), the other two positive patient samples were diagnosed with RRMS and were negative in our CBA. The anti-MOG reactivity observed by FACS and ELISA was congruent for the two sera 1771 and 2246, these showed the highest reactivity against conformationally intact MOG (Table 6). Overall, we did not observe a correlation between the results obtained by FACS and ELISA (Figure 17B, Spearman $r=0.16$, $p = 0.07$). Also 1 of 87 HC (2016-18) tested positive by ELISA but not by FACS. Our results show that the ELISA with a display of MOG with a site directed

biotinylation at the C-terminus is more sensitive than the ELISA with a conventional binding of MOG to a maxisorp plate.

3.6 Affinity purified anti-MOG abs from patients 1771 and 2246

Among the analyzed patient sera, those from two patients (1771 and 2246) were the only ones who showed anti-MOG reactivity by FACS and ELISA and cross-reactivity to rat MOG. Therefore, MOG-specific abs from these patients were affinity purified in order to perform an *in vivo* analysis of their pathogenic potential. The detailed analysis of these serum samples and the establishment and validation of the affinity purification are described in the next sections.

3.6.1 Detailed analysis of patient sera 1771 and 2246

Patient 1771, a 46 years old female, was diagnosed with relapsing bilateral ON and with CAPS, a rare, inherited autoinflammatory disease. We performed a longitudinal analysis of the anti-MOG reactivity for an observation time of 26 months, during that period the patient did not obtain any treatment and the disease course was stable. The anti-MOG abs were of the IgG1 isotype and the IgM class, we did not observe any significant fluctuation of the anti-MOG response during the observation time (Figure 18A). Reactivity due to MOG-specific abs of the IgG class was observed up to a dilution of 1:12150 at which the MFI ratio was 6.2 (Figure 18B). Since the anti-MOG abs were planned to be used for transfer experiment in Lewis rat and since rat and mouse MOG show differences in their amino acid sequence (Breithaupt, Schäfer et al. 2008), we tested also the reactivity to rat MOG and observed a strong binding (Figure 18C): the binding percentage of MOG-specific IgG and IgM for rat MOG was $19 \% \pm 0.38$ and $15.5 \% \pm 0.98$, respectively. We could detect also an anti-MOG reactivity in the CSF, however, we did not observe an intrathecal production of anti-MOG IgG since the MFI ratio of the CSF (72.44) was lower than the MFI ratio of the corresponding serum (86.34) adjusted to the same IgG concentration (Figure 18D). Abs of the IgG and the IgM classes showed a similar reactivity to the different mutant variants of MOG. (Figure 18E): anti-MOG reactivity was directed against P42, localized in the CC' loop on MOG.

Patient 2246, a 49 years old male, was diagnosed with a severe relapsing unilateral ON and showed a stable disease course during an observation time of 35 months. Two months after the first sample collection, a therapy with the immunosuppressive drug Azathioprine (AZA) was started. The analysis of the second follow-up sample showed a strong reduction of the anti-MOG reactivity, which remained stable for the rest of the observation period (Figure 19A). Anti-MOG reactivity could be detected up to a serum dilution of 1:12150, MFI ratio was 3.53 (Figure 19B).

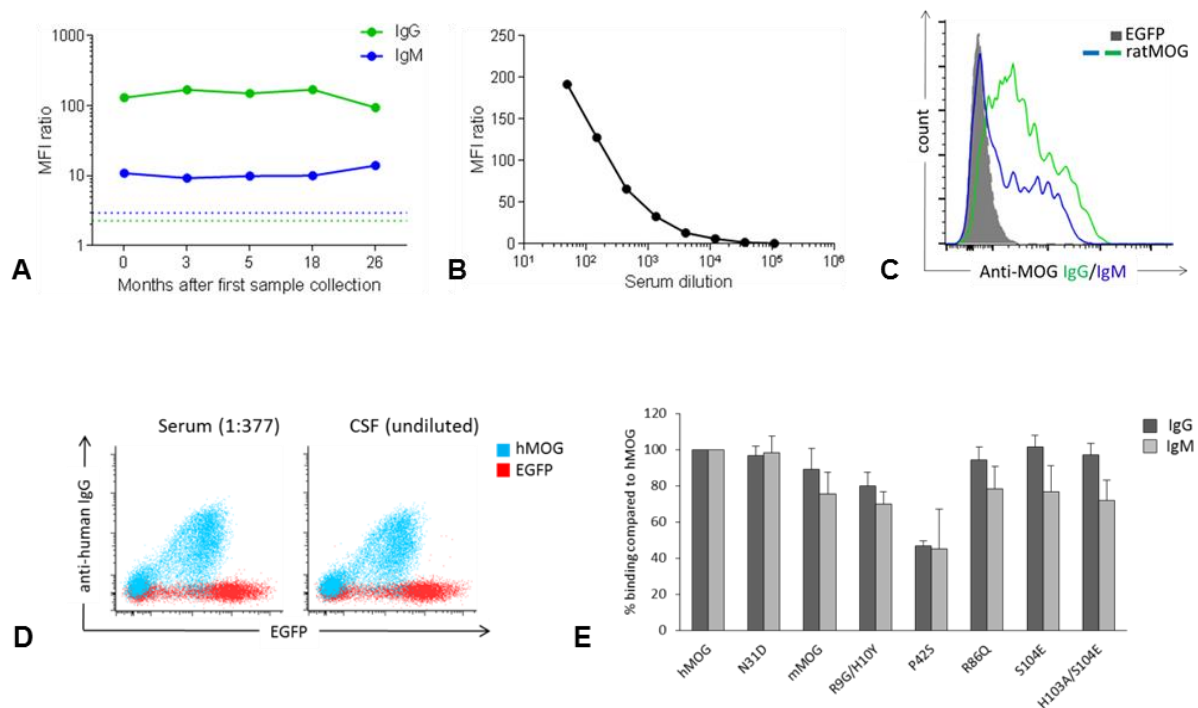


Figure 18: Detailed analysis of the anti-MOG reactivity in patient 1771 by FACS: for longitudinal analysis, sera of the different time points were diluted 1:50 and incubated with HeLa cells transfected with EGFP (control cell) or hMOG-EGFP. Anti-MOG reactivity was detected by using as secondary anti-human IgG (green line) or anti-human IgM (blue line). MFI ratio was calculated as follows: MFI (MOG-EGFP)/MFI (EGFP). Green and blue dashed lines represent the corresponding cutoff value (2.27 for IgG and 2.96 for IgM) (A). Sera from the first time point was diluted from 1:50 up to 1:109350 dilution and analyzed for anti-MOG IgG (B). IgG and IgM Abs were also tested for binding to rat MOG (C). Serum and CSF of the first time point were adjusted to the same IgG concentration (22 µg/ml) and tested for anti-MOG reactivity. The MFI ratio of the CSF was 72.44, while that of the serum sample was 86.34 (D). Comparison of the recognized epitopes on MOG by MOG-specific IgG and IgM: HeLa cells transfected with different variants of hMOG or with mMOG were incubated with a 1:50 dilution of the sera and MOG-reactivity due to abs of the IgG or the IgM class was analyzed. Mean \pm SEM, n=2 (E).

Sera from this patient showed a high reactivity against rat MOG (MFI ratio was 141.4) (Figure 19C). MOG-specific abs had the IgG1 subclass (Figure 19D). The analysis of the reactivity against different MOG epitopes revealed that the anti-MOG response in this patient was directed against H103 of the FG'loop and R9 and H10 of the AA' loop. Moreover, we observed a stronger binding to the P42S mutant than to the wt MOG (Figure 19E).

3.6.2 Establishment and validation of affinity purification of MOG-specific abs

For the establishment of an affinity purification protocol we first tried to use NHS columns with covalently conjugated hMOG. The mAb 8-18C5 was used as a positive control and the eluted antibody was tested by FACS for binding to conformationally intact hMOG expressed on the surface of HeLa cells (Figure 20, upper histograms). Importantly, while the mAb 8-18C5 was completely absorbed by this column, the anti-MOG Abs from the patient 1771 were largely unbound as seen by high anti-MOG reactivity in the flow through.

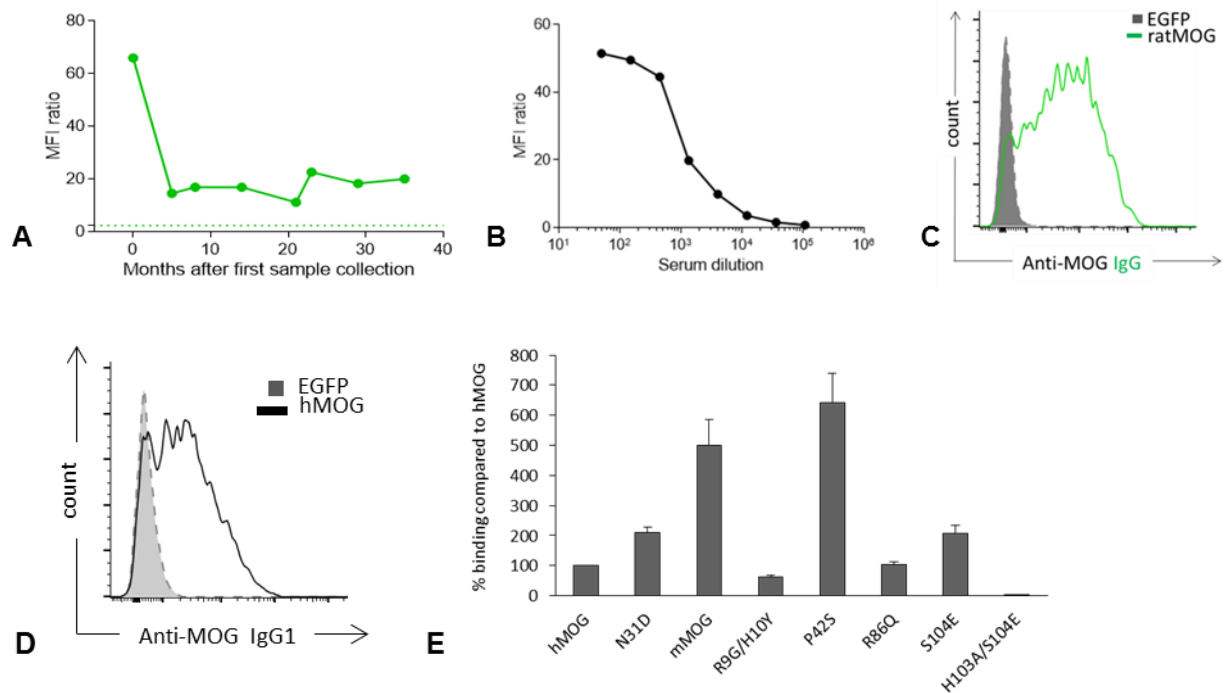


Figure 19: Detailed analysis of the anti-MOG reactivity in patient 2246 by FACS: for longitudinal analysis, sera of the different time points were diluted 1:50 and incubated with HeLa cells transfected with EGFP (control cell) or MOG-EGFP. Anti-MOG reactivity was detected by using as secondary anti-human IgG (green line). MFI ratio was calculated as follows: MFI (MOG-EGFP)/ MFI (EGFP). Green dashed line represents the corresponding cutoff value (2.27) (A). Serum from the first time point was diluted from 1:50 up to 1:109350 dilution and analyzed for anti-MOG reactivity (B). Abs were also tested for binding to ratMOG (C). MOG-specific abs were of the IgG1 subclass (D). Analysis of the recognized epitopes on MOG: HeLa cells transfected with different variants of hMOG or with mMOG were incubated with a 1:50 dilution of the sera and MOG-reactivity due to abs of the IgG class was analyzed. Mean \pm SEM, $n=3$ (E).

Only a very small amount (1.2 μ g) of anti-MOG could be recovered after loading of 20 ml plasma on this column. Both the eluted fractions of the 8-18C5 antibody and of the patient sample 1771 showed anti-MOG reactivity (Figure 20, lower histograms). As an alternative approach, we biotinylated hMOG at the Avi-Tag linked to the C-terminus and bound the protein to streptavidin sepharose columns. EDTA blood from patients 1771 and 2246 was collected at different time points during the observation period and corresponded to a total plasma volume of 600 ml and 1200 ml, respectively. More details about the amount of unpurified and purified abs are provided in table 10. Eluted abs were separated by SDS-Page and visualized by Coomassie blue staining, bands of interest were cut out and analyzed by mass spectrometry (Figure 21). We could identify by mass spectrometry in the eluted sample from patient 2246 abs of the IgG class, while the eluted sample from patient 1771 contained both abs of the IgG and the IgM class.

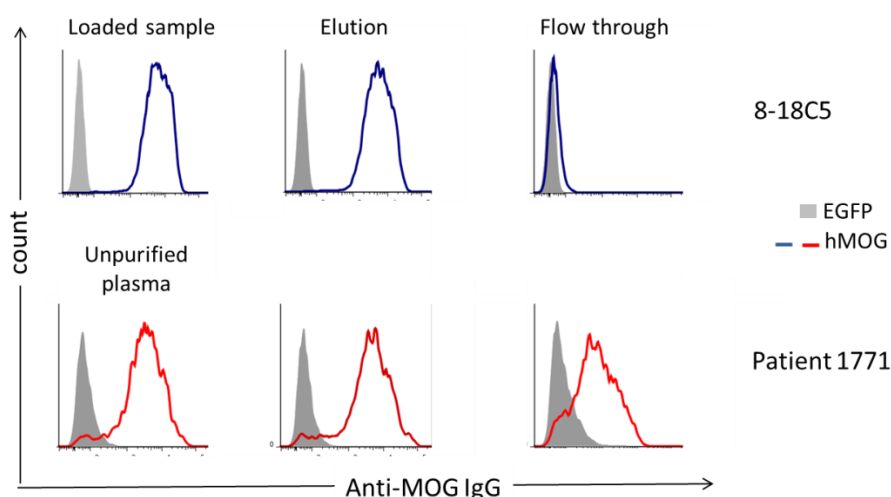


Figure 20: Binding of the eluted fractions of the 8-18C5 mAb and patient 1771 to native hMOG. HeLa cells were transiently transfected with EGFP (control) or hMOG-EGFP and incubated with the starting material (loaded sample and unpurified plasma, respectively), eluted abs and the flow through. All samples were adjusted to a concentration of 12 $\mu\text{g/ml}$. All fractions tested in the CBA were purified by using an NHS column loaded with hMOG.

This is consistent with our CBA results, which showed that among the identified anti-MOG positive patients, patient 1771 was the only one who, apart from anti-MOG IgG, had also anti-MOG abs from the IgM class (Figure 21).

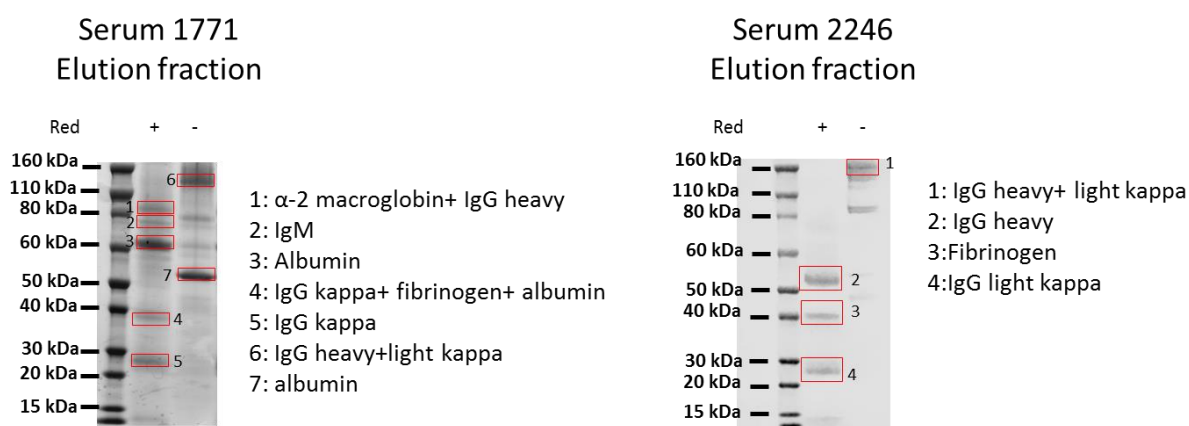


Figure 21: Elution fractions of material from ON patients 1771 and 2246 purified by using biotinylated hMOG. Eluted abs were dialyzed against PBS and 21 μl of each fraction was analyzed using SDS-Page and Coomassie blue staining under reducing and not reducing conditions. The bands in the red boxes were cut out and analyzed by mass spectrometry.

Both preparations showed also lower amounts of albumin, fibrinogen and α -2 macroglobin. The eluted fractions were quantified by IgG and IgM ELISA (see section 2.2.8.3 for detailed protocol) and the enrichment of MOG-specific abs in the eluted fractions was analyzed by FACS and ELISA.

Table 10: IgG and IgM concentration of unpurified plasma and purified fractions

Sample ID	Gender	Diagnosis	Therapy	Amount of Abs in the unpurified sample (mg)	Amount of purified Abs (µg)
1771	female	Relapsing bilateral ON and CAPS	no	IgG: 1339 IgM: 23.45	IgG: 471.4 IgM: 54.66
2246	male	Relapsing unilateral ON	AZA	IgG: 1500	IgG: 571.2

3.6.3 Validation of affinity purification by FACS and ELISA

For FACS analysis, HeLa cells were transfected as usual with EGFP and hMOG-EGFP and incubated with unpurified plasma material or purified abs adjusted to the same antibody concentration (12 µg/ml; 600 ng/50.000 cells) (Figure 22A).

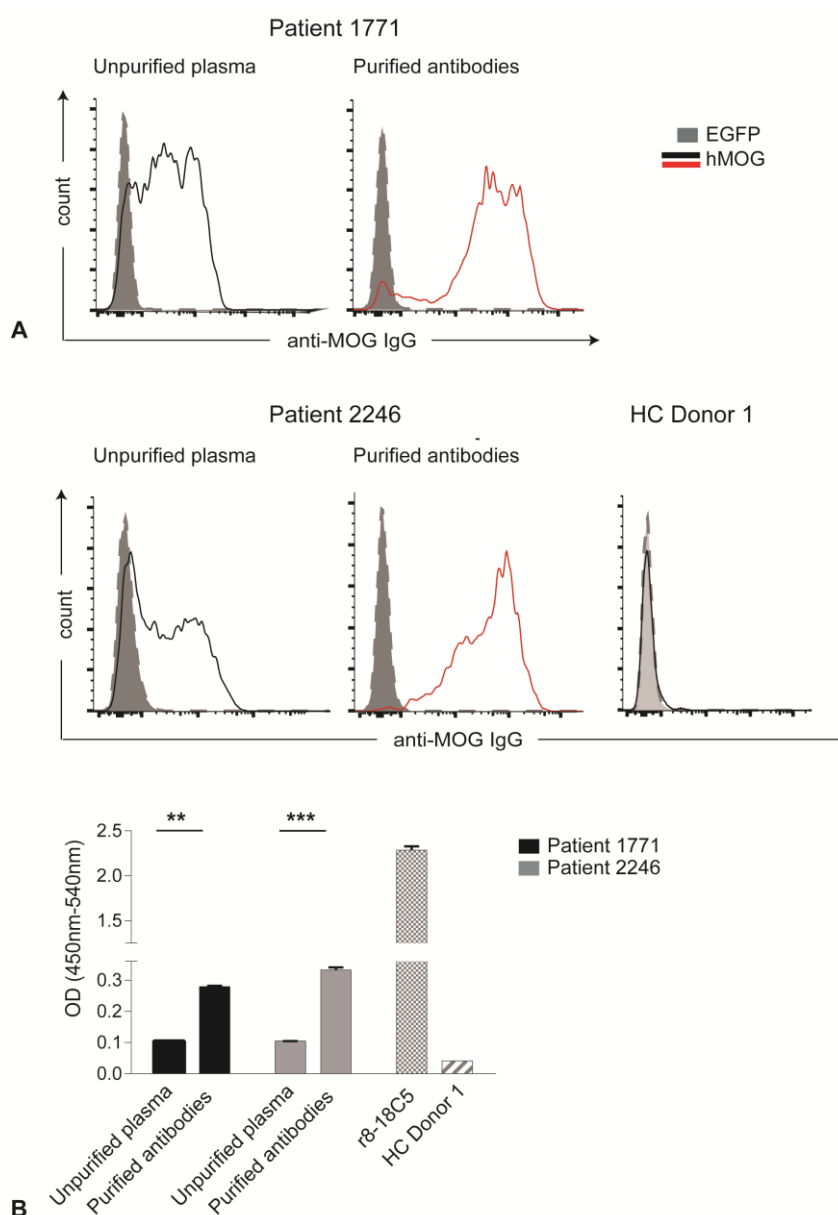


Figure 22: Binding analysis of affinity purified MOG-specific abs by FACS and ELISA. Unpurified plasma and purified abs from patients 1771 and 2246 were tested for reactivity to full length hMOG-

EGFP (black and red line) at a concentration of 12µg/ml. EGFP cells (in grey) were used as a control. Abs from the HC Donor 1 were used as a negative control (A). Unpurified plasma and purified abs were tested by ELISA for reactivity against recombinant hMOG; the r8-18C5 mAb and IgG from HC Donor 1 were used as positive and negative control, respectively. Unpurified material, purified abs and HC IgG were adjusted to a concentration of 6µg/ml, the r8-18C5 mAb was used at 0.5µg/ml (B). Error bars represent SDs and asterisks represent significance based on Student's t test as compared with the unpurified fraction (** $p < 0.005$; *** $p < 0.0005$; **** $p < 0.0001$).

The eluted fraction of both patients showed an enrichment of MOG-specific abs by FACS: the FACS ratio of the purified abs was 12.7 and 17.6 times higher than the FACS ratio of the unpurified material, respectively in patient 1771 and 2246. Both antibody preparations showed also by ELISA a significantly higher reactivity compared to the unpurified fraction (Figure 22B). We quantified by ELISA the binding of the affinity purified abs to recombinant hMOG and calculated the dissociation constant (K_D) which was 7 nM for the IgG purified from patient 1771 and 45.95 nM for the IgG purified from patient 2246. The K_D of the positive control mAb 8-18C5 was 2.4 nM (Figure 23A). The affinity purified abs recognized also the not glycosylated MOG variant (Figure 23B).

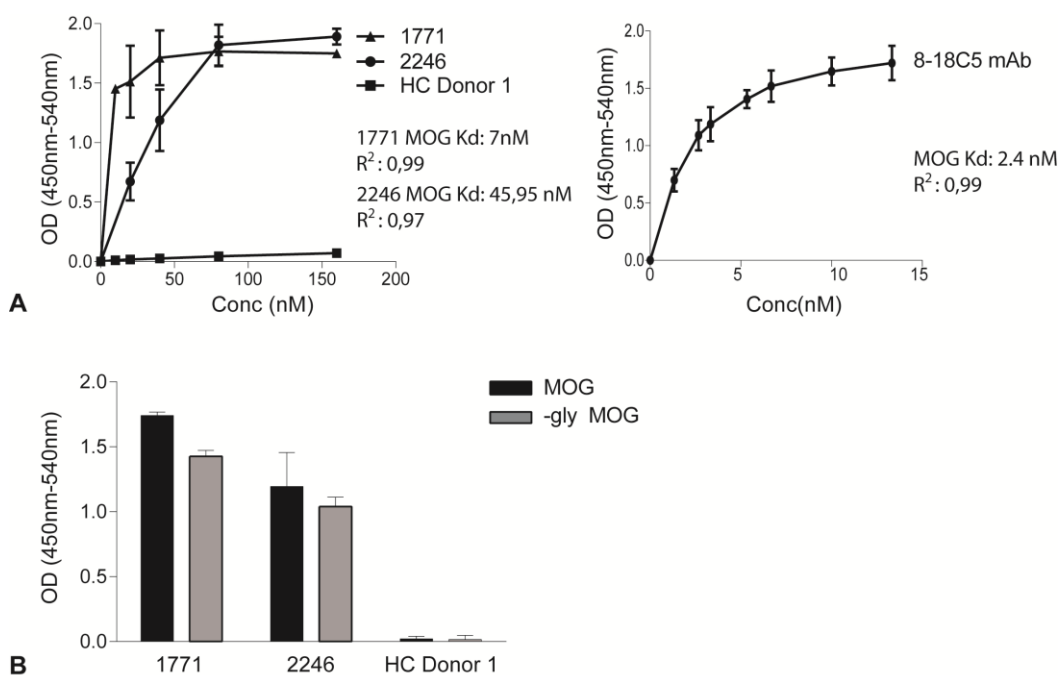


Figure 23: Binding features of affinity purified abs by ELISA. Saturation experiments were performed by ELISA to determine the affinities of the purified abs from patients 1771 and 2246 for recombinant hMOG. The 8-18C5 mAb and the IgG from HC Donor 1 were used as positive and negative control, respectively. $n=3$. Error bars represent SDs. (A). Binding to the unglycosylated MOG variant by ELISA. $n=2$. Error bars represent SDs. (B)

Affinity purified abs from patient 2246 were obtained in a higher yield and where therefore also used for indirect immunohistochemistry experiments on rat brains: we observed a strong labeling on myelin in the cerebral and cerebellar white matter whereas control IgG remained

negative (Figure 24). This staining was carried out by our collaboration partner Prof. Romana Höftberger of the Medical University of Vienna.

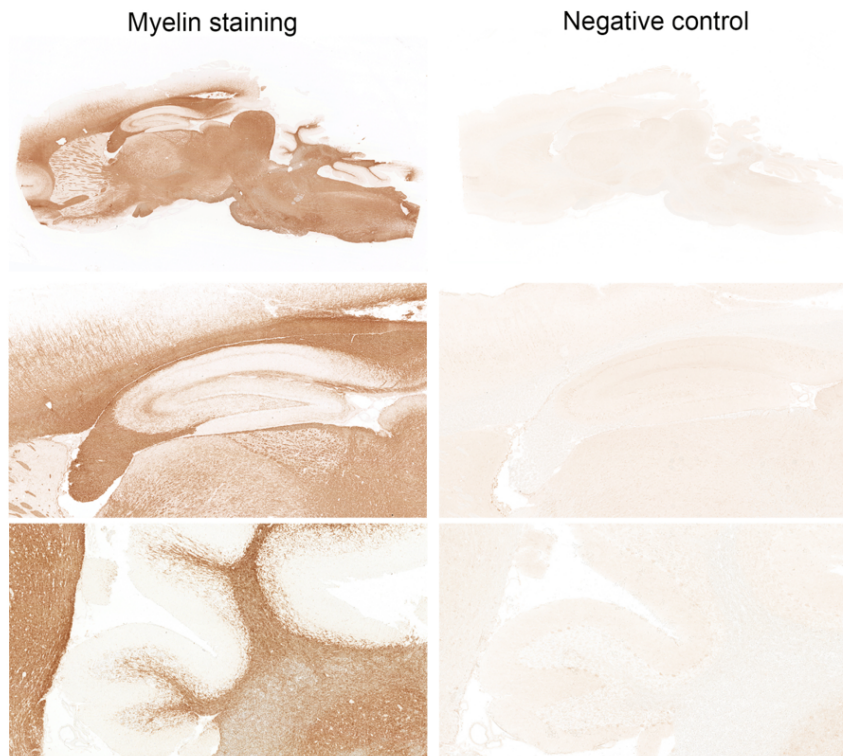


Figure 24: Indirect immunohistochemistry of affinity purified abs from patient 2246 on non-perfused rat brain. IgG from a MOG-negative patient with a psychiatric disorder was used as negative control (picture prepared from Prof. Romana Höftberger). Staining of the cerebral and cerebellar area are shown in detail in the middle and lower figure, respectively. Affinity purified abs and negative control were used at a concentration of 3 µg/ml.

3.6.4 Pathogenicity of affinity purified abs against MOG

Affinity purified abs from patients 2246 and 1771 were used to investigate their potential pathogenicity by *in vivo* experiments performed in Lewis rats (see section 2.2.11 for detailed protocol). These abs were analyzed for reactivity against mMOG and rat MOG in FACS (Figure 25A) and ELISA (Figure 25B). For the transfer experiments, EAE was induced in Lewis rats by the injection of MOG-specific T cells (T MOG-GFPn). Two days after EAE induction, affinity purified MOG specific IgG from patients 1771 and 2246, the mAb 8-18C5 and total IgG from HC Donor 1 were injected intrathecally.

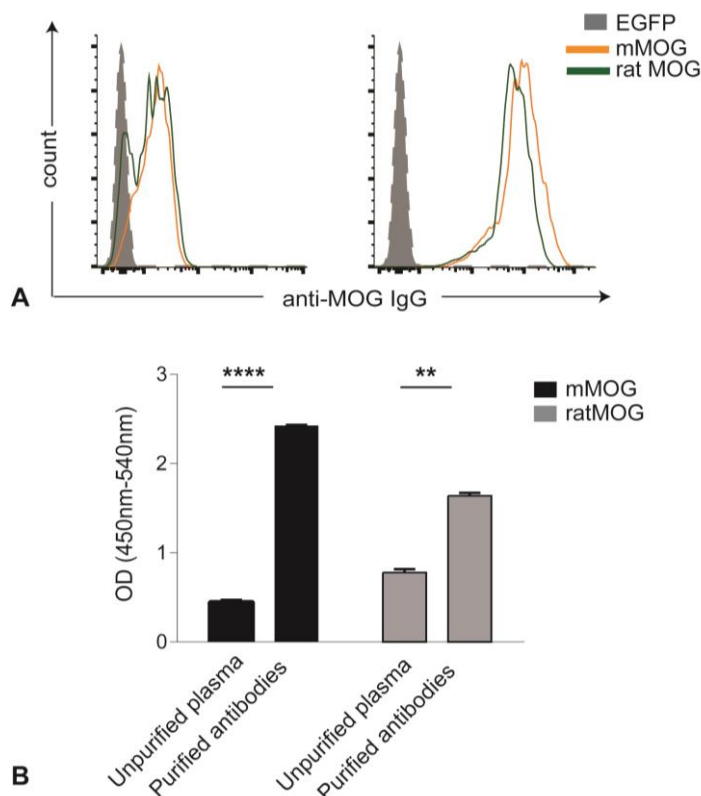


Figure 25: Binding analysis of affinity purified MOG-specific abs to mMOG and rat MOG by FACS and ELISA. Binding of purified abs to HeLa cells transfected with full length mMOG-EGFP and ratMOG-EGFP. HeLa cells transfected with EGFP only (in grey) were used as a control. Abs were used at a concentration of 12 μ g/ml (A); Reactivity by ELISA of unpurified plasma and purified abs against mMOG and rat MOG. Unpurified material and purified abs were adjusted to a concentration of 6 μ g/ml. n=2. Error bars represent SDs and asterisks represent significance based on Student's t test as compared with the unpurified fraction (** p < 0.005; *** p < 0.0005; **** p < 0.0001) (B).

Both the mAb 8-18C5 and the abs from patients 1771 and 2246 induced an increase of disease severity and a significant weight loss, while the negative control did not show any effect (Figure 26). Rats treated with the abs obtained from patients 1771 and 2246 showed five days after EAE induction a clinical score of 2.25 ± 1.06 and of 1.75 ± 0.35 SD, respectively. Rats treated with the mAb 8-18C5 had at the same time point a clinical score of 2.75 ± 1.06 SD. The animals were sacrificed 72 hours after antibody injection and brains and spinal cords were prepared for immunohistochemical analysis. Animal experiments were performed in cooperation with Dr. Naoto Kawakami.

3.6.5 Histopathological analysis

Pathological analysis of the spinal cord revealed in animals treated with the patient's abs or with the mAb 8-18C5 inflammation reflected by the massive subpial infiltration of CD3+T-lymphocytes. This was absent in the animals treated with the abs from HC Donor 1 (Figure 25 A-C).

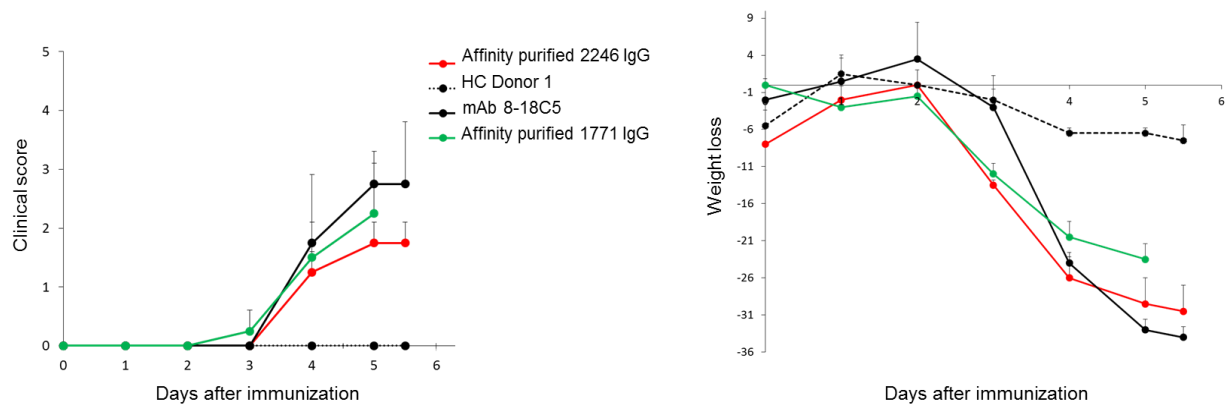


Figure 26: Clinical score and weight loss in Lewis rats treated with patient derived MOG-specific abs. EAE was induced in $n=8$ female Lewis rats by the intravenous injection of 8×10^6 MOG-specific T cells. Two days after injection of the MOG-specific T cells, 90 μ g of each antibody were injected intrathecally. Abs from patients 1771 and 2246 are indicated by the red and green line, respectively, the mAb 8-18C5 by the black line and the negative control HC Donor 1 by the dashed line. Rats were scored daily for disease severity and weight change. Values = mean \pm SD (2 animals per antibody).

Also activated macrophages, visualized by ED1 staining, were observed in the subpial area in rats treated with the anti-MOG abs, this was less pronounced in the animals treated with control abs where macrophages were found in the perimeningeal area (Figure 27D-F). Luxol fast blue staining (LFB) of the spinal cord and the optic nerve showed in animals treated with the patient's abs and the 8-18C5 antibody a mild perivascular demyelination, which was not observed in the animals treated with the control abs (Figure 27G-I). Reactivity for C9neo suggesting terminal complement activation was observed in the perivascular area in animals treated with the mAb 8-18C5 and to a lower extent in the animals treated with the patient's abs, whereas it was minimal in the control animals (Figure 27J-L). Subpial deposition of human IgG was observed only in rats treated with the patient's abs (Figure 27M-O).

3.7 Recombinant abs from patient 2246

To obtain MOG-specific B cells from patient 2246, two different approaches were used: first, B cells were activated and differentiated to Ig-secreting cells *in vitro*, tested for anti-MOG reactivity, and then sorted with a MOG-tetramer; second, MOG-specific B cells were directly sorted *ex vivo*.

3.7.1 MOG-specific B cells identified after *in vitro* stimulation

We used cryopreserved PBMC and induced differentiation of B cells to Ig-secreting cells by adding TLR7+8 ligand R848 and IL-2 (Pinna, Corti et al. 2009). B cell subpopulations were identified as follows: memory B cells ($CD19^+$, $CD27^+$, $CD38^-$); plasmablasts ($CD19^+$, $CD27^+$, $CD38^+$); naïve B cells ($CD19^+$, $CD27^-$, $CD38^-$). MOG-specific B cells were identified by

staining with a FITC-labeled mMOG tetramer and belonged mainly to the memory B cell subpopulation (5.68% compared to 0.22% of the HC) (Figure 28A).

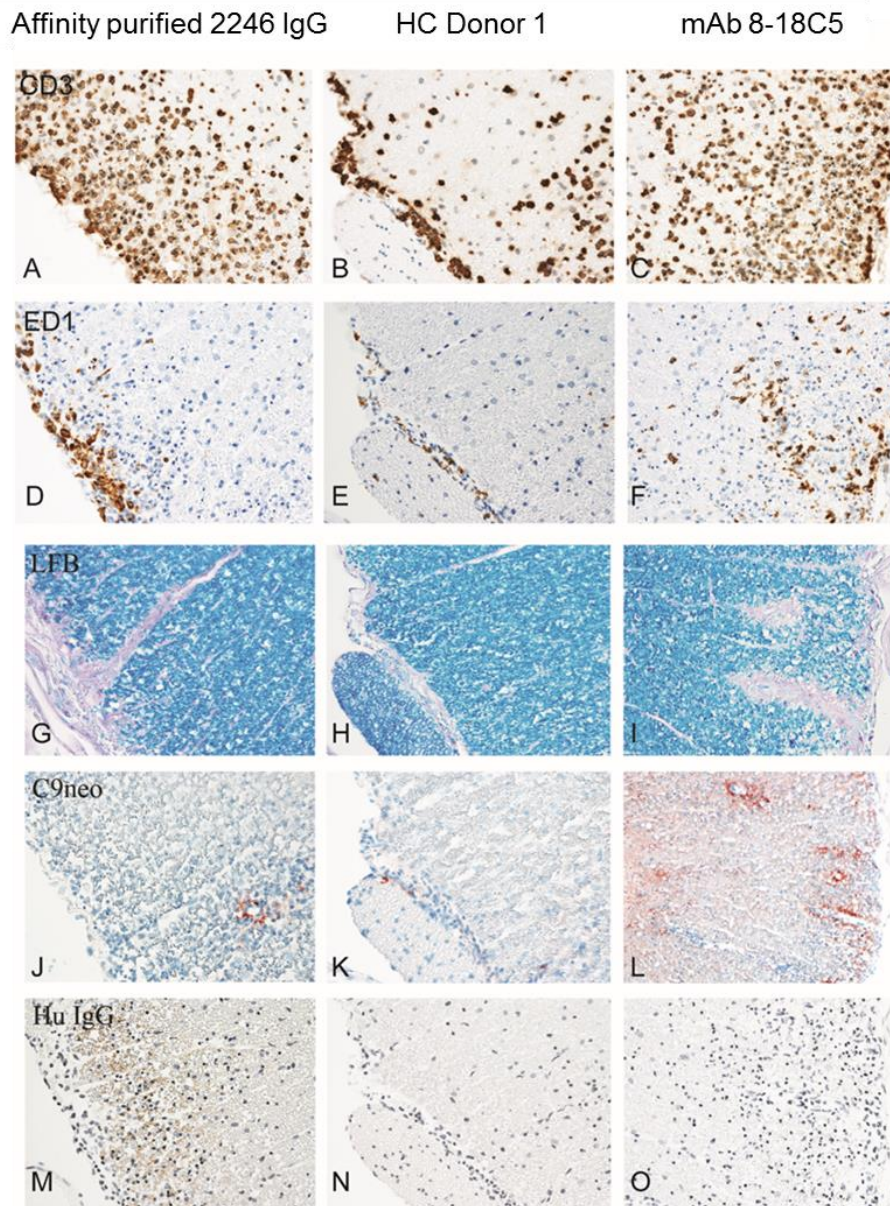


Figure 27: Histopathological analysis of inflammation, demyelination and complement activation. Tissue infiltration by CD3⁺ T-lymphocytes (A and C), absent in B. ED1 staining of activated macrophages in subpial area (D and F), less pronounced macrophage deposition in E. Perivascular Luxol fast blue (LFB) staining in G and I, absent in H. Immunoreactivity for activated complement (C9neo antigen) in the perivascular area (L) and to a lower extend in J and K. Staining for human IgG (M), absent in N and O.

In parallel to these tetramer stainings, the supernatants (SN) of the *in vitro* stimulated cells were analyzed for abs to MOG in our CBA (Figure 28B and C). We could detect abs that recognize full length hMOG and mMOG in the SN of the patient's cells, while the SN of the HC did not show any anti-MOG reactivity. The stimulated cells of the other wells were cryopreserved and used later for single cell sorting (Figure 28D) using the murine MOG tetramer (kindly provided by Dr. G. Krishnamoorthy).

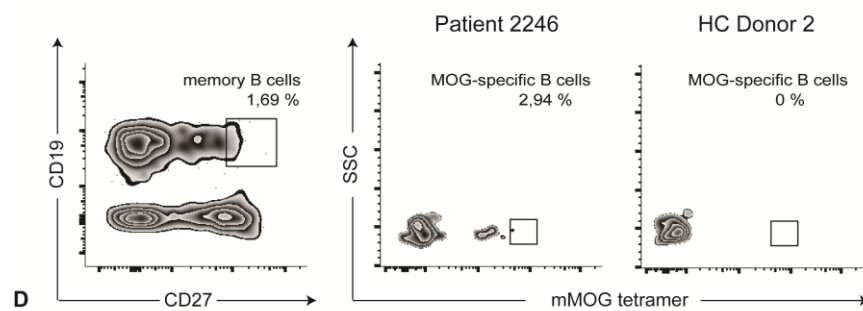
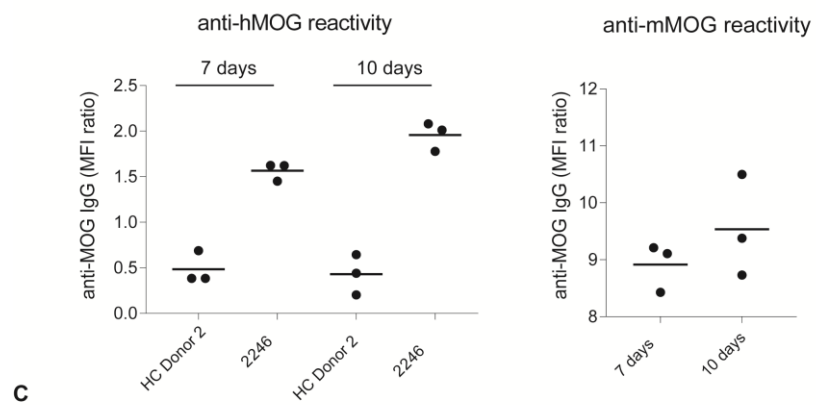
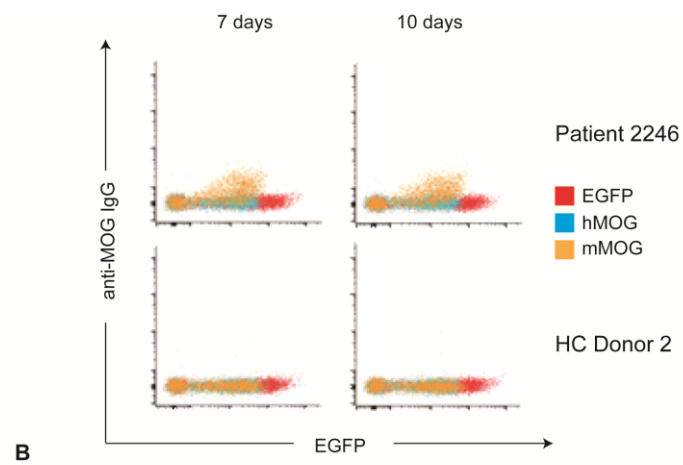
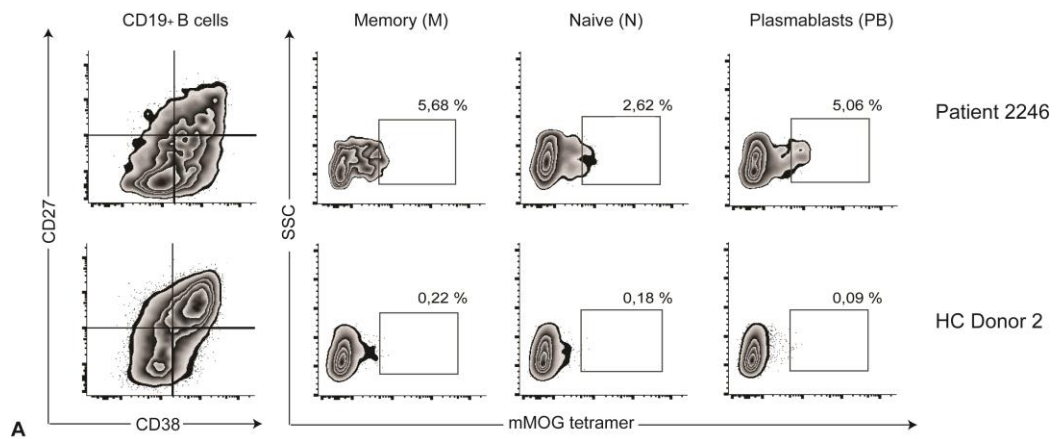


Figure 28: Phenotype of MOG-specific B cells in patient 2246. CD19⁺ B cells of the stimulated wells were divided into subpopulations (naive B cells (N), memory B cells (M) and plasmablasts (PB)), based on the expression of CD27 and CD38 (A). M: CD19⁺, CD27⁺, CD38⁻; PB: CD19⁺, CD27⁺, CD38⁺; N: CD19⁺ CD27⁻). Cells shown here were stimulated for 7 days (A). Detection of MOG-specific abs in the SN of stimulated B cells from patient 2246 and HC Donor 2. HeLa cells were transfected with EGFP, hMOG-EGFP and mMOG-EGFP and then incubated with undiluted SN to test for anti-MOG IgG by flow cytometry. Cells were stimulated for 7 (left plot) and 10 days (right plot). Shown is one representative well /conditions (B) and a summary of all tested wells (C). Gating strategy for single cell sorting of *in vitro* stimulated PBMC from patient 2246: memory B cells (CD19⁺, CD27⁺) stained by the mouse MOG tetramer were sorted. Stimulated cells from HC Donor 2 were used as negative control. Frequencies represent tetramer-positive B cells among memory B cells (CD19⁺, CD27⁺) (C).

MOG tetramer-positive B cells of patient 2246 represented 2.94 % of CD19⁺ CD27⁺ B cells. The cells displayed in 28D were single cell sorted. From one of them we generated a H₂L₂-chain pair which was used to obtain full length recombinant abs.

3.7.2 Validation of human MOG tetramers and staining of PBMC *ex vivo*

The extracellular domain of hMOG was produced recombinantly in HEK 293 EBNA 1 cells, enzymatically biotinylated at the Avi-tag and then incubated with fluorescently labeled streptavidin in order to generate a tetramer. The BCR-binding activity of this tetramer was validated with splenocytes from MOG-Ig knock-in mice (Litzenburger, Fässler et al. 1998). APC and FITC labeled tetramers were compared. The APC-labeled tetramers showed a more efficient staining of splenocytes from IgH^{MOG} knock-in mice than the FITC labeled tetramers (Figure 29A) and were therefore used for the staining of PBMC from patients with MOG-specific abs. These included patients with a low (patient 467) and high (patients 1771 and 2246) anti-MOG reactivity in the CBA (Figure 29B). We identified MOG-positive B cells (CD19⁺) in patient 2246 and a weak staining of cells from patient 467 and 1771. However, we observed also a labelling of few B cells in a control donor who tested negative for anti-MOG reactivity in our CBA (Figure 29B). We optimized the staining by using negatively selected B cells instead of whole PBMC and gated on class-switched memory B cells. This allowed us to reduce the unspecific binding in HC cells (Figure 29C). This gating strategy was used for single sorting of freshly isolated B cells from patient 2246 (Figure 29D). MOG tetramer-binding B cells represented 0.51 % of class-switched memory B cells. The cells displayed in 29C were single cell sorted. From four of them we could generate H₂L₂-chain pairs which were used to obtain full length recombinant abs.

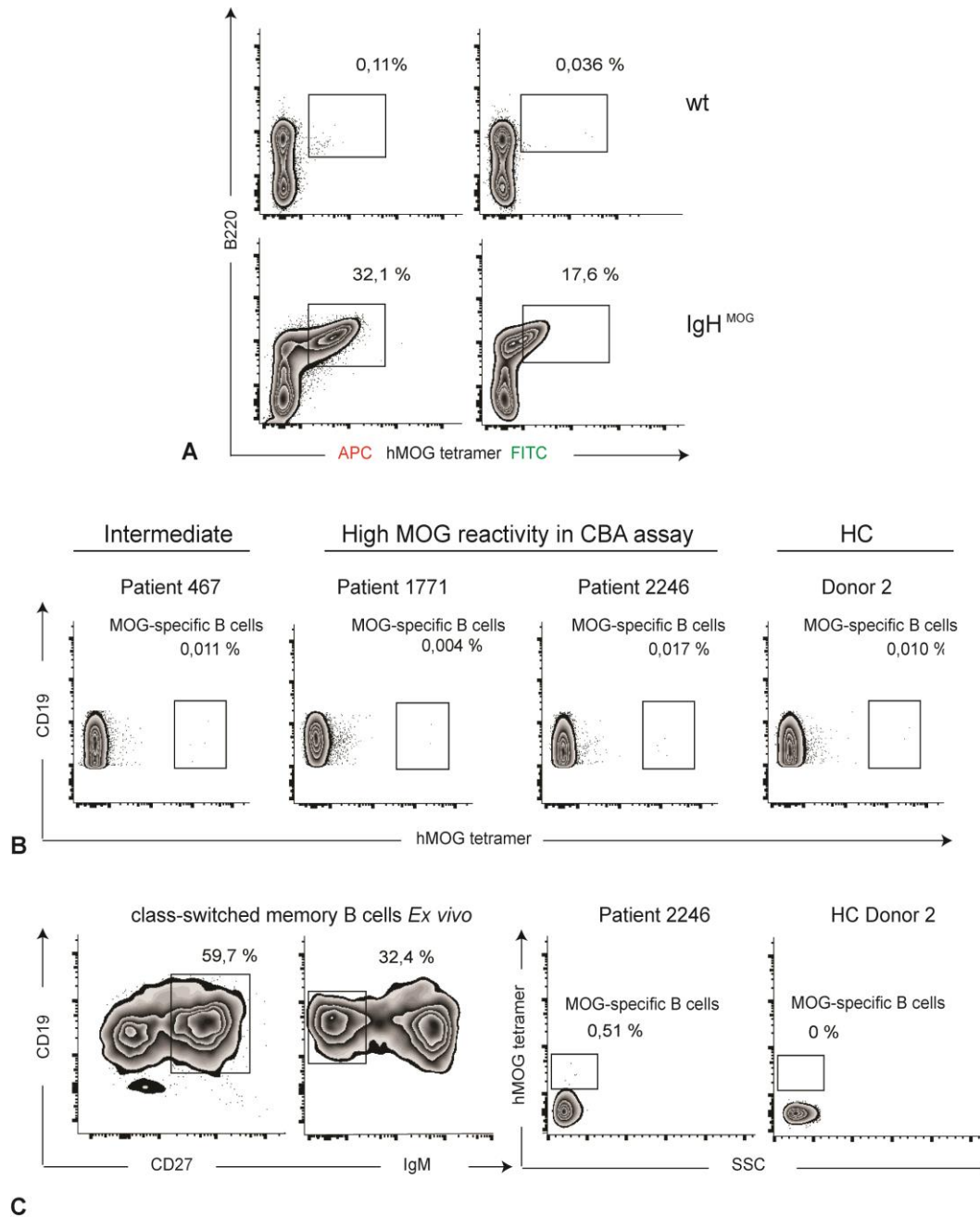


Figure 29: Validation of hMOG tetramers and staining of PBMC *ex vivo*. The extracellular part of hMOG was expressed in HEK 293 EBNA 1 cells, biotinylated enzymatically and allowed to form a tetramer with streptavidin-APC or streptavidin-FITC conjugate. MOG-tetramers were incubated with splenocytes from IgH^{MOG} knock-in (Litzenburger, Fässler et al. 1998) and control mice (A). Staining of PBMC from patients 467, 1771 and 2246 and HC with an anti-CD19 antibody and APC-labeled hMOG tetramer (B). Optimized staining of class-switched memory B cells (CD19⁺, CD27⁺, IgM⁺) with APC-labeled human MOG tetramer (n=2) (C). Gating strategy for single cell sorting of fresh isolated B cells from patient 2246. Freshly isolated B cells from HC were used as negative control. Frequencies represent tetramer-positive B cells among class-switched memory B cells (CD19⁺, CD27⁺, IgM⁺) (C, left).

3.7.3 Recombinant expression of IgG from patient 2246

We obtained from the single cell sorting of MOG-specific B cells from patient 2246 five recombinant IgG clones: one from the *in vitro* stimulated PBMC (r2246_D7) and four from the *ex vivo* isolated B cells (r2246_E6, r2246_E3, r2246_A2 and r2246_F6). Single cell PCR and recombinant antibody expression are described in detail in sections 2.2.1 and 2.2.6. The amount of purified antibody/volume of cell suspension was variable and ranged from 0.25 – 5.4 µg/ml. The five isolated MOG-specific B cells were not clonally related since they had different VH-D-JH and VK-JK gene rearrangements (Table 11).

Table 11: Alignment of CDR3 protein sequences and V_H-D-J_H and V_K-J_K gene segment use

Antibody ID	V-D-J Junction	V	D	J	V-J Junction	V	J
2246_D7	<u>C</u> ARHPLGSGD ^{WG} PGDYAWDS.....	V4-39	D4-17	J4	<u>C</u> QQYYSNPYT..... ^{FG}	V4-1	J2
2246_E6	<u>C</u> ASHRDDVWSGYSNYYHYGLDV..... ^{WG}	V3-11	D3-3	J4	<u>C</u> QQSHSFPLT..... ^{FG}	V1-39	J4
2246_E3	<u>C</u> ASYVVGPTFDLS ^{WG} DY.....	V1-2	D1-26	J4	<u>C</u> QHRSNWPPFT..... ^{FG}	V3-11	J3
2246_A2	<u>C</u> ASETWNRGILRPGP..... ^{WG}	V4-61	D5-12	J5	<u>C</u> QHYGGSPSFT..... ^{FG}	V3-20	J3
2246_F6	<u>C</u> ARDIPAAGLFLDF..... ^{WG}	V3-7	D6-13	J4	<u>C</u> QRYNTYSRDLT..... ^{FG}	V1-5	J4

Eluted fractions were pooled and visualized by Coomassie blue staining and Western blot (Figure 30).

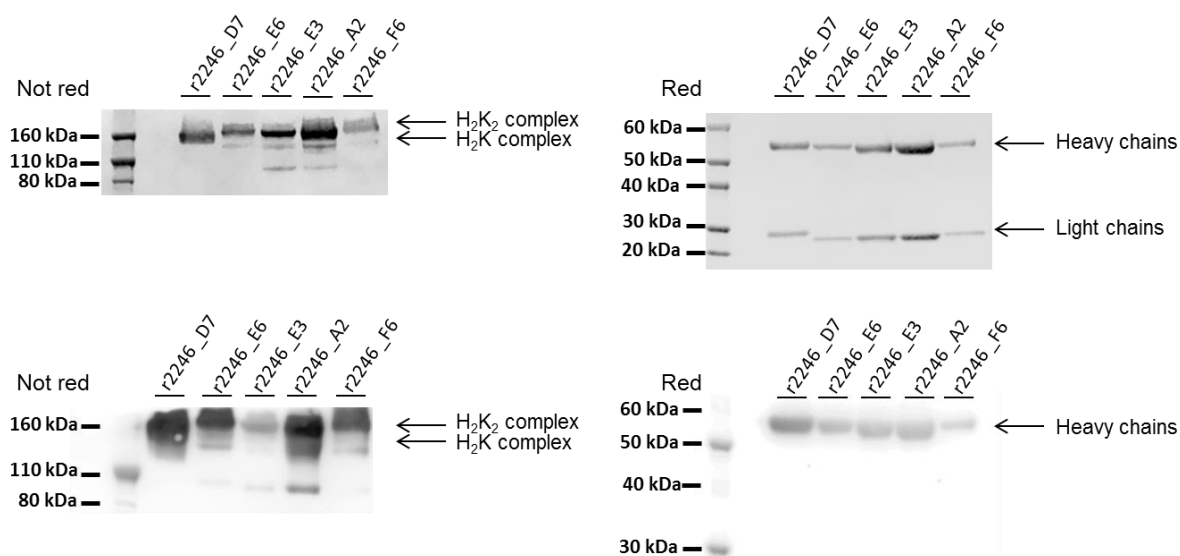


Figure 30: Visualization of recombinant abs by Coomassie staining and Western blot. Eluted fractions of recombinant abs were analyzed by Coomassie blue staining (upper figures) and Western Blot (lower figures). 1 µg of each antibody was loaded on the gel under not reducing (Not red) and reducing (Red) conditions. Western blot was performed by using an HRP-anti-His antibody.

3.7.4 Functional analysis of recombinant abs from patient 2246

Recombinant abs were analyzed for anti-MOG reactivity by ELISA and flow cytometry. Four of these five abs showed by ELISA reactivity against recombinant hMOG. The binding was quantified by calculating the binding constant (K_D) (Figure 31 and Table 12).

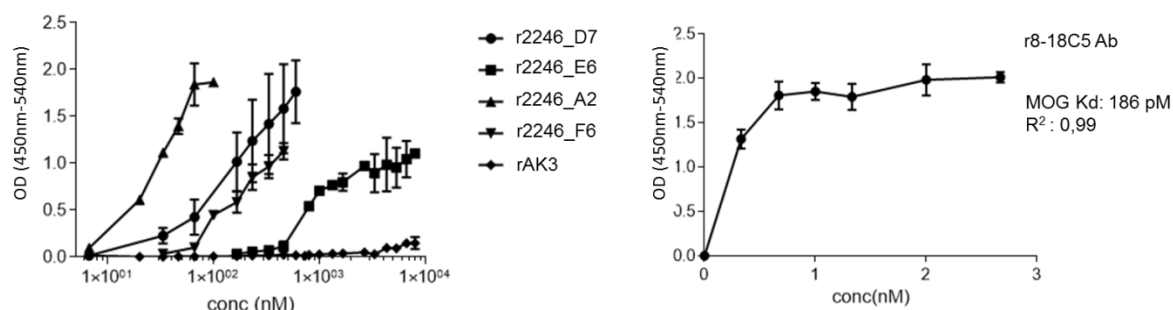


Figure 31: Binding of hMOG by abs generated from MOG-specific B cells. Saturation binding experiments were performed to determine the affinity of recombinant abs to human MOG. K_D values are shown in Table 13. The humanized r8-18C5 mAb was used as positive control. $n \geq 2$, error bars represent SDs.

We probed these abs also for binding to other glycoproteins present in the CNS (NF155, NF186 and OmgP) generated in the same HEK 293 expression system as MOG (data summarized in Table 12). The r2246_E6 antibody was the only one which did not show reactivity to the other antigens, this was however accompanied by a low binding affinity to MOG (704.6 nM) (Table 12).

Table 12: Reactivity of recombinant abs and binding quantification against hMOG

Antibody ID	reactivity (ELISA)	reactivity (FACS)	kD (hMOG)
r2246_D7	MOG; NF155	/	277.6 nM
r2246_E6	MOG	/	704.6 nM
r2246_E3	/	/	/
r2246_A2	MOG; omgP; NF155; NF186	/	28.4 nM
r2246_F6	MOG; NF155; NF186	/	385 nM

None of the generated abs showed by flow cytometry reactivity against full length human and murine MOG (Figure 32, data shown for r2246_D7).

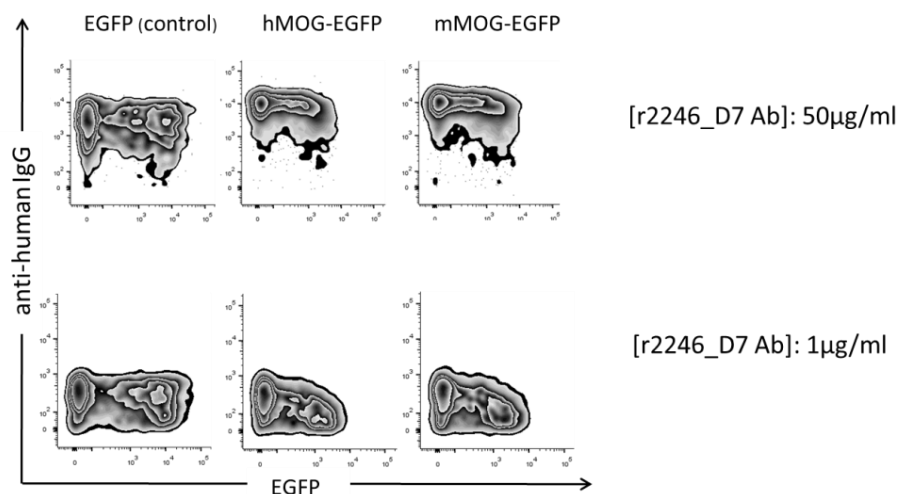


Figure 32: Binding of r2246_D7 to full length MOG by FACS. HeLa cells were transfected with full length hMOG-EGFP and mMOG-EGFP. Antibody was used at a concentration of 1 µg/ml and 50 µg/ml. HeLa cells transfected with EGFP only were used as control cells.

3.7.5 Transfer of human recombinant abs in Lewis rats

In order to determine the potential pathogenicity of the human recombinant abs described above, we performed *in vivo* experiments in Lewis rats. The recombinant antibody used for these experiments was r2246_D7 since it showed both higher affinity to MOG and less binding to the tested antigens compared to the other recombinant abs. Mild EAE was induced by intravenous injection of 8×10^6 MOG-specific T cells (T MOG-GFPn). Two days after EAE induction, 500 µg of the r2246_D7 antibody were injected intrathecally. The murine 8-18C5 mAb and the humanized r8-18C5 antibody were used as positive controls, while the rAb3 and a commercial mouse IgG1 antibody were used as negative controls. Both the murine 8-18C5 mAb as the humanized r8-18C5 antibody induced an increase of disease severity, while the human r2246_D7 antibody did not show any effect (Figure 32). Rats treated with the positive controls showed four days after EAE induction an increase of the clinical score, reaching at day five a maximum value of 2.5 for the murine mAb 8-18C5, and then completely recovered at day nine.

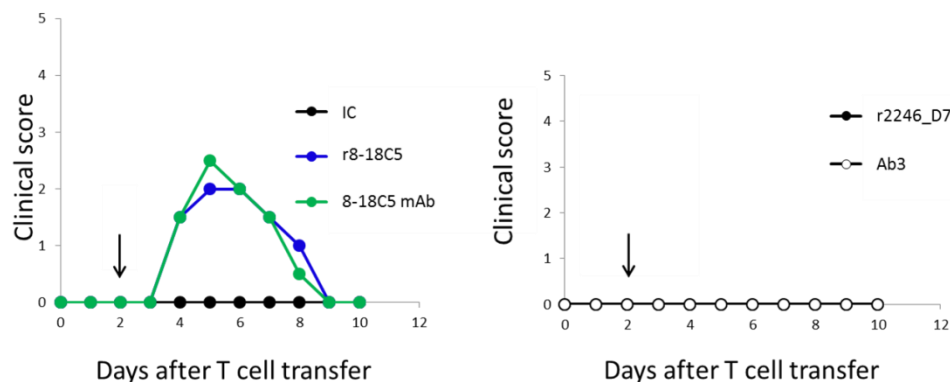


Figure 32: Clinical score in Lewis rats treated with recombinant MOG-specific abs. EAE was induced in n=2 male Lewis rats by the intravenous injection of 8×10^6 MOG-specific T cells. Two days after EAE induction, 500 μ g of each antibody were injected intravenously. Isotype control (IC), the humanized r8-18C5 antibody and the murine 8-18C5 mAb are indicated by the black, the blue and the green lines, respectively (left). The r2246_D7 and the negative control Ab3 are indicated by the full and empty circle symbol, respectively (right). Rats were scored daily for disease severity and weight change (not shown).

4 Discussion

4.1 Clinical spectrum of patients with abs to MOG

In this study, 17 sera from adult patients from the Institute of Clinical Neuroimmunology showed reactivity against conformation-intact MOG. In adults, abs to MOG have been described in several autoimmune disorders with partly overlapping features (Figure 33): they occur in a subset of AQP4-antibody negative NMO patients and patients with ON but are absent in most patients with classical adult MS. We here show, to our knowledge for the first time, that abs to MOG can occur also in adult patients with classical RRMS and clinical features reminiscent of NMOSD.

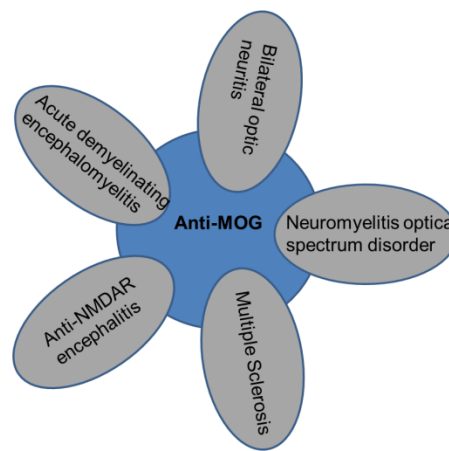


Figure 33: Overlapping features of MOG-antibody-associated CNS disorders. Abs to MOG are detected in a proportion of patients with different clinically defined CNS diseases: MS (childhood MS, especially before puberty and classic adult MS with a NMOSD-like phenotype), NMOSD, bilateral ON, ADEM and anti-NMDA-receptor (NMDAR)-antibody-associated encephalitis. Some patients with abs against MOG have clinical features that overlap with different autoimmune disorders, but fall outside current classification schemes. Modified from (Hohlfeld, Dornmair et al. 2016).

We observed the highest reactivity against MOG in patients diagnosed with ON and NMOSD. Our findings confirm previous studies which describe the presence of abs to MOG in proportions of patients with ON and anti-AQP4 abs negative NMOSD (Mader, Gredler et al. 2011, Kitley, Woodhall et al. 2012, Ramanathan, Reddel et al. 2014)

Among our cohort of patients with abs to MOG, three were also diagnosed with an autoinflammatory disease. These include two patients with FMF and one patient with CAPS. However, there was no anti-MOG reactivity when we analyzed a larger group of patients with similar diagnosis. Classically, autoinflammatory diseases were considered of being unrelated to autoantigen-specific T cells and B cells (Masters, Simon et al. 2009, Guler, Kaptanoglu et al. 2012, Onur, Aral et al. 2013) . However, there is evidence that the NLRP3 inflammasome, which is hyperactivated in CAPS patients, is also involved in humoral immunity (Kumar,

Kumagai et al. 2009). Further studies have to clarify whether there is an association between autoinflammatory diseases and the appearance of autoantibodies to MOG.

Two of the HC analyzed in our study had reactivity to MOG close to the cutoff value. Abs against conformation-intact MOG in HC have been described previously (Lalive, Menge et al. 2006). However, animal experiments have shown that abs to MOG are not pathogenic on their own, but perform a second hit, when the integrity of the blood-brain barrier is compromised by an already ongoing inflammatory process (Linington and Lassmann 1987, Schluesener, Sobel et al. 1987, Littenburger, Fässler et al. 1998).

Abs to MOG are more likely to be present during the early phases of childhood MS and are rather rare in adult MS. The first part of this study allowed us to make in this context two important observations: first, abs to MOG can occur in single patients with neuropathologically defined MS pattern II and a relapsing-remitting disease course; second, abs to MOG can also be found in a subset of adult patients who fulfill the McDonalds criteria for MS and have clinical features of NMOSD. These patients will be described in more detail in the next sections.

The clinical and pathological features of index patient 1819 are different from previously reported anti-MOG positive cases (Kitley, Waters et al. 2014, Sato, Callegaro et al. 2014, Titulaer, Hoftberger et al. 2014). More in detail, the disease in this patient was different from NMOSD because it did not reveal any optic nerve involvement and recurrent myelitis affected less than two vertebral segments (no LETM). On the other hand, despite a relapsing-remitting disease course, it could not be classified as typical MS because no OCB and no MS periventricular lesions were observed in this patient. Longitudinal analysis of anti-MOG reactivity revealed an association with the clinical course. Therefore, MOG-specific abs may serve as a biomarker with therapeutic implications. We observed an intense increase in anti-MOG reactivity after initiation of therapy with rituximab (32 months after disease onset). The observation that the recognized epitope pattern remained stable over time supports the idea that this increase is due to preexisting MOG-specific antibody secreting cells and memory B cells, and not to epitope spreading. The mechanisms of this increase in anti-MOG reactivity is not clear, but a previous study performed in NMO patients showed that rituximab therapy resulted in an increase of the B-cell survival factor BAFF (Pellkofer, Krumbholz et al. 2011). Interestingly, a transient increase in abs to AQP4 was previously observed in some patients after rituximab therapy and was linked to elevated BAFF levels (Nakashima, Takahashi et al. 2011). At the time point of increase of anti-MOG reactivity the patient developed a massive, bilateral, parieto-occipital white matter lesion and a brain biopsy was performed (results of histopathological analysis will be discussed in detail in section 4.2).

In this study, five adult MS patients tested positive for anti-MOG reactivity. These patients fulfilled the diagnostic criteria for MS because they had typical MS lesions on cranial MRI, positive OCBs in the CSF and a typical relapsing-remitting MS disease course. Clinically they were characterized by severe myelitis and/or ON. It has already been postulated that some patients with abs to MOG may represent a subgroup of optico-spinal MS (Zamvil and Slavin 2015), this hypothesis is supported by our findings but also expanded by the fact that our patients had otherwise rather typical MS. Longitudinal analysis of anti-MOG reactivity for an observation time up to nine years, showed that abs to MOG tend to fluctuate over time and intermittently fell below our detection limit (2.27). The high relapse rates and lack of satisfactory response to several DMTs in these five patients, strongly suggest that patients with MS who have abs to MOG may be at higher risk to develop progressive disease and need escalating therapies. It is difficult to estimate the occurrence of abs to MOG in adult MS: our data suggests that it may range between 5 % (in a selected cohort with specific clinical features, like group one in this study) and less than 1% in unselected MS groups. One limitation of our study is the relatively small number of anti-MOG-positive patients diagnosed with MS, but it is still the largest and best-defined cohort of anti-MOG-positive adult MS described so far. In addition, since no serum sample from the time of clinical onset was available, we do not know whether the production of abs to MOG is a primary or secondary event. Previous studies in pediatric patients identified MOG-specific abs at the first demyelinating event, arguing therefore for a primary event in these patients (Brilot, Dale et al. 2009, Probstel, Dornmair et al. 2011). On the other hand, recent animal studies showed that an autoimmune reaction to MOG can occur upon a toxic oligodendrocyte death (Traka, Podojil et al. 2016).

4.2 Histopathology of anti-MOG encephalomyelitis

Histopathological analysis of the brain biopsy performed in index patient 1819 revealed severe demyelination with features defined previously as “pattern II MS” (Lucchinetti, Brück et al. 2000). This is distinct from the astrocytopathy described in NMO (Misu, Höftberger et al. 2013). The lesions observed in this patient had a zonal configuration on MRI, this supports the findings of the histopathological examination, such as the centrifugal expansion reflected by densely packed macrophages at the lesion edge and the preservation of CNPase-positive, premyelinating oligodendrocytes within the lesion edge and center. The sites of ongoing demyelination at the early active lesion part showed deposition of IgG and activated complement. Moreover, complement activation was restricted to the area of active demyelination. This was unexpected, since blood-brain barrier damage with leakage of serum proteins was also seen in the periplaque white matter and within the lesion center.

The detailed analysis of antibody binding showed that not glycosylated MOG is much better recognized than glycosylated MOG. Presumably, glycosylation is reduced at the site of active inflammation facilitating as a consequence binding of abs to MOG on myelin sheaths resulting in complement activation. The deposition of IgG and the activation of complement observed in this patient are typical of MS pattern II. The presence of abs to MOG in patients with these neuropathological features is an important issue: the fact that among a total of five analyzed patients with pattern II MS, we could identify only one with abs to MOG indicates that MS type II in itself might be heterogeneous and is possibly associated with abs against different antigens. However, our findings and two recently published reports (Di Pauli, Hoftberger et al. 2015, Jarius, Metz et al. 2016), indicate that at least a subgroup of MS type II might be associated with abs to MOG.

Our study with different groups of patients diagnosed with MS showed that many patients with clinical MS and MS histopathology type II do not have abs to MOG (Spadaro, Gerdes et al. 2015, Spadaro, Gerdes et al. 2016). These observations confirm findings from other studies (Jarius, Metz et al. 2016). Thus, for these patients the actual target of the pathogenic autoantibody response remains to be identified.

4.3 Features of abs to MOG

Our CBA allowed us to determine the IgG subclass in 8 of 17 patients: all had the complement activating isotype IgG1 and are therefore potentially pathogenic. Also previous studies revealed the IgG1 subtype to be the dominant isotype of MOG-specific abs (McLaughlin, Chitnis et al. 2009). Patient 1771 showed in addition also an anti-MOG response mediated by abs of the IgM class. IgM abs can activate the complement system and some of them might be pathogenic as observed in IgM monoclonal gammopathy associated neuropathies (Mata, Borsini et al. 2011). IgM recognizing conformation-intact MOG have been observed in children during a first episode of demyelination (Brilot, Dale et al. 2009). Patient 1771 tested positive for anti-MOG IgM for the whole observation period. Patients who produce IgM during an active IgG response against the same antigen have also been observed in previous studies (Suwannalai, Willemze et al. 2011, Filippidou, Krashias et al. 2016), but the exact mechanism behind that is not clear. However, the fact that the anti-MOG IgG and IgM of our patient showed the same epitope specificity suggests that these anti-MOG IgM are not the result of the triggering of naïve B cells, but are mainly produced upon antigen stimulation (Murphy, Travers et al. 2009). The CSF of patient 1771 was negative for OCB and showed an anti-MOG reactivity which was lower than the response observed in the serum, when serum and CSF were tested at equal IgG concentrations.

These data suggest mainly a peripheral production of abs to MOG and are in line with previous findings (Dale, Tantsis et al. 2014, Ramanathan, Reddel et al. 2014).

The MOG-specific abs of the adult patients analyzed in this study recognized in an equal proportion one single epitope and multiple epitopes on MOG. Intriguingly, patients with ON or NMOSD were more likely to recognize only one epitope, while the majority of MS patients and all encephalomyelitis patients recognized multiple epitopes. The analysis of the epitopes involved in antibody binding showed interindividual heterogeneity, confirming thereby previous findings (Mayer, Breithaupt et al. 2013). Abs of patient 1819 showed an epitope recognition pattern which has not yet been observed so far: three different loops are involved in this patient's antibody binding to MOG. The nearly complete loss of binding to the MOG mutants R9G/H10Y and S104E indicated that both regions are bound simultaneously, consistent with the distance between amino acids and the observed maximum dimensions of single epitopes of up to 21 x 28 Å (Ramaraj, Angel et al. 2012).

Binding of abs to different mutants of conformation-intact MOG were analyzed previously in pediatric patients, however these abs were not suitable for the investigation of their pathogenic potential in animal models due to low reactivity to murine MOG (Mayer, Breithaupt et al. 2013). Transfer experiments have been performed with human sera and whole IgG from adult patients, however, the exact epitopes involved in binding to MOG were not known (Zhou, Srivastava et al. 2006, Saadoun, Waters et al. 2014, Flach, Litke et al. 2016, Kinzel, Lehmann-Horn et al. 2016). To our knowledge no transfer experiments employing affinity purified patient-derived MOG-specific abs with known epitope recognition pattern have been performed so far. On the other hand, epitopes on MOG recognized by murine abs are known: the mAbs 8-18C5 and Z2, which were used in animal models for the investigation of a pathogenic role of abs to MOG, bind to MOG via the FG' loop (Breithaupt, Schäfer et al. 2008). In addition, also other parts of the surface of MOG which do not belong to the FG' loop are recognized by pathogenic murine mAbs (Piddlesden, Lassmann et al. 1993).

The extracellular domain of human and murine MOG have a > 95% sequence identity (Mayer, Breithaupt et al. 2013). The main differences concern R9, P42 and R86, substituted in murine MOG by G9, S42 and Q86, respectively. Additionally, amino acid residue H10 is substituted by a tyrosine residue in mMOG but not in rat MOG (Breithaupt, Schäfer et al. 2008). Most of the patients analyzed previously did not recognize murine MOG because their antibody response to MOG was directed against P42 (Mayer, Breithaupt et al. 2013). In this study we observed that 3 ON patients (3202, 1771 and 2246) with abs to MOG showed high reactivity to murine MOG: in two of them this reactivity was present despite the binding to P42, probably explained by the recognition of Q86. Patient 2246 recognizes the MOG mutant

P42S much stronger than hMOG. In addition, binding to murine MOG in this patient is also mediated by H103, similarly to the pathogenic mAb 8-18C5 and Z2. Since H103 is conserved among species (Breithaupt, Schäfer et al. 2008), this subset of abs in patient 2246 could play a potential pathogenic role. We performed the affinity purification of MOG-specific abs by using human MOG, this allowed us to get rid of the abs that recognize only S42, which are not relevant in our patient since this amino acid is replaced by P42 in hMOG. The affinity purified antibody fraction obtained from this patient was still able to bind to rat MOG both in our CBA as well as to myelin in rat brains. Abs to MOG in patient 1771 showed binding to the CC' loop of MOG. These abs were also affinity purified and used in our *in vivo* experiments. This is to our knowledge the first time that the *in vivo* pathogenicity of abs to MOG is investigated by using human abs recognizing the CC'loop on hMOG.

4.4 Repertoire of abs to MOG

The ELISA used to screen patient sera in this study was performed by using MOG produced in a human cell system. The protein was site-specific biotinylated and then bound to the ELISA plate in the same way as it is oriented on the cell membrane. This immunoassay based on the streptavidin-biotin system allowed higher sensitivity when compared to the conventional assay. Even though it is common view that only CBAs can identify abs to MOG that may have a pathogenic role *in vivo* (Brehm, Piddlesden et al. 1999, Ohtani, Kohyama et al. 2011), a direct comparison between a CBA and a streptavidin-based ELISA has to our knowledge not yet been done before. We analyzed a total of 116 patients with both assays and found that even by using this highly sensitive ELISA we could not identify all anti-MOG positive patients that scored positive in our CBA: 5 of 116 patients were positive in both assays, while two patients tested positive only by ELISA. The lack of correlation of the results we obtained with these two different methods strongly suggests the existence of a broad repertoire of MOG-specific abs in at least a subset of patients. Our data show that this MOG ELISA can be useful to predict whether abs to MOG from patients that scored positive in a CBA can be affinity purified with recombinantly produced MOG: abs from patients 1771 and 2246 that scored positive in both assays, similarly to the mAb 8-18C5, could be affinity purified while the affinity purification of abs from patient 3202, who scored negative in the ELISA, did not succeed. In addition, our analysis provides direct evidence that a subset of anti-MOG positive patients have autoantibodies able to bind both the soluble recombinant protein as well as the cell-bound protein. Abs with these features have not been described in patients before, while the murine mAb 8-18C5 has these properties. Abs to MOG in some patients (Haase, Guggenmos et al. 2001) as well as the mAb Y11 (Brehm, Piddlesden et al. 1999) are able to bind both linear MOG peptides as well as cell-bound MOG but the

pathogenic potential has been investigated only for the latter (Piddlesden, Lassmann et al. 1993). The affinity of the purified abs to MOG was lower than the one observed for the mAb 8-18C5 in the ELISA, however, they are still considered high affinity abs since their K_D value was in the low nanomolar range.

To investigate the pathogenic effects of MOG-specific abs *in vivo* we used, beside the affinity purification, an additional experimental approach: we isolated from patient 2246, both MOG-specific B cells directly *ex vivo* as well as PBMCs which were stimulate *in vitro* to differentiate to antibody-secreting cells. This procedure was performed by using fluorescently labeled human and mouse MOG tetramers. The isolated cells were single-cell sorted and used to generate recombinant abs. Antigen-specific B cells circulate at very low frequency in peripheral blood and proliferate at a very low rate under steady-state conditions (Lanzavecchia and Sallusto 2009, Yoshida, Mei et al. 2010), therefore their identification can be challenging. We chose to use antigen tetramers since they determine an increase of the avidity of BCR labeling and of the brightness of staining. Moreover, the employment of fluorescently labeled streptavidin eliminates the need to modify the antigen with a fluorophore, a procedure that can cause epitope destruction. Our tetramers bound to MOG-specific B lymphocytes from transgenic knock-in mice (Litzenburger, Fässler et al. 1998), suggesting that the recombinant MOG we used for tetramer formation exhibits the correct folding. Since we wanted to generate abs reactive against rodent MOG to use in our animal model, we used also a mMOG tetramer and single cell-sorted *in vitro* stimulated B cells. MOG-specific B cells in patient 2246 were mainly of the memory subtype, moreover, we could identify also a small proportion of early plasmablasts, which still carry their BCR on the surface. The *in vitro* stimulated B cells from this patient produced abs that showed anti- MOG reactivity in our CBA. In addition, we used a hMOG tetramer to isolate MOG-specific B cells directly from the peripheral blood of this patient. Also here we could identify a small proportion of cells belonging to the memory subtype. In total, we generated from the single cells sorted cells five recombinant abs. Four out of five of these abs showed reactivity against MOG by ELISA, but did not bind to MOG in our CBA. In addition, they showed cross-reactivity to other antigens produced in the same human cell system as MOG. The autoreactivity we observed reminds of findings obtained with human immunoglobulins generated from randomly selected B cells: about 20 % of all abs produced by human mature B-lymphocytes are autoreactive and 4 % of these are polyreactive (Wardemann, Yurasov et al. 2003). Abs with these features are produced by circulating B cells that escaped the first BCR-dependent bone marrow selection checkpoint (Wardemann, Yurasov et al. 2003), a mechanism that triggers apoptosis or reediting for autoreactive BCR (Meffre and Wardemann 2008).

4.5 Pathogenicity of abs to MOG

Our study shows, to our knowledge for the first time, that MOG-specific abs affinity purified from the blood of two patients with demyelinating diseases were pathogenic in animals. This reveals that abs to MOG are not only a biomarker that helps to stratify patients with inflammatory diseases of the CNS. While our findings in index patient 1819 suggest a potential pathogenic role of abs to MOG, with here now show a direct proof of their pathogenicity in patients 2246 and 1771. Previous transfer studies, performed with concentrated sera from MS patients, showed that abs to MOG can exacerbate CNS damage and cellular immunity has been suggested as the main effector mechanism (Zhou, Srivastava et al. 2006). These results are difficult to interpret because pathogenicity could be caused by pathogenic compounds beyond abs to MOG. IgG from NMO patients that tested positive for abs to MOG can directly damage myelin *in situ*, independent of preexisting disease and of complement activation (Saadoun, Waters et al. 2014). These data strongly suggest that abs to MOG from different patients can exert their pathogenicity by using different effector mechanisms. The affinity purified abs from both patients tested positive for anti-MOG reactivity in our CBA and induced EAE exacerbation in Lewis rats. In addition, the histopathological analysis of rats who received affinity purified abs from patient 2246 reveals two important finding: first, the demyelination observed in these animals is complement mediated; second, MOG-specific abs are able to enhance in the CNS the local activation of MOG-specific T cells. Based on these findings, further experiments need to be performed in order to clarify whether MOG-specific B cells can also mediate demyelination in conjunction with T cells with another antigen specificity. MOG lesions in this study were characterized by a massive leucocyte infiltration, similarly to a recent finding (Flach, Litke et al. 2016). While in this latter case no disease relevant MOG abs mediated demyelination was observed, the injection of the abs from our patient induced a subpial demyelination. This was also present at the level of the optic nerve and consequently suggests that these abs exert a pathogenic role in this patient who was diagnosed with a severe ON. The injection of the r2246_D7 antibody, obtained from MOG-specific B cells present in the peripheral blood of patient 2246, did not induce disease exacerbation in Lewis rats. This antibody showed reactivity against the extracellular domain of MOG but did not bind full length MOG in our CBA. The lack of pathogenic potential of this antibody in our *in vivo* experiments confirms that abs that do not recognize cell-bound MOG are not pathogenetically relevant *in vivo*.

4.6 Conclusions

Abs to MOG induce demyelination in different animal models, therefore, the identification of patients with MOG-specific abs may have diagnostic and therapeutic implications. In the first part of this study we show that abs to MOG can occur in patients with overlapping features of

NMOSD and MS. Our findings in index patient 1819 with MOG-associated encephalomyelitis suggest that abs to MOG can contribute to demyelination: these abs recognize conformation-intact MOG; they can access the CNS via the locally opened blood-brain barrier; they are of the complement activating isotype; the histology in this patient resembles anti-MOG mediated demyelination in animals and MS type “pattern II”; the observed association between anti-MOG reactivity and clinical course and the improvement after IA indicate the presence of pathogenic abs. Similar findings were made subsequently also by other two groups (Di Pauli, Hoftberger et al. 2015, Jarius, Metz et al. 2016). We here show that abs to MOG can also be found in a small proportion of adult MS with a specific phenotype. Further studies have to clarify whether patients with MS and abs to MOG may be at higher risk of progressive disease. Our study reveals that especially patients with concomitant severe spinal cord and brainstem lesions should be tested for anti-MOG reactivity. The longitudinal analysis of abs to MOG we performed in these patients showed that the anti-MOG reactivity tends to fluctuate over time, indicating that repeated analysis may be helpful if clinical features are compatible with MOG-associated MS. In summary, the results from the first part of this study broaden the spectrum of diseases associated to MOG-specific abs and therefore support the emerging hypothesis that MOG-antibody associated diseases might be a separated entity.

The role of abs to MOG in the pathogenesis of demyelinating diseases is still unresolved and the observation that only a subset of these abs recognizes both human and murine MOG, limits the employment of animal studies as experimental approach. Whether affinity purified and recombinant abs to MOG are pathogenic *in vivo* has not yet been investigated. These questions were addressed in the second part of this study. Abs to conformation-intact murine MOG were affinity purified from two adult patients diagnosed with ON. In addition, recombinant abs from one of this patient were generated. While affinity purified abs showed to be pathogenic *in vivo* by inducing demyelination and inflammation, recombinant abs did not induce any pathological effect. Taken together, our results with recombinant and affinity purified abs revealed a broad repertoire of abs against MOG, which occurred in the same patient (2246). Even though MOG-abs associated ON has been shown to have a more favorable outcome than AQP4-abs associated NMOSD (Sato, Callegaro et al. 2014, Hoftberger, Sepulveda et al. 2015), the potential pathogenic role of abs to MOG in adult ON observed in this study is supported by the fact that MOG-abs associated ON is characterized by a more pronounced retinal atrophy (Havla, Kumpfel et al. 2016), optic nerve swelling (Ramanathan, Reddel et al. 2014) and by longer optic nerve lesions (Akaishi, Sato et al. 2016, Ramanathan, Prelog et al. 2016) compared to patients with no abs to MOG. In conclusion, these findings strongly suggest abs to MOG as a potential emerging marker of ON.

5 References

't Hart, B. A., J. D. Laman, et al. (2004). Modelling of multiple sclerosis: lessons learned in a non-human primate. The Lancet Neurology. 3: 588-597.

Adelmann, M., J. Wood, et al. (1995). "The N-terminal domain of the myelin oligodendrocyte glycoprotein (MOG) induces acute demyelinating experimental autoimmune encephalomyelitis in the Lewis rat." J Neuroimmunol 63(1): 17-27.

Akaishi, T., D. Sato, et al. (2016). "MRI and retinal abnormalities in isolated optic neuritis with myelin oligodendrocyte glycoprotein and aquaporin-4 antibodies: a comparative study." J Neurol Neurosurg Psychiatry 87(4): 446-448.

Beck, R., J. Trobe, et al. (2003). "High- and low-risk profiles for the development of multiple sclerosis within 10 years after optic neuritis: experience of the optic neuritis treatment trial." Arch Ophthalmol 121(7): 944-949.

Beltran, E., B. Obermeier, et al. (2014). "Intrathecal somatic hypermutation of IgM in multiple sclerosis and neuroinflammation." Brain 137(Pt 10): 2703-2714.

Berger, T., P. Rubner, et al. (2003). "Antimyelin antibodies as a predictor of clinically definite multiple sclerosis after a first demyelinating event." N Engl J Med 349(2): 139-145.

Bourquin, C., A. Schubart, et al. (2003). "Selective unresponsiveness to conformational B cell epitopes of the myelin oligodendrocyte glycoprotein in H-2b mice." J Immunol 171(1): 455-461.

Brädl, M., T. Misu, et al. (2009). "Neuromyelitis optica: pathogenicity of patient immunoglobulin in vivo." Ann Neurol 66(5): 630-643.

Brändle, S., B. Obermeier, et al. (2016). "Distinct oligoclonal band antibodies in multiple sclerosis recognize ubiquitous self-proteins." Proc Natl Acad Sci U S A 113(28): 7864-7869.

Brehm, U., S. Piddlesden, et al. (1999). "Epitope specificity of demyelinating monoclonal autoantibodies directed against the human myelin oligodendrocyte glycoprotein (MOG)." J Neuroimmunol 97(1-2): 9-15.

Breithaupt, C., B. Schäfer, et al. (2008). "Demyelinating myelin oligodendrocyte glycoprotein-specific autoantibody response is focused on one dominant conformational epitope region in rodents." J Immunol 181(2): 1255-1263.

- Brilot, F., R. C. Dale, et al. (2009). "Antibodies to native myelin oligodendrocyte glycoprotein in children with inflammatory demyelinating central nervous system disease." Ann Neurol 66(6): 833-842.
- Brunner, C., H. Lassmann, et al. (1989). "Differential ultrastructural localization of myelin basic protein, myelin/oligodendroglial glycoprotein, and 2',3'-cyclic nucleotide 3'-phosphodiesterase in the CNS of adult rats." J Neurochem 52(1): 296-304.
- Clements, C., H. Reid, et al. (2003). "The crystal structure of myelin oligodendrocyte glycoprotein, a key autoantigen in multiple sclerosis." Proc Natl Acad Sci 100(19): 11059-11064.
- Cohen, J. A., A. J. Coles, et al. (2012). "Alemtuzumab versus interferon beta 1a as first-line treatment for patients with relapsing-remitting multiple sclerosis: a randomised controlled phase 3 trial." The Lancet 380(9856): 1819-1828.
- Confavreux, C., S. Vukusic, et al. (2000). "Relapses and progression of disability in multiple sclerosis." N Engl J Med 343(20): 1430-1438.
- Dale, R., E. Tantsis, et al. (2014). "Antibodies to MOG have a demyelination phenotype and affect oligodendrocyte cytoskeleton."
- Delarasse, C., P. Daubas, et al. (2003). "Myelin/oligodendrocyte glycoprotein-deficient (MOG-deficient) mice reveal lack of immune tolerance to MOG in wild-type mice." J Clin Invest 112(4):544-553
- Derfuss, T., K. Parikh, et al. (2009). "Contactin-2/TAG-1-directed autoimmunity is identified in multiple sclerosis patients and mediates gray matter pathology in animals." Proc Natl Acad Sci U S A 106(20): 8302-8307.
- Di Pauli, F., R. Hoftberger, et al. (2015). "Fulminant demyelinating encephalomyelitis: Insights from antibody studies and neuropathology." Neurol Neuroimmunol Neuroinflamm 2(6): e175.
- Di Pauli, F., S. Mader, et al. (2011). "Temporal dynamics of anti-MOG antibodies in CNS demyelinating diseases." Clin Immunol 138(3): 247-254.
- Durocher, Y., S. Perret, et al. (2002). "High-level and high-throughput recombinant protein production by transient transfection of suspension-growing human 293-EBNA1 cells." Nucleic Acids Res 30(2): E9.

- Fernandez-Carbonell, C., D. Vargas-Lowy, et al. (2015). "Clinical and MRI phenotype of children with MOG antibodies." Mult Scler 22(2): 174-184.
- Filippidou, N., G. Krashias, et al. (2016). "The association between IgG and IgM antibodies against cardiolipin, β 2-glycoprotein I and Domain I of β 2-glycoprotein I with disease profile in patients with multiple sclerosis." Mol Immunol 75: 161-167.
- Fischer, M. T., I. Wimmer, et al. (2013). "Disease-specific molecular events in cortical multiple sclerosis lesions." Brain 136(Pt 6): 1799-1815.
- Flach, A. C., T. Litke, et al. (2016). "Autoantibody-boosted T-cell reactivation in the target organ triggers manifestation of autoimmune CNS disease." Proc Natl Acad Sci U S A 113(12): 3323-3328.
- Genain, C. P., M. H. Nguyen, et al. (1995). "Antibody facilitation of multiple sclerosis-like lesions in a nonhuman primate." J. Clin. Invest. 96(6): 2966-2974.
- Gori, F., B. Mulinacci, et al. (2011). "IgG and IgM antibodies to the refolded MOG(1-125) extracellular domain in humans." J Neuroimmunol 233(1-2): 216-220.
- Guler, E., E. Kaptanoglu, et al. (2012). "Autoantibodies are not associated with familial mediterranean fever." Acta Reumatol Port 37(2): 144-148.
- Haase, C., J. Guggenmos, et al. (2001). "The fine specificity of the myelin oligodendrocyte glycoprotein autoantibody response in patients with multiple sclerosis and normal healthy controls." J Neuroimmunol 114(1-2): 220-225.
- Hampe, C., L. Petrosini, et al. (2013). "Monoclonal antibodies to 65kDa glutamate decarboxylase induce epitope specific effects on motor and cognitive functions in rats." Orphanet J Rare Dis.
- Hauser, S., E. Waubant, et al. (2008). "B-cell depletion with rituximab in relapsing-remitting multiple sclerosis." N Engl J Med. 358(7): 676-688.
- Hauser, S. L., G. Comi, et al. (2015). "Efficacy and safety of ocrelizumab in relapsing multiple sclerosis - results of the interferon-beta-1a-controlled, double-blind, Phase III OPERA I and II studies." Mult Scler 21: 61-62 [Abstract 190].
- Havla, J., T. Kumpfel, et al. (2016). "Myelin-oligodendrocyte-glycoprotein (MOG) autoantibodies as potential markers of severe optic neuritis and subclinical retinal axonal degeneration." J Neurol.

- Heigl, F., R. Hettich, et al. (2013). "Immunoadsorption in steroid-refractory multiple sclerosis: clinical experience in 60 patients." Atheroscler Suppl 14(1): 167-173.
- Hickman, S., C. Dalton, et al. (2002). "Management of acute optic neuritis." Lancet 360(9349): 1953-1962.
- Hoffmann, F. and E. Meinl (2014). "B cells in multiple sclerosis: good or bad guys?: An article for 28 May 2014 - World MS Day 2014." Eur J Immunol 44(5): 1247-1250.
- Hoftberger, R., M. Sepulveda, et al. (2015). "Antibodies to MOG and AQP4 in adults with neuromyelitis optica and suspected limited forms of the disease." Mult Scler 21(7): 866-874.
- Hohlfeld, R., K. Dornmair, et al. (2016). "The search for the target antigens of multiple sclerosis, part 2: CD8+ T cells, B cells, and antibodies in the focus of reverse-translational research." The Lancet Neurology 15(3): 317-331.
- Jarius, S., I. Metz, et al. (2016). "Screening for MOG-IgG and 27 other anti-glial and anti-neuronal autoantibodies in 'pattern II multiple sclerosis' and brain biopsy findings in a MOG-IgG-positive case." Mult Scler 22(12): 1541-1549.
- Jarius, S., K. Ruprecht, et al. (2016). "MOG-IgG in NMO and related disorders: a multicenter study of 50 patients. Part 2: Epidemiology, clinical presentation, radiological and laboratory features, treatment responses, and long-term outcome." J Neuroinflammation 13(1): 280.
- Jarius, S. and B. Wildemann (2010). "AQP4 antibodies in neuromyelitis optica: diagnostic and pathogenetic relevance." Nat Rev Neurol 6(7):383-392.
- Johns, T. and C. Bernard (1997). "Binding of complement component C1q to myelin oligodendrocyte glycoprotein: a novel mechanism for regulating CNS inflammation." Mol Immunol 34(1): 33-38.
- Kebir, H., K. Kreymborg, et al. (2007). "Human TH17 lymphocytes promote blood-brain barrier disruption and central nervous system inflammation." Nat Med 13(10): 1173-1175.
- Keegan, M., F. König, et al. (2005). "Relation between humoral pathological changes in multiple sclerosis and response to therapeutic plasma exchange." The Lancet 366(9485): 579-582.
- Kim, S. M., M. R. Woodhall, et al. (2015). "Antibodies to MOG in adults with inflammatory demyelinating disease of the CNS." Neurol Neuroimmunol Neuroinflamm 2(6): e163.

- Kinzel, S., K. Lehmann-Horn, et al. (2016). "Myelin-reactive antibodies initiate T cell-mediated CNS autoimmune disease by opsonization of endogenous antigen." Acta Neuropathol 132(1): 43-58.
- Kitley, J., M. I. Leite, et al. (2013). "Longitudinally extensive transverse myelitis with and without aquaporin 4 antibodies." JAMA Neurol 70(11): 1375-1381.
- Kitley, J., P. Waters, et al. (2014). "Neuromyelitis optica spectrum disorders with aquaporin-4 and myelin-oligodendrocyte glycoprotein antibodies: a comparative study." JAMA Neurol 71(3): 276-283.
- Kitley, J., M. Woodhall, et al. (2012). "Myelin-oligodendrocyte glycoprotein antibodies in adults with a neuromyelitis optica phenotype." Neurology 79(12): 1273-1277.
- Krumbholz, M., T. Derfuss, et al. (2012). "B cells and antibodies in multiple sclerosis pathogenesis and therapy." Nat Rev Neurol 8(11): 613-623.
- Krumbholz, M. and E. Meinl (2014). "B cells in MS and NMO: pathogenesis and therapy." Semin Immunopathol 36(3): 339-350.
- Krupp, L., M. Tardieu, et al. (2013). "International Pediatric Multiple Sclerosis Study Group criteria for pediatric multiple sclerosis and immune-mediated central nervous system demyelinating disorders: revisions to the 2007 definitions." Mult Scler 19(10): 1261-1267.
- Kuhle, J., C. Pohl, et al. (2007). "Lack of association between antimyelin antibodies and progression to multiple sclerosis." N Engl J Med 356(4): 371-378.
- Kumar, H., Y. Kumagai, et al. (2009). "Involvement of the NLRP3 inflammasome in innate and humoral adaptive immune responses to fungal beta-glucan." J Immunol 183(12): 8061-8067.
- Kutzelnigg, A., C. F. Lucchinetti, et al. (2005). "Cortical demyelination and diffuse white matter injury in multiple sclerosis." Brain 128(Pt 11): 2705-2712.
- Lalive, P. H., M. G. Hausler, et al. (2011). "Highly reactive anti-myelin oligodendrocyte glycoprotein antibodies differentiate demyelinating diseases from viral encephalitis in children." Mult Scler 17(3): 297-302.
- Lalive, P. H., T. Menge, et al. (2006). "Antibodies to native myelin oligodendrocyte glycoprotein are serologic markers of early inflammation in multiple sclerosis." Proc Natl Acad Sci U S A 103(7): 2280-2285.

- Lanzavecchia, A. and F. Sallusto (2009). "Human B cell memory." Curr Opin Immunol 21(3): 298-304.
- Lassmann, H., C. Brunner, et al. (1988). "Experimental allergic encephalomyelitis: the balance between encephalitogenic T lymphocytes and demyelinating antibodies determines size and structure of demyelinated lesions." Acta Neuropathol 75(6): 566-576.
- Lebar, R., C. Lubetzki, et al. (1986). "The M2 autoantigen of central nervous system myelin, a glycoprotein present in oligodendrocyte membrane." Clin Exp Immunol. 66(2): 423-434.
- Lennon, V., D. Wingerchuk, et al. (2004). "A serum autoantibody marker of neuromyelitis optica: distinction from multiple sclerosis." Lancet 364(9451): 2106-2112.
- Lindert, R., C. Haase, et al. (1999). "Multiple sclerosis: B- and T-cell responses to the extracellular domain of the myelin oligodendrocyte glycoprotein." Brain 122(Pt 11): 2089-2100.
- Linington, C., M. Bradl, et al. (1988). "Augmentation of demyelination in rat acute allergic encephalomyelitis by circulating mouse monoclonal antibodies directed against a myelin/oligodendrocyte glycoprotein." Am J Pathol 130(3): 443-454.
- Linington, C. and H. Lassmann (1987). "Antibody responses in chronic relapsing experimental allergic encephalomyelitis: correlation of serum demyelinating activity with antibody titre to the myelin/oligodendrocyte glycoprotein (MOG)." J Neuroimmunol 17(1): 61-69.
- Litzenburger, T., R. Fässler, et al. (1998). "B lymphocytes producing demyelinating autoantibodies: development and function in gene-targeted transgenic mice." J Exp Med. 188(1): 169-180.
- Lucchinetti, C., W. Brück, et al. (2000). "Heterogeneity of multiple sclerosis lesions: implications for the pathogenesis of demyelination." Ann Neurol 7(3): 115-121.
- Lucchinetti, C., R. Mandler, et al. (2002). "A role for humoral mechanisms in the pathogenesis of Devic's neuromyelitis optica." Brain 125(Pt 7): 1450-1461.
- Mader, S., V. Gredler, et al. (2011). "Complement activating antibodies to myelin oligodendrocyte glycoprotein in neuromyelitis optica and related disorders." J Neuroinflammation 8: 184.

- Marta, C. B., A. R. Oliver, et al. (2005). "Pathogenic myelin oligodendrocyte glycoprotein antibodies recognize glycosylated epitopes and perturb oligodendrocyte physiology." Proc Natl Acad Sci U S A 102(39): 13992-13997.
- Masters, S., A. Simon, et al. (2009). "Horror autoinflammaticus: the molecular pathophysiology of autoinflammatory disease (*)." Annu Rev Immunol 27: 621-668.
- Mata, S., W. Borsini, et al. (2011). "IgM monoclonal gammopathy-associated neuropathies with different IgM specificity." Eur J Neurol 18(8): 1067-1073.
- Mayer, M. and E. Meinl (2012). "Glycoproteins as targets of autoantibodies in CNS inflammation: MOG and more." Ther Adv Neurol Disord 5(3): 147-159.
- Mayer, M. C., C. Breithaupt, et al. (2013). "Distinction and temporal stability of conformational epitopes on myelin oligodendrocyte glycoprotein recognized by patients with different inflammatory central nervous system diseases." J Immunol 191(7): 3594-3604.
- McLaughlin, K. A., T. Chitnis, et al. (2009). "Age-dependent B cell autoimmunity to a myelin surface antigen in pediatric multiple sclerosis." J Immunol 183(6): 4067-4076.
- Meffre, E. and H. Wardemann (2008). "B-cell tolerance checkpoints in health and autoimmunity." Curr Opin Immunol 20(6): 632-638.
- Misu, T., R. Höftberger, et al. (2013). "Presence of six different lesion types suggests diverse mechanisms of tissue injury in neuromyelitis optica." Acta Neuropathologica 125(6): 815-827.
- Murphy, K., P. Travers, et al. (2009). "Janeway Immunobiology, 9th Edition." Garland Science.
- Nakashima, I., T. Takahashi, et al. (2011). "Transient increases in anti-aquaporin-4 antibody titers following rituximab treatment in neuromyelitis optica, in association with elevated serum BAFF levels." J Clin Neurosci 18(7): 997-998.
- Neuteboom, R., M. Boon, et al. (2008). "Prognostic factors after a first attack of inflammatory CNS demyelination in children." Neurology 71(13): 967-973.
- O'Connor, K. C., K. A. McLaughlin, et al. (2007). "Self-antigen tetramers discriminate between myelin autoantibodies to native or denatured protein." Nat Med 13(2): 211-217.
- Obermeier, B., R. Mentele, et al. (2008). "Matching of oligoclonal immunoglobulin transcriptomes and proteomes of cerebrospinal fluid in multiple sclerosis." Nat Med 14(6): 688-693.

- Ohtani, S., K. Kohyama, et al. (2011). "Autoantibodies recognizing native MOG are closely associated with active demyelination but not with neuroinflammation in chronic EAE." Neuropathology 31(2): 101-111.
- Onur, H., H. Aral, et al. (2013). "Anti-CCP Antibodies Are Not Associated with Familial Mediterranean Fever in Childhood." Int J Rheumatol 2013(498581).
- Pelayo, R., M. Tintoré, et al. (2007). "Antimyelin antibodies with no progression to multiple sclerosis." N Engl J Med 356(4): 426-428.
- Pellkofer, H., M. Krumbholz, et al. (2011). "Long-term follow-up of patients with neuromyelitis optica after repeated therapy with rituximab." Neurology 76(15): 1310-1315.
- Pham-Dinh, D., M. Matteit, et al. (1993). "Myelin/oligodendrocyte glycoprotein is a member of a subset of the immunoglobulin superfamily encoded within the major histocompatibility complex." Proc. Natl. Acad. Sci. 90(17): 7990-7994.
- Piddlesden, S., H. Lassmann, et al. (1993). "The demyelinating potential of antibodies to myelin oligodendrocyte glycoprotein is related to their ability to fix complement." Am J Pathol 143(2): 555-564.
- Pinna, D., D. Corti, et al. (2009). "Clonal dissection of the human memory B-cell repertoire following infection and vaccination." Eur J Immunol 39(5): 1260-1270.
- Probstel, A. K., K. Dornmair, et al. (2011). "Antibodies to MOG are transient in childhood acute disseminated encephalomyelitis." Neurology 77(6): 580-588.
- Ramanathan, S., K. Prelog, et al. (2016). "Radiological differentiation of optic neuritis with myelin oligodendrocyte glycoprotein antibodies, aquaporin-4 antibodies, and multiple sclerosis." Mult Scler 22(4): 470-482.
- Ramanathan, S., S. W. Reddel, et al. (2014). "Antibodies to myelin oligodendrocyte glycoprotein in bilateral and recurrent optic neuritis." Neurol Neuroimmunol Neuroinflamm 1(4): e40.
- Ramaraj, T., T. Angel, et al. (2012). "Antigen-antibody interface properties: composition, residue interactions, and features of 53 non-redundant structures." Biochim Biophys Acta 1824(3): 520-532.
- Reindl, M., F. Di Pauli, et al. (2013). "The spectrum of MOG autoantibody-associated demyelinating diseases." Nat Rev Neurol 9(8): 455-461.

- Reindl, M., C. Linington, et al. (1999). "Antibodies against the myelin oligodendrocyte glycoprotein and the myelin basic protein in multiple sclerosis and other neurological diseases: a comparative study." Brain 122(Pt 11): 2047-2056.
- Rostasy, K., S. Mader, et al. (2012). "Anti-myelin oligodendrocyte glycoprotein antibodies in pediatric patients with optic neuritis." Arch Neurol 69(6): 752-756.
- Saadoun, S., P. Waters, et al. (2010). "Intra-cerebral injection of neuromyelitis optica immunoglobulin G and human complement produces neuromyelitis optica lesions in mice." Brain 133(Pt 2): 349-361.
- Saadoun, S., P. Waters, et al. (2014). "Neuromyelitis optica MOG-IgG causes reversible lesions in mouse brain." Acta Neuropathol Commun 2: 35.
- Saini, H., R. Rifkin, et al. (2013). "Passively transferred human NMO-IgG exacerbates demyelination in mouse experimental autoimmune encephalomyelitis." BMC Neurol 13(104).
- Sato, D. K., D. Callegaro, et al. (2014). "Distinction between MOG antibody-positive and AQP4 antibody-positive NMO spectrum disorders." Neurology 82(6): 474-481.
- Schluesener, H., R. Sobel, et al. (1987). "A monoclonal antibody against a myelin oligodendrocyte glycoprotein induces relapses and demyelination in central nervous system autoimmune disease." J Immunol 139(12): 4016-4021.
- Serafini, B., B. Rosicarelli, et al. (2004). "Detection of ectopic B-cell follicles with germinal centers in the meninges of patients with secondary progressive multiple sclerosis." Brain Pathol 14(2): 164-174.
- Sorensen, P., S. Lisby, et al. (2014). "Safety and efficacy of ofatumumab in relapsing-remitting multiple sclerosis: a phase 2 study." Neurology 82(7): 573-581.
- Spadaro, M., L. A. Gerdes, et al. (2016). "Autoantibodies to MOG in a distinct subgroup of adult multiple sclerosis." Neurol Neuroimmunol Neuroinflamm 3(5): e257.
- Spadaro, M., L. A. Gerdes, et al. (2015). "Histopathology and clinical course of MOG-antibody-associated encephalomyelitis." Ann Clin Transl Neurol 2(3): 295-301.
- Spadaro, M. and E. Meinl (2016). "Detection of Autoantibodies Against Myelin Oligodendrocyte Glycoprotein in Multiple Sclerosis and Related Diseases." Methods Mol Biol 1304: 99-104.
- Suwannalai, P., A. Willemze, et al. (2011). "The fine specificity of IgM anti-citrullinated protein antibodies (ACPA) is different from that of IgG ACPA." Arthritis Res Ther 13(6): R195.

- Titulaer, M. J., R. Hoftberger, et al. (2014). "Overlapping demyelinating syndromes and anti-N-methyl-D-aspartate receptor encephalitis." Ann Neurol 75(3): 411-428.
- Traka, M., J. R. Podojil, et al. (2016). "Oligodendrocyte death results in immune-mediated CNS demyelination." Nat Neurosci 19(1): 65-74.
- Trebst, C., S. Jarius, et al. (2014). "Update on the diagnosis and treatment of neuromyelitis optica: recommendations of the Neuromyelitis Optica Study Group (NEMOS)." J Neurol 261(1): 1-16.
- von Büdingen, H., F. Mei, et al. (2015). "The myelin oligodendrocyte glycoprotein directly binds nerve growth factor to modulate central axon circuitry." J Cell Biol 210(6): 891-898.
- Von Büdingen, H. C., M. Gulati, et al. (2010). "Clonally expanded plasma cells in the cerebrospinal fluid of patients with central nervous system autoimmune demyelination produce "oligoclonal bands"." J Neuroimmunol 218(1-2): 134-139.
- Wardemann, H., S. Yurasov, et al. (2003). "Predominant autoantibody production by early human B cell precursors." Science 301(5638): 1374-1377.
- Wingerchuk, D., Lennon VA, et al. (2007). "The spectrum of neuromyelitis optica." Lancet Neurol 6(9): 805-815.
- Wingerchuk, D., Lennon VA, et al. (2006). "Revised diagnostic criteria for neuromyelitis optica." Neurology 66(10): 1485-1489.
- Wu, X., M. Zhou, et al. (2013). "Myelin oligodendrocyte glycoprotein induces aquaporin-4 autoantibodies in mouse experimental autoimmune encephalomyelitis." J Neuroimmunol 261(1-2): 1-6.
- Xiao, B., C. Linington, et al. (1991). "Antibodies to myelin-oligodendrocyte glycoprotein in cerebrospinal fluid from patients with multiple sclerosis and controls." J Neuroimmunol 31(2): 91-96.
- Yoshida, M., Y. Tamura, et al. (2000). "Immusorba TR and Immusorba PH: basics of design and features of functions. 1998." Ther Apher 4(2): 127-134.
- Yoshida, T., H. Mei, et al. (2010). "Memory B and memory plasma cells." Immunol Rev. 237(1): 117-139.
- Zamvil, S. and A. Slavin (2015). "Does MOG Ig-positive AQP4-seronegative opticospinal inflammatory disease justify a diagnosis of NMO spectrum disorder?" Neurol Neuroimmunol Neuroinflamm 2(1): e62.

Zhou, D., R. Srivastava, et al. (2006). "Identification of a pathogenic antibody response to native myelin oligodendrocyte glycoprotein in multiple sclerosis." Proc Natl Acad Sci U S A 103(50): 19057-19062.

6 List of Abbreviations

Abs	Antibodies
Amp	Ampicillin
BCA	Bicinchoninic acid
BCR	B-cell receptor
BSA	Bovine serum albumin
CIS	Clinically isolated syndrom
CSF	Cerebrospinal fluid
DMSO	Dimethyl sulfoxide
DNA	Deoxyribonucleic acid
EAE	Experimental autoimmune encephalomyelitis
EBNA	Epstein-Barr virus nuclear antigen
EDTA	Ethylenediaminetetraacetic acid
EGFP	Esmerald green fluorescent protein
ELISA	Enzyme-linked immunosorbent assay
FCS	Fetal calf serum
FITC	Fluorescein isothiocyanate
HC	Healthy controls
HEK 293	Human embryonic kidney cell line
HeLa	Cervical cancer cell line Henrietta Lacks
His-Tag	Polyhistidine tag
hMOG	Human MOG
HRP	Horseradish peroxidase
Kan	Kanamycin
LB media	Luria-Bertani media
LDS	Lithium dodecyl sulfate
mAb	Monoclonal antibody
MFI	Mean fluorescence intensity
MOG	Myelin oligodendrocyte glycoprotein
MRI	Magnetic resonance imaging
MS	Multiple sclerosis
NaOH	Sodium hydroxide
NF	Neurofascin
NHS	N-hydroxysuccinimide
NIND	Non inflammatory neurological diseases
Ni-NTA	Nickel-nitrilotriacetic acid
NMOSD	Neuromyelitis optica spectrum disorders
OCB	Oligoclonal band
omgP	Oligodendrocyte myelin glycoprotein
ON	Optic Neurities
PBS	Phosphate buffered saline
PBST	Phosphate buffered saline with Tween-20
PCR	Polymerase chain reaction
PE	Phycoerythrin
PLEX	Plasma exchange
PVDF	Polyvinylidene fluoride

RRMS	Relapsing-remitting multiple sclerosis
RT-PCR	Reverse-transcript polymerase chain reaction
SDS-PAGE	Sodium dodecyl sulfate polyacrylamide gel electrophoresis
SPMS	Secondary-progressive multiple sclerosis
TMB	3,3',5,5'-Tetramethylbenzidine

7 Publications and Conferences

7.1 Publications

- **Spadaro M**, Kawakami N, Winklmeier S, Beltran E, Höftberger R, Schuh E, Thaler F, Gerhards R, Jenne D, Lassmann H, Hohlfeld R, Kümpfel T, Meinl E. *Pathogenicity and repertoire of human autoantibodies against MOG. In preparation.*
- Havla J, Kümpfel T, Schinner R, **Spadaro M**, Schuh E, Meinl E, Hohlfeld R, Outteryck O. *Myelin-oligodendrocyte-glycoprotein (MOG) autoantibodies as potential markers of severe optic neuritis and subclinical retinal axonal degeneration.* J Neurol, 2016 Jan 264(1):139-151. doi: 10.1007/s00415-016-8333-7.
- **Spadaro M**, Gerdes LA, Krumbholz M, Ertl-Wagner B, Thaler FS, Schuh E, Metz I, Blaschek A, Dick A, Brück W, Hohlfeld R, Meinl E, Kümpfel T. *Autoantibodies to MOG in a distinct subgroup of adult multiple sclerosis.* Neurol Neuroimmunol Neuroinflamm, 2016 Jun 30;3(5):e257. doi: 10.1212/NXI.0000000000000257.
- Ligocki AJ, Rivas JR, Rounds WH, Guzman AA, Li M, **Spadaro M**, Lahey L, Chen D, Henson PM, Graves D, Greenberg BM, Frohman EM, Ward ES, Robinson W, Meinl E, White CL, Stowe AM, Monson NL. *A distinct class of Antibodies may be an indicator of gray matter autoimmunity in early and established relapsing remitting Multiple Sclerosis patients.* ASN Neuro, 2015 21;7(5). doi: 10.1177/1759091415609613.
- **Spadaro M**, Gerdes LA, Mayer MC, Ertl-Wagner B, Laurent S, Krumbholz M, Breithaupt C, Högen T, Straube A, Giese A, Hohlfeld R, Lassmann H, Meinl E, Kümpfel K. *Histopathology and clinical course of MOG-associated encephalomyelitis.* Ann Clin Transl Neurol, 2015 Mar;2(3):295-301. doi: 10.1002/acn3.164.

7.2 Conferences

- **Spadaro M**, Gerdes LA, Krumbholz M, Ertl-Wagner B, Thaler FS, Schuh E, Metz I, Blaschek A, Dick A, Brück W, Hohlfeld R, Meinl E, Kümpfel T. *Autoantibodies to myelin oligodendrocyte glycoprotein antibodies in a small proportion of adult multiple sclerosis patients. European committee for treatment and research in multiple sclerosis (ECTRIMS), Barcelona 2015. (Poster presentation).*
- **Spadaro M**, Gerdes LA, Mayer MC, Ertl-Wagner B, Laurent S, Krumbholz M, Breithaupt C, Högen T, Straube A, Giese A, Hohlfeld R, Lassmann H, Meinl E, Kümpfel T. *Histopathology and clinical course of MOG-antibody associated encephalomyelitis. 15th European School of Neuroimmunology, Prague 2015.*
- **Spadaro M**, Gerdes LA, Mayer MC, Schuh E, Hoffmann F, Laurent S, Lassmann H, Hohlfeld R, Kümpfel T, Meinl E. *Myelin oligodendrocyte glycoprotein antibodies in patients with different inflammatory diseases of the CNS. 12th International Congress of Neuroimmunology, Mainz 2014. (Poster presentation).*

- **Spadaro M**, Gerdes LA, Mayer C, Schuh E, Laurent S, Krumbholz M, Linn L, Högen T, Kammermeier S, Giese A, Straube A, Lassmann H, Hohlfeld R, Meinl E, Kümpfel T. *Antikörper gegen Myelin Oligodendrozyten Glykoprotein (MOG) bei Erwachsenen mit verschiedenen Enzephalitiden. 87th Congress of the Deutsche Gesellschaft für Neurologie (DGN), Munich 2014. (Oral presentation)*

8 Curriculum Vitae

HIGHER EDUCATION	PhD candidate, Institute of clinical Neuroimmunology (Klinikum Großhadern) and International Max Planck Research School (IMPRS-LS) Martinsried, Germany 05/2013-12/2016 <i>Supervision:</i> Prof. R. Hohlfeld and Prof. E. Meinel	
	Master of Science in Biology, University of Messina Messina, Italy 03/2009-11/2010, Final grade: 110/110 cum Laude <i>Supervision:</i> Prof. E. Tellone, Department of Organic and Biological Chemistry	
	Bachelor's Degree in Biology, University of Messina Messina, Italy 09/2004-03/2009, Final grade: 110/110 cum Laude <i>Supervision:</i> Prof. FR. Trischitta, Department of human Physiology and Pharmacology	
CAREER DEVELOPMENT TRAINING	Business Fundamentals (V20), Ludwigs-Maximilians Universität Munich, Germany 10/2015-01/2016	
COMPETENCE TRAINING	COMMUNICATION Scientific Writing PROJECT MANAGEMENT Time and Project management Career mentoring and management GRAPHIC DESIGN Adobe Illustrator	
LANGUAGES	ITALIAN	bilingual proficiency
	GERMAN	bilingual proficiency
	ENGLISH	fluent spoken and written
SOFTWARE SKILLS	STANDARD	Microsoft office Word, Excel, Power Point, Outlook
	DATA ANALYSIS	GraphPad
	GRAPHIC DESIGN	Adobe Illustrator, Photoshop CS